MASS TRANSFER AND ENGINEERING ASPECTS ON AIR POLLUTION CONTROL EQUIPMENT

By Hans T. Karlsson

Doctoral dissertation

1981

Department of Chemical Engineering

Lund Institute of Technology - Sweden

Digitized by the Internet Archive
in 2026

https://archive.org/details/IA41553424_0016

MASS TRANSFER
AND ENGINEERING ASPECTS
ON AIR POLLUTION CONTROL EQUIPMENT

by

Hans T. Karlsson
MSc, Sm

Department of Chemical Engineering, Lund Institute of Technology
P.O.Box 740, S-220 07 Lund 7, Sweden

By due permission of the chancellor's office at Lund University for obtaining a doctorate, the thesis will be defended publicly in lecture-hall C at the Chemical Center, Lund, on June 1, 1981 at 9.15 am, in accordance to the university statute, Chapter 8, § 32.

Faculty opponent: Dr. Daniel Simonsson, Assistant Professor
the Royal Institute of Technology

Organization
LUND UNIVERSITY
Department of Chemical Engineering
Lund Institute of Technology
P.O.Box 740
S-220 07 Lund 7, Sweden

Document name
DOCTORAL DISSERTATION

Date of issue
May 5, 1981

CODEN: LUTKDH/(TKKT/1002)/1-168/(1981)

Author(s)
Hans T. Karlsson

Sponsoring organization

Title and subtitle

Mass Transfer and Engineering Aspects on Air Pollution Control Equipment

Abstract

Models for evaluation of experiments and scale-up of equipment for air pollution control are discussed. The expressions for calculation of the enhancement factor in irreversible gas-liquid reactions are improved. Models are presented for the scale-up of dry-injection removal processes. A new type of laboratory absorber is discussed and used in the evaluation of gas-liquid reactions. An integral method is presented for evaluation of kinetic data.

Specific processes for control of NO_x and SO_2 are discussed. NO_x removal for nitric acid plants, pickling baths, and coal-fired power plants is experimentally and theoretically investigated. A comprehensive assessment study of SO_2 removal is presented; the study is focused on process chemistry, scrubber systems, instrumentation and technology.

Key words
Gas-solid reactions, multi-jet absorber, kinetics, catalysts, oxides of nitrogen, and sulfur dioxide.

Classification system and/or index terms (if any)

Supplementary bibliographical information

Language
English

ISSN and key title

ISBN

Recipient's notes

Number of pages
168

Price

Security classification

Distribution by (name and address) Hans T. Karlsson, Department of Chemical Engineering, Lund Institute of Technology, P.O.Box 740, S-220 07 Lund 7, Sweden

I, the undersigned, being the copyright owner of the abstract of the above-mentioned dissertation, hereby grant to all reference sources permission to publish and disseminate the abstract of the above-mentioned dissertation.

Signature Hans Karlsson Date April 22, 1981

DOKUMENTDATABLAD enl SIS 61 41 21

UNIV.
LEIDEN
BIBL.

The Noble Art of Assessing the True Status

TABLE OF CONTENTS

Summary

	Page
INTODUCTION	1
OBJECTIVE AND SCOPE	1
MODELLING AND EVALUATION OF EXPERIMENTS	2
Background	2
The enhancement factor for gas-liquid reactions	2
Dry-injection removal	4
Modelling of the multi-jet absorber	5
Integral evaluation method	8
SPECIFIC PROCESSES FOR AIR POLLUTION CONTROL	10
Background	10
NO_x removal at a nitric acid plant	11
Wet scrubbing of NO_x with H_2O_2	15
NO_x removal at steel pickling plants	16
NO_x removal at a coal-fired power plant	19
Wet scrubbing of SO_2 in the U.S.	20
ACKNOWLEDGEMENT	22
NOTATION	23
REFERENCES	24

Appendices

I. Karlsson, H.T. and Bjerle, I.
On the Enhancement Factor for Instantaneous Irreversible Gas/Liquid Reactions.
Trans IChemE, 58(2), 138 (1980).

II. Karlsson, H.T. and Bjerle, I.
A Simple Approximation of the Error Function.
Comp. & Chem. Eng., 4(1), 67 (1980).

III. Karlsson, H.T. and Bjerle, I.
A General Explicit Enhancement Factor for Irreversible Gas-Liquid Reactions with Gas-Side Resistance.
Chem. Eng. Sci., 35(4), 1005 (1980).

IV. Karlsson, H.T., Klingspor, J. and Bjerle, I.
Adsorption of Hydrochloric Acid on Solid Slaked Lime for Flue Gas Clean Up.
Journal manuscript.

TABLE OF CONTENTS
(Continued)

V. Karlsson, H.T., Åberg, S. and Bjerle, I.
An Experimental Investigation of Mass Transfer from a Gas Flow to Liquid Jets.
Int. J. Heat Mass Transfer, 23(3), 355 (1980).

VI. Karlsson, H.T. and Bjerle, I.
Absorption of NO and NO_2 in a H_2O_2 Solution Using a Multi-Jet Absorber.
Technical report, Dept. of Chem. Eng., 31 pp., April, 1981.

VII. Karlsson, H.T. and Rosenberg, H.S.
Technical Aspects of Lime/Limestone Scrubbers for Coal-Fired Power Plants. Part I: Process Chemistry and Scrubber Systems.
APCA Journal, 30(6), 710 (1980).

VIII. Karlsson, H.T. and Rosenberg, H.S.
Technical Aspects of Lime/limestone Scrubbers for Coal-Fired Power Plants. Part II: Instrumentation and Technology.
APCA Journal, 30(7), 822 (1980).

IX. Karlsson, H.T. and Rosenberg, H.S.
Selective Catalytic Oxidation of NO to NO_2.
Technical report, Battelle, 29 pp., January, 1981.

INTRODUCTION

Air pollution is a byproduct from a process called human activities in an industrialized society. However, there is a continuous stream of emerging processes for control of air pollutants from stationary sources. The development is an inevitable result of the burning of large amounts of fossil fuels, along with an awareness of the impacts of pollutants on the environment and human beings.

Flue gas cleaning (FGC) processes represent a comparatively new technology. Consequently there is a need of research and development. Firstly, the theoretical aspects of FGC is not well understood. Reaction mechanisms have to be outlined and models describing mass transfer with chemical reaction need to be developed. Secondly, new and better FGC processes, as well as improvement of the now existing, is desirable.

OBJECTIVE AND SCOPE

This thesis comprises some thoughts and conclusions from work with air pollution control problems since the fall 1976. The work has been continued in terms of a number of programs or projects sponsored by individual organisations and companies, and has then continuously been complemented with theoretical considerations.

The projects have dealt with gaseous pollutants rather than particulates, and furthermore, mobile sources are not discussed in the thesis. The work has been focused on add-on processes. Pollution control can also be accomplished by developing modifications of the emitting process. However, the problem will in that case tend to deal with other engineering disciplins than chemical engineering.

The summary has been divided into one theoretical part and one part describing practical experience of processes, although there exists no such clear cut in the appendices or in the reality. The theoretical part discusses a few models for mass transfer with chemical reaction in heterogenous systems. The models are vital parts when dimensioning equipment and/or necessary intruments for the evaluation of kinetic data.

The second part contains a number of "case studies" of NO_x and SO_2 removal. SO_2 and NO_x are certainly the most important gaseous pollutants to be considered.

MODELLING AND EVALUATION OF EXPERIMENTS

Background

Scale-up from laboratory investigations to full-scale systems is often made on basis of incomplete or poor information in order to attempt to save time and money. On the other hand, the process chemistry can be too complex to allow a thorough outline. In many cases the reaction systems are of multi component type with two or more phases present. Key factors for an increased improvement of FGC processes are models describing mass transfer with chemical reaction and proper methods for evaluation of kinetic data. The latter factor may include theoretical as well as experimental techniques.

The most obvious use of models for mass transfer with chemical reaction is to increase the reliability of the scale up procedure. This will minimize investment risks. Secondly, the models will increase the understanding of the process, which uncovers feasible options to improve the removal efficiency and/or save expensive reactants. Hence, an increased process flexibility to optimize design is obtained. Thirdly, when assessing the status of full scale units and demonstration plants, the models indicate what parameters are essential to get a proper characterization.

If a reaction system is too complex to allow experimental data to be described by a model, better understanding of the process can be achieved by means of a model for a similar or more simple reaction system. The behavior of different parameters of such a model can give a good quantitative idea of the real reaction system.

Enhancement Factor for Gas-Liquid Reactions

The most frequently used device for control of gaseous pollutants is the scrubber. Basically, the size of a scrubber is determined from a set of conservation equations and the global rate of absorption in every gas/liquid contact point. The conservation equations depend on the hydrodynamic conditions and the flow pattern pertinent to the specific type of scrubber. The mass transfer rate, on the other hand, is expressed by a set of general equations for all types of absorbers.

Principally, the gaseous pollutant is removed from the gas phase and transported into the liquid by diffusion. The absorption rate can be

enhanced by a chemical reaction in the liquid phase. It is now generally accepted that the reaction rate for many gas-liquid reactions of practical importance can be represented by an m-, n:th-order irreversible rate expression. In 1948 van Krevelen and Hoftijzer (2) derived an approximate expression for the enhancement factor (the factor by which the absorption rate is increased by reaction) for a second order irreversible reaction. The derivation was based on the film theory; however, the relationship was later shown to be valid for the penetration theory. The validity was also extended to m-, n:th-order reactions.

To obtain better relationship, surprisingly little effort has followed the publication by van Krevelen and Hoftijzer (2). To date, exact solutions exist only for the two limiting cases: pseudo-m:th-order reaction and instantaneous reaction.

The classical implicit expression for the enhancement factor involves three deficiencies:

- The general expression gives the enhancement factor implicitly.
- In the case where gas-side resistance is involved, the concentration of the gaseous species at the interface is given implicitly.
- When an instantaneous reaction occurs in a quiscent liquid and the diffusion coefficients for the reacting species diverge considerably from each other, the commonly used approximation is invalid.

In Appendix III a relationship is given in order to delete the first deficiency mentioned. The equation is about as accurate as the implicit equation when compared to the true film theory (numerical solution). The present approximation was obtained in the following way: The enhancement factor (E) depends on the reaction parameter (γ) and the limiting case of an instantaneous reaction (E_i). The relationship has an approximate symmetri axis in $\gamma = E_i$, if considering a log-log scale and assuming $E > 3$. A relationship related to the harmonic mean value of E_i and γ was inferred from this finding. The equation has a simple mnemonic form.

The second deficiency was eliminated by introducing the straightforward harmonic mean value (Appendix III). The accuracy is about 20 percent. However, highest deviation is obtained at a great gas phase resistance. This means that the deviation in the mass transfer rate (which is indeed the most important parameter) is still no more than 5 percent, since the influence

of the enhancement factor decreases with increasing gas phase resistance.

Appendix I gives a derivation of an approximate solution of the enhancement factor for an instantaneous reaction in a quiesent liquid. This should delete deficiency number three. The derivation is based on a class of equations by Hastings (4), and an approximation of the error function shown in Appendix II. The equation was found to be superior to other commonly used approximations. The deviation from the exact implicit expression is no more than 5 percent for $E_i \geq 2$ (the range $1 \leq E_i \leq 2$ is of little practical importance); the ratio of the diffusion coefficients covers a range of five orders of magnitude.

Dry-Injection Removal

An emerging tecnology for removal of gaseous species from flue gas is injection of a solid reactant into the flue gas stream and subsequent capture of the solids in a baghouse filter. The equipment required for such a process is very simple and poses minimal addition to costs for flue gases which require control of the particulates along with the gaseous pollutant.

Appendix IV presents a model to calculate the removal efficiency for a process involving dry-injection. There are two feasible modes to operate the process concept. The first assumes that the solids are continuously injected into the flue gas stream at a given stoichiometric ratio with respect to the gaseous species. When the solids have been captured on the baghouse filter cloth, a homogeneous cake with continuously increasing thickness is formed. The solids are then removed from the filter cloth and the procedure is repeated in cycles. In the second mode of operation, all the solids used for a cycle is injected into the ductwork at the beginning of a cycle to precoat the filter cloth. The filter cake is then retained on the cloth for the entire cycle to remove the gaseous pollutant. Furthermore, it is possible to neglect the reaction during the transport of the solids from the injection point to the filter cloth.

In order to obtain an appropriate kinetic expression on which to base the model, a reaction system of practical importance (ie. slaked lime and hydrochloric acid) was examined experimentally. The reaction was found to be of first order with respect to the two reactants (second order totally). The model was based on this kinetic expression and the conservation equation, containing the convective, transient, and reaction terms.

Hence, two coupled partial differential equations were used to describe the system. The discrepancy of the two modes of operation was accounted for by using different boundary conditions.

The equations were solved by applying a constant pattern approach. For the continuous injection model this implicates that each point on the concentration curve of gaseous species moves out from the cloth with the same velocity as the interface where solids are added. For the precoating model on the other hand this means that the width of the concentration front tends toward a constant value as the wave moves through the bed of solids. The solutions are in terms of fraction removed gaseous pollutant:

$$\eta = \alpha - \alpha \ln \left[\frac{\alpha \exp [N(1-1/\alpha)] - 1}{\alpha - 1} \right] / N \qquad (1)$$

and

$$\eta = \alpha \ln \left[\frac{1 + \exp [N]}{1 + \exp [N(1-1/\alpha)]} \right] / N \qquad (2)$$

respectively. Here α and N are the stoichiometric ratio (solids/gas) and number of transfer units (rate constant multiplied by gas residence time at final thickness of solids), respectively.

The differential equations have recently been solved numerically by Wilhelmsson (5) to obtain exact solutions of the models. The solutions were compared to Equations (1) and (2), and the agreement was found to be excellent for all conditions encountered in practical applications. When a constant pattern exists, it is said that the conditions are favorable. Equation (1) was found to have favorable conditions for all values of α and N, and no discrepancy was found when compared to the numerical solution. Equation (2) has favorable conditions for $N > 5$, giving less than 0.13 percent deviation. When $N = 2$ and $\alpha = 1$, Equation (2) deviates by about 4 percent from the exact solution. However, when $N < 2$, the removal efficiency is not great.

Modelling of the Multi-Jet Absorber

Appendices V and VI describe a new type of laboratory reactor for investigation of gas-liquid reactions. The principle is based on the features of the well-known laminar jet absorber, ie. well-defined mass transfer properties. However, a large number of jets are utilized rather

than a single one. Such an approach offers a design where the gas is contacted with the liquid in a plug flow pattern. Thus, parameters as mass transfer interfacial area and gas residence time can be set at values similar to those of full scale absorbers. This feature provides direct scale-up, which is of importance when complex reaction systems are studied, in which case the kinetic data are hard to evaluate.

Generally speaking two different types of laboratory absorbers exist. The first type has well-defined mass transfer properties and is suitable for the evaluation of reaction mechanisms and of kinetic data. The second type has properties similar to full scale absorbers and is suitable for direct scale-up. The multi-jet absorber was constructed in order to combine these two properties. If experiments are performed in the multi-jet absorber, useful information is obtained even if the reaction mechanism is too complex to outline.

The mass transfer coefficient in the gas phase is outlined in Appendix V. The problem is complex since both the motion of the jets and the perpendicular gas flow generate boundary layers. The both limiting cases, ie. flow, perpendicular and parallel to the jets, respectively, can be estimated. However, the intervening transit region presents a problem.

It was found that a correlation for perpendicular flow can be used to describe experimental data (and a theoretical model) for parallel flow by replacing Reynold's number with a dimensionless group that depends on the residence time of the jet. By using the anology with a plane surface geomentry, and considering the data by Kays et al. (6) for a rotating cylinder placed in a perpendicular gas stream, a relationship was derived for the transit region. The configuration of the liquid jets was also taken into consideration in the relationship, which is expressed in terms of a j_d-equation.

In order to outline the applicability of the multi-jet absorber in evaluating kinetic data for gas-liquid reactions, some absorption experiments were performed as shown in Appendix VI. The reaction of NO_2 with water was considered appropriate since the system has been thoroughly outlined in the literature. Absorption of NO_2 in water can be represented by the following set of formulae:

$$2\,NO_2 \rightleftarrows N_2O_4$$

$$N_2O_4 + H_2O \rightarrow HNO_3 + HNO_2$$

$$3\,HNO_2 \rightarrow HNO_3 + H_2O + 2\,NO$$

The following equation was derived for this system:

$$\psi = H_D^{-1} \sqrt{(k_D D_{DL})}\, \theta \qquad (3)$$

A total of 30 data points are plotted in Figure 1 using the parameters of this equation. The straight line corresponds to a least-square fit, and the slope is given in table 1, along with data from other investigations. In conclusion, data are obtained from the multi-jet absorber with fair accuracy. As can be seen, data from nine studies vary a factor three.

The general treatment for absorption of a number of species in the multi-jet absorber, includes two equations for every species (i):

$$\frac{d\, p_{iG}}{d\, t} = R\, T_G\, A_V\, N_i \qquad (4)$$

$$N_i = k^o_{iL}\, E\, p_{ii}\, H_i^{-1} = k_{iG}\, (p_{iG} - p_{ii}) \qquad (5)$$

subject to:

$$\begin{cases} t = 0 \\ p_{iG} = (p_{iG})_o \end{cases} \qquad \begin{cases} t = \theta \\ p_{iG} = p_{iG} \end{cases}$$

A complex reaction scheme including three species is studied in Appendix VI.

FIGURE 1. PLOT OF EQ. (3) FOR ABSORPTION OF NO_2 IN WATER AT 20 °C

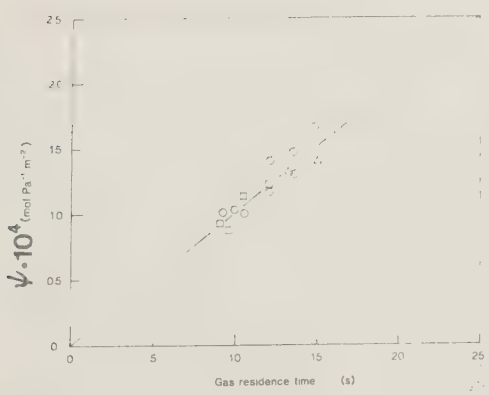

TABLE 1. KINETIC DATA FOR THE REACTION BETWEEN NITROGEN TETROXIDE AND WATER AT 20 °C

Investigation (Reference)	$H_D^{-1} \sqrt{(k_D D_{DL})} * 10^5$ (mol Pa^{-1} s^{-1} m^{-2})
Present study	1.0
Kramers et al. (7)	0.77
Wendel & Pigford (8)	0.53
Decker et al. (9)	1.0
Corriveau (10)	0.52
Gerstacker (11)	0.9-1.0
Kameoka & Pigford (12)	0.63
Caudle & Denbigh (13)	1.0
Kamiyama & Inoue (14)	1.58

Integral Evaluation Metod

The following equation is discussed in Appendix VI:

$$\kappa = \frac{C_o^{1-\delta}}{\theta(1-\delta)} \left[1 - (C/C_o)^{1-\delta}\right] \qquad (6)$$

This relation is the integrated result of the conservation equation for a plug flow or batch reactor with an irreversible reaction; the equation necessitates absence of volume changes. In its simplest form, δ and κ are the reaction order and rate constant, respectively. Equation (6) may also represent systems with complex chemistry and allow influence of mass transfer on the reaction rate. However, in that case δ and κ will have other meanings and the reaction order and rate constant are given implicitly from these paramenters.

There is no simple method available for the evaluation of δ and κ from experiments. For instance, various δ values can be assumed and then $\kappa\theta$ is plotted as a function of θ. A straight line indicates that the assumed δ value was an appropriate choice. However, poor planning of the experiments and/or improper treatment of the data may give a straight line for different δ values. A numerical method can also be used. By assuming various δ values, a mean value of κ can be estimated from all experiments as a function of δ. The true reaction order is reflected in minimal standard deviation with respect to κ. Again, poor planning of the experiments may cause uncertainty in the evaluation.

It would be beneficial to find a graphic method by which δ and κ could be evaluated from a straight-line plot. Such a method readily shows trends and deviations in the δ value. Scattered points which are obviously in error can be easily noticed and eliminated from the evaluation.

Rohsenow and Hartnett (15) show how to use the collocation method to find approximate solutions to differential equations. The method was used, as shown in Appendix VI, to find a workable formula for evaluation purposes. An example is given with two collocation points, ie. $\delta = 0$ and $\delta = 2$, in which case Equation (6) degenerates into:

$$\ln\left[(C_o - C)/\theta\right] = \delta \ln\left[\sqrt{(C_o C)}\right] + \ln[\kappa] \qquad (7)$$

The approximation has the following properties:

- The error in κ is no more than 2 percent if $C/C_o \geq 0.5$ and $0 \leq \delta \leq 2$. By expanding the validity to $0 \leq \delta \leq 3$, the ratio C/C_o must be greater than 0.7 to obtain less than 2 percent error. However, if $C/C_o < 0.5$, the error is still not great.

- When the true δ value coincides with one of the collocation points, Equation (7) is exact; if the δ value is reasonably close to one of the collocation points, the accuracy is sufficient.

From the last property, it can be inferred that the true reaction order can be obtained with a high accuracy even if the conversion is great (small C/C_o value). This because one of the original collocation points can be replaced by the evaluated value of δ. Thus, an iterative procedure is followed.

Figure 2 displays a plot of data from absorption of NO_2 in a H_2O_2 solution, using the paramenters of Equation (7). The slope was found to be two, indicating an instantaneous combination of two NO_2 molecules to form the tetroxide in the gas phase, followed by reaction between the tetroxide and water; the latter reaction being the rate determining step.

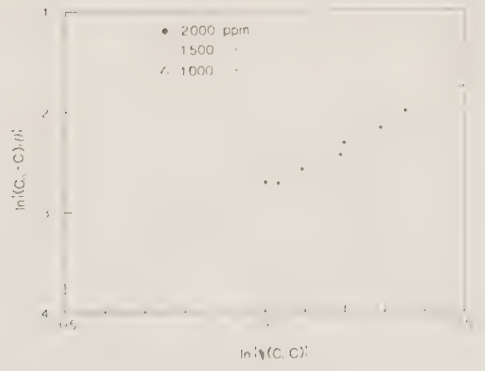

TABLE 2. EVALUATION OF KINETIC DATA FOR REACTION OF NO_2 WITH A H_2O_2 SOLUTION AT 20 ^{o}C.

SPECIFIC PROCESSES FOR AIR POLLUTION CONTROL

Background

The far most dominating gaseous pollutants are NO_x and SO_2. The yearly man-made emission of sulfur species is $90 * 10^6$ tons S, out of which 70 percent stem from coal combustion. The natural emission is about $150 * 10^6$ tons S/year. Oxides of nitrogen are emitted to an amount of $500 * 10^6$ tons NO/year; about 10 percent of this is man-made.

There are probably more than 50 individual processes developed for removal of SO_2. However, 80 percent of all flue gas desulfurization (FGD) processes in operation are based on wet scrubbing using a lime/limestone slurry. These throwaway processes produce a sludge that has to be disposed of. Hence, large land areals are required to store the sludge. Other throwaway processes in operation include single and double alkali.

Regenerable processes are in general more complex and less developed than throwaway processes. They produce, sulfuric acid, SO_2 or elemental sulfur as a byproduct. However, none of these products has a great market value. The dominating regenerable processes are Magnesium Oxide, Citrate and Wellman-Lord.

Contrary to SO_2 removal, NO_x emissions may in many cases be reduced by manipulating the emitting process. However, the NO_x problem is still more difficult to solve, and the processes are in general less developed than FGD processes.

The leading process for NO_x removal is catalytic reduction with ammonia. Other dry processes to be encountered are adsorption on molecular sieve and noncatalytic reduction with ammonia.

There are many wet processes for NO_x removal in various development stages. However, many of them have been abandoned as they are too complex or expensive and/or not enough efficient.

Air pollution control processes in general can be considered as chemical factories. This is especially true for regenerable processes, in which case the pollutant is converted into a useful byproduct. However, in addition to the problems usually encountered in chemical plants, a number of circumstances aggravate the problem of implementing a process:

- There is no return on investment, except in some rare cases. It is now well established that a return on investment claimed during the early stages of development, for many flue gas clea-

ning (FGC) processes from which a byproduct can be obtained, were in serious error. It turned out that these processes have a higher annualized cost than comparable throwaway processes.

- The air pollution problem is often converted into a water pollution problem. This is also true for some regenerable processes.

- The large amounts of gas to be treated present big engineering problems, since the gas is diluted with respect to the pollutant. Also, it is often a question of a "dirty" environment with large amounts of fly ash present.

- The "chemical plant" has in many cases to be incorporated into activities related to engineering disciplines other than chemical engineering, eg. SO_2 control for utility boilers and NO_x removal at steel pickling plants.

Case Study
NO_x Removal at a Nitric Acid Plant

Background

The Swedish Environmental Protection Board (SwEPA) had alleged the need of control of NO_x at Supra's nitric acid plants at Köping. Accordingly, the SwEPA and Supra initiated a joint effort to establish an appropriate control method. The following three metods were considered for a thourough investigation: selective catalytic reduction with ammonia, adsorption on molecular sieve, and absorption in a solution of urea. Since a comprehensive experimental effort was necessitated for the latter control method, our department was requested to participate.

The plant under consideration is of low pressure type (1.7 atm) and comprises a series of 9 absorption towers. The capacity is roughly $140 * 10^3$ tons HNO_3/year, and the tail gas contains about 2800 ppm NO_x.

Experimental; Absorption of NO_x in a Urea Solution

The objective of the experimental program was to establish appropriate operating conditions for scrubbing of NO_x in a urea solution. The influence of the following parameters was considered: the gas residence time, the concentration of nitric acid in the scrubbing solution, the temperature, and the degree of oxidation (ie. NO_2/NO_x). At the time of the initiation of the study (early in 77), enough information on scrubbing with urea was not available for the conditions to be encountered at Köping.

The experiments were performed in a multi-jet absorber, with a specific mass transfer area of 120 m^{-1}. The laboratory reactor was considered appropriate , as it has well-defined properties that can be set similar to those of full scale units. It was suggested to use absorption tower number 9 for the scrubbing with urea. Accordingly, reference tests were performed in the multi-jet absorber, using a 2 percent nitric acid solution (no urea present) to scrub NO_x. The gas residence time was screened, using conditions similar to those of absorbtion in tower 9, in order to make the removal efficiency coincide for the two cases. A gas residence time of about 20 s in the multi-jet absorber was found to reflect the conditions for absorption tower 9 in the best way. Although the suggested method was considered as the only availbale one to translate the laboratory experiments, some dissimilarities were not accounted for. For instance, the higher pressure in the full scale unit (1.7 atm) would tend to make the laboratory result a little too conservative.

Experimental Result

The influence of the urea concentration was not examined experimentally, as several sources had shown absence of influence; the urea concentration was set at 1 percent by weight in all experiments.

The tail gas has an oxidation degree of about 25 percent. It would be possible to add NO_2 in order to enhance the absorption of NO_x. However, the experiments showed that such a measure will have a negative effect on the overall removal, since the added NO_2 increases the NO_x concentration.

At an oxidation degree of 25 percent, the nitric acid concentration has a large effect on the removal efficiency of NO_x. However, when the concentration is increased above 10 percent, no significant increase is obtained.

The gas residence time was shown to have a marked effect on the removal at values lower than those to be encountered in absorption tower 9. However, the effect seems to drop rapidly at higher values. Thus, the "reference level" is probably close to optimum.

The most interesting result was obtained when investigating the influence of the temperature on the removal efficiency. The dependency is displayed in Figure 3, using two different concentrations of nitric acid. As can be noted, a great enhancement in the removal can be obtained by lowering the temperature from 20 to 0 ^{o}C.

Process Chemistry

The process chemistry for absorption of NO_x in a urea solution is not clearly understood. However, it is generally accepted that nitrous acid reacts with urea according to:

$$HNO_2 + (NH_2)_2CO + HNO_3 \rightarrow N_2 + CO_2 + NH_4NO_3 + H_2O$$

$$2\,HNO_2 + (NH_2)_2CO \rightarrow 2\,N_2 + 3\,H_2O + CO_2$$

From Ringbakken et al. (16) it can be concluded that the first reaction dominates in acidic systems.

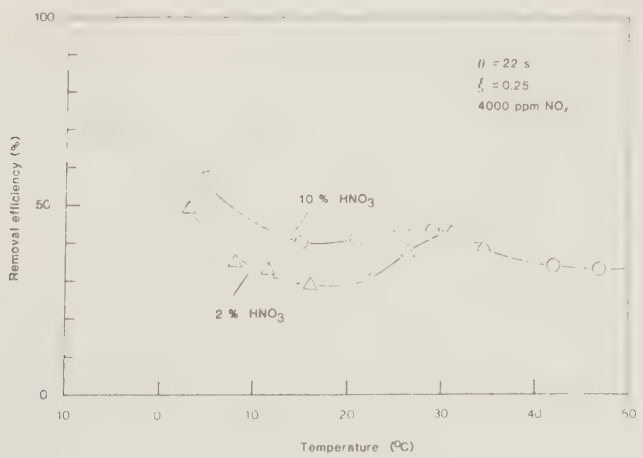

FIGURE 3. REMOVED NO_x AS A FUNCTION OF THE TEMPERATURE.

In addition, the present study has pointed out that NO reacts with urea, giving the following two overall reactions:

$$NO + 4\,HNO_3 + 3(NH_2)_2CO \rightarrow 3\,N_2 + 3\,CO_2 + 3\,NH_4NO_3 + 2\,H_2O$$

$$2\,NO_2 + (NH_2)_2CO \rightarrow N_2 + CO_2 + NH_4NO_3$$

Process Concept

A flow sheet of the suggested process is shown in Figure 4. The reactants used in absorption tower 9, ie. urea and nitric acid, are available from the product line of Supra. The bleed stream contains ammonium nitrate which, as a useful byproduct, is sent to an evaporator for recovery.

The scrubbing solution has the following composition: 0.5 - 2 percent urea, 1.5 - 5 percent nitric acid, and 10 - 15 percent ammonium nitrate. The recirculated liquor is cooled to 2 - 3 ^{o}C before it is introduced into the absorption tower in order to obtain optimal absorption.

From the experiments, the removal efficiency of NO_x was estimated to 50 - 60 percent. Since a small amount NO_x is removed in the absence of urea, the actual decrease in the emission level is only 45 percent. The figures have later been verified by Norsk Hydro.

The cost data for the process are shown in table 2. Although the process is very simple in design, it is very expensive. In light of the poor reduction of the NO_x emission, ie. from 2800 to 1500 ppm, the process was abandoned.

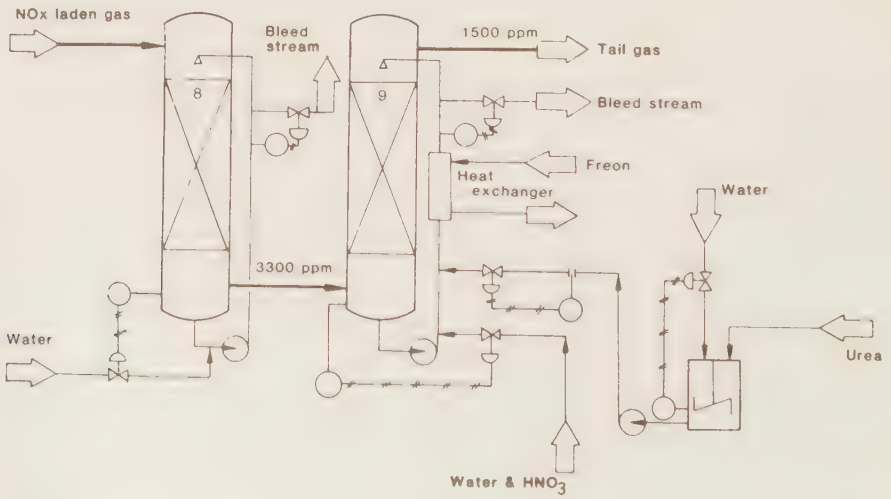

FIGURE 4. DETAILED FLOW SHEET OF THE UREA PROCESS (COURTESY SUPRA).

Discussion

The overall project has shown that selective catalytic reduction with ammonia is a superior method for reduction of NO_x at a nitric acid plant. Accordingly, a decision has been made to install such a process which is expected to be in operation within 1 or 1.5 years. Rough cost figures are given in table 3 for obtaining a 85 percent reduction in NO_x, corresponding to 500 ppm NO_x in the tail gas. When compared to the urea process, catalytic reduction is not only more efficient but also less costly.

Late in 79, Supra retrofitted a nitric acid plant in Landskrona with a catalytic reduction process. The process has since then operated smoothly to meet the standard of 500 ppm NO_x.

Case Study

Wet Scrubbing of NO_x with H_2O_2

EKA is a large Swedish producer of H_2O_2. At the time the SwEPA had taken action to abate NO_x emissions from nitric acid factories in Sweden, EKA and Supra initiated negotiations to outline the feasibility of using H_2O_2 for tail gas scrubbing.

The French Ugine Kuhlmann is one company among others that has developed a process for scrubbing of NO_x with a H_2O_2 solution. However, not enough information was available for assessing the applicability, and our department got involved in the problem.

TABLE 2. ROUGH COST DATA FOR UREA PROCESS (MID 81 FIGURES)

CAPITAL INVESTMENT		
Cooling, Process control, Dissolution	7 MSkr*	
OPERATING COST		
Urea	2.0	MSkr/Year
Nitric acid	0.3	-"-
Steam	0.8	-"-
Electricity	0.2	-"-
Personnel	0.7	-"-
Maintenance	0.4	-"-
Total	4.4	MSkr/Year
CREDIT		
Recovered byproducts	1.5	MSkr/Year
TOTAL YEARLY COST		
Depreciation (10 years/15 % interest)	1.4	MSkr/Year
Operating cost	4.4	-"-
Credit	./.1.5	-"-
Total	4.3	MSkr/Year

* 10^6 Swedish kronor

TABLE 3. ROUGH COST DATA FOR SELECTIVE CATALYTIC REDUCTION WITH AMMONIA (MID 81 FIGURES)

CAPITAL INVESTMENT		
Reactor and Construction	9 MSkr	
OPERATING COST		
Catalyst (5 years lifetime)	0.2	MSkr/Year
Ammonia	0.5	-"-
Maintenance	0.1	-"-
Total	0.8	MSkr/Year
TOTAL YEARLY COST		
Depreciation (10 years/15 % interest)	1.8	MSkr/Year
Operating cost	0.8	-"-
	2.6	MSkr/Year

The simultaneous absorption of NO and NO_2 in a H_2O_2 solution was extensively studied. Three gaseous species react with H_2O_2, ie. NO, N_2O_4 and N_2O_3, and the reaction products are water and nitric acid. The rate constant was determined for the first species, as well as the influence of the nitric acid strength on the absorption rate. The rate limiting steps for N_2O_4 and N_2O_3 were found to be the hydrolytic reactions; kinetic data were determined. Nitric acid has a slight influence on the hydrolysis of the latter species.

When considering cost data, H_2O_2 has a very limited application for the scrubbing of NO_x. The reactant is very expensive and it will add unacceptably to the operating cost. Only small units are feasible, in which case the only alternative may be a high capital investment.

The removal efficiency of NO_x in a reasonably sized scrubber is low. Hence, there are probably no, or very limited, practical applications of wet scrubbing of NO_x with H_2O_2.

The study is described in greater detail in Appendix VI.

Case Study
NO_x Removal at Steel Pickling Plants

The Swedish steel works have a large number of pickling plants for the treatment of a varity of steel products. The material is pickled in a mixture of hydrofluoric and nitric acids in order to improve the surface properties. During the process, large amounts of NO_x and HF are released. The gaseous species are withdrawn from the pickling bath and discharged into a stack. Generally, the processes have been constructed or retrofitted with wet scrubbers to remove NO_x and HF; the scrubbing liquor is water or a sodium hydroxide solution. The scrubbers have all been working poorly, which was first noticed from the coloured plumes due to large amounts of NO_x being emitted to the atmosphere. Action was taken and a committee was founded with representatives from the Swedish steel works, Jernkontoret, the SwEPA and our department. The objective of the committee work can be summarized as:

- Evaluation of existing scrubbers for the removal of NO_x and HF
- Screening and evaluation of commercial technology and potential methods for NO_x removal
- Laboratory and full scale investigations of selected methods for NO_x removal

- Evaluation of feasible options.

The work has been extended over a long period of time because of severe difficulties to cope with:

- The legislation is extremely stringent but not well-defined
- The processes are dissimilar and often operated intermittent with an emission varying from one hundred to several thousand ppm NO_x.

Five scrubber systems were selected at random to be subjected to evaluation. The removal efficiency of NO_x was measured with a chemiluminescent instrument to obtain the true status of the scrubbers. The removal efficiency was in all cases very low and actual values ranged from zero to 33 percent. The latter figure corresponds to a very favorable case where two scrubbers with 1" packing are used in series. The gas contact time is more than 20 s, and the ratio NO_2/NO_x is as high as 0.50.

When calculating the required tower height to remove a reasonable amount of NO_x, it can be inferred that there is no way to scrub NO_x with a sodium hydroxide solution. The problem is exacerbated when the amount NO dominates over NO_2, which is the usual case. For instance, when the ratio NO_2/NO_x is 0.33, which is a typical value when pickling steel, there is an upper limit of 67 percent removal considering the oxidation of NO to NO_2 to be very slow.

Of the methods available for removal of NO_x, selective catalytic reduction with ammonia and adsorption on molecular sieve were abandoned because of cost considerations. Especially since the plants in general are small, large investments can not be tolerated. In addition, the presence of HF may cause unacceptable interactions, catalytic reduction requires a considerable increase of the gas temperature, and an adsorption process requires treatment of the recovered NO_x.

Three vendors offered wet scrubbing systems; wet scrubbing in a H_2O_2 solution using a "new type of packing" catalytic oxidation of NO to NO_2 using activiated carbon with subsequent absorption of NO_2, and wet scrubbing in an alkaline $KMnO_4$ solution. The first two methods were abandoned because it is doubtful if they work. Previous findings indicate that the methods are poor, especially when a high removal efficiency is required in the low range concentration of NO_x. The third method requires a complex control system; sulfite ion has to be added to the scrubbing liquor when the ratio NO_2/NO_x diverges from 0.5. Since no demonstration

unit exists, it is hard to assess the true status. The process was precluded from further considerations because of these two deficiencies.

Two feasible methods for control of NO_x when pickling steel have prevailed as a result of the investigations. By adding urea or H_2O_2 to the pickling bath, the amount of released NO_x can be suppressed considerably. These two reactants are known to react with nitrous acid, which may be an intermediate in the complex reaction series where nitric acid reacts with a metal to generate oxides of nitrogen. The mechanisms are different for the two reactants; H_2O_2 oxidizes HNO_2 to HNO_3, which means that every mole abated NO_x is recovered in form of regenerated nitric acid. Urea, on the other hand, reduces HNO_2 to ammonia under the conditions to be encountered when pickling steel. Only part of the complex process chemistry is known, and further investigations are necessary.

The methods have been tested in the laboratory and at several full scale facilities at the steel works. Both the methods are excellent options. In general, the reduction in the NO_x emission is great at a stoichiomentric ratio of one. There are two main parameters that affect the removal efficiency at a set stoichiometric ratio. The efficiency increases when the distance from the pickled metal surface to the gas/liquid interface increases and when the concentration of NO_x decreases.

Preliminary cost data indicate the two methods to be about equal. Urea requires a higher investment cost than H_2O_2 because of a more complex method for adding the urea to the pickling bath. On the other hand, H_2O_2 is more expensive than urea, so the annualized costs for the two methods are about equal. However, the use of H_2O_2 implicates a credit for the recovered nitric acid which makes it superior. In addition, when using urea, the formation of ammonia may cause a problem.

The use of urea or H_2O_2 for NO_x reduction implies another feature. Since the operation of the existing scrubbers can be focused on the absorption of HF, actions can be taken to recover this species rather than to dispose of the scrubbing liquor. It is known that HF has a great solubility in water. Accordingly, HF can be absorbed efficiently in water. The scrubbing liquor can be recirculated to allow the HF content to build up to a level where the bleed stream can be used in the pickling process.

Case Study

NO_x Removal at a Coal-Fired Power Plant

Recently stated US Federal research goals have emphasized the need of NO_x control technologies for power plants, which are one of the principal sources of man-made NO. Since Tennessee Valley Authority (TVA) is at the same time a Federal agency and a large producer of electricity, it follows that TVA is interested in assessing and developing technologies for NO_x control. Generally speaking, two types of control technologies have been considered for NO_x; combustion modification and stack gas treatment. However, if coal-fired utility boilers are required to achieve an emission level of 100 ppm of NO_x by 1985, stack gas treatment may be the only available technology to meet this standard in the required time frame. Accordingly, TVA requested Battelle's Columbus Laboratories to conduct a study on work in the area of NO_x removal from the standpoint of developing a flue gas treatment system for a coal-fired power plant. The scope of work includes laboratory studies on selective catalytic oxidation of NO to the more readily absorbed NO_2.

Experiments were performed on a uniform engineering basis in a fixed bed reactor using 14 different catalysts. Parameters such as space velocity, temperature, and gas composition were set to reflect the conditions at a coal-fired power plant. Screening of the catalysts was started at a relatively low space velocity of 1,500 hr^{-1}. The temperature range investigated was 150 to 800 F. The composition of the simulated flue gas was chosen to reflect the conditions when burning high sulfur coal. This was done because wet scrubbing processes under development for simultaneous removal of SO_2 and NO_x require a molar ratio of SO_2 to NO_x of at least three.

The experimental results are very encouraging. A Fe_2O_3/MnO/ZnO catalyst prepared at Battelle yielded over 70 percent oxidation of NO to NO_2 in simulated flue gas at a temperature of 200 F and a space velocity of 1,500 hr^{-1}. The optimum temperature for most of the catalysts tested appears to be around 200 F. This temperature is very suitable for an add-on process since particulates can be removed in a dry collection device ahead of the catalyst bed. The flue gas can then be spray cooled to 200 F with water. After catalytic oxidation of NO to NO_2, the flue gas can be sent to a limestone scrubber for removal of SO_2 and NO_2.

The experimental results have revealed an additional problem with regard to catalytic oxidation of NO in flue gas. After about 14 hours of run time, the catalyst activity starts to decrease. No explanation has yet been found for this effect. Additional work is needed to solve the problem of catalyst deactivation as well as to find a more active catalyst. The study is described in greater detail in Appendix IX.

Assessment Study
Lime/Limestone Scrubbing of SO_2 in the U.S.

Ironically enough early efforts to control air pollution relied on the conversion from coal to oil. Today the energy situation has made coal more attractive. Parallel to the conversion back to coal, a large number of flue gas desulfurization (FGD) systems have been constructed in the U.S. and all over the world.

There are almost 100 operational FGD systems in the U.S. Of these, 80 percent are based on absorption of SO_2 in a lime/limestone slurry with subsequent disposal of the sludge. This principle constitutes the leading technology and may be regarded as commercially available if low sulfur coals are fired.

Great progress has been obtained in FGD, and scaling is now much less of a problem. The difference between lime and limestone is also smaller due to progress in process chemistry and design. The trend today is slowly turning towards utilization of limestone instead of the more expensive lime. Of the plants under construction or planned in the U.S., more than twice as many are based on limestone than on lime.

In spite of the effort, there are still severe problems to be solved. It is an exaggeration to state that the majority of the systems accomplish their purpose. Problems may be identified on two levels. On the first level, problems directly related to the ability to operate a process can be found. There is a need of characterization of full-scale systems, because there is a big gap between these and pilot-plants. Thus, more accurate data are needed for the design. There is also a need of a failure mechanism analysis, as it is not generally known what causes downtime for FGD systems. To improve the performance, better dampers, expansion joints, pumps, valves, and instruments are required. The most severe problems as to construction materials, still to be solved, is stack corrosion.

The third big problem is related to waste disposal and loop closure. The performance for closed loop operation is in general poor, especially when high sulfur coals are fired. The waste disposal problem is probably the part of the FGD technology that needs most development work.

Problems on the second level are related to process optimization. There is a large number of important problems in this category with difficult interlocking considerations. For instance, the removal efficiency involves problems such as modification of process chemistry, choice of materials of construction for reheat and stack, liquid-to-gas-ratio, number of absorbers, and reheat method. The optimal set of variables has to be identified when the standards are tightened up.

The mass transfer and engineering aspects of wet scrubbing of SO_2 are discussed more in detail in Appendices VII and VIII.

Significance to Swedish conditions

For Sweden, the most attractive FGD system at short sight, is probably limestone scrubbing, burning low sulfur coal, with forced oxidation to form a gypsum sludge. This sludge may be dewatered, stabilized with fly ash and lime, and then disposed of. Only lime/limestone scrubbing, burning low sulfur coal, and Wellman-Lord may be considered as commercial technologies. The big price difference between lime and limestone makes the former reactant less attractive. This will be aggravated at long sight since expensive fuel is needed to produce lime from limestone.

Some actions can be taken in order to eliminate usual deficiencies encountered in the operation of FGD systems:

Staff requirement

The staff should be of the right branch. It is of utmost importance that the staff is experienced in trouble shooting and in operating FGD systems.

Spare modules

If vital parts of the FGD system are duplicated they can be cleaned and maintained on a rolling schedule basis. Although it does not ensure a smooth operation at short sight, it ensures the emission standard to be met. Additionally, at long sight, it keeps the parts in good shape.

Overhaul

There is a need of a thourough overhaul of the complete FGD system every year.

Prescrubber

Chloride interacts with the scrubber chemistry and aggravates corrosion. It would be beneficial to have a prescrubber with a separate loop ahead of the SO_2 absorber. The HCl containing liquor can be neutralized and disposed of.

Reheat

When the flue gas passes through the scrubber it is cooled to its adiabatic saturation temperature. The flue gas has to be reheated sufficiently to avoid stack corrosion. Most U.S. systems are designed for 10 to 30 ^{o}C reheat. However, entrained drops and mist consume heat when evaporating and the actual reheating may not be sufficient. In Japan, the flue gas is usually reheated in the order of 30 to 80 ^{o}C.

Lime/Limestone grind

By finely grinding the lime/limestone, a great removal efficiency of SO_2 can be achieved, as well as improved load-following capability. According to Japanese experience this will suppress scaling.

Absorber design

It is generally believed that scaling can be prevented by using simple scrubbers. Accordingly, most modern scrubbers in the U.S. are constructed without internals. However, with no internals, the removal is not high, which may cause scaling in the mist eliminators. According to Japanese experience, a key factor for scale prevention is a continuous flow of slurry over all parts of the internals.

ACKNOWLEDGEMENT

This thesis contains work performed at the Department of Chemical Engineering, The Lund Institute of Technology, and at the Chemical Process Development Section, Battelle's Columbus Laboratories.

First of all I would like to express my deep gratitude to my thesis advisor, Professor Ingemar Bjerle, for his hospitableness and deep pockets.

I would also like to thank my friend and teacher Dr. Harvey S. Rosenberg at Battelle, for having uncovered the mystery of flue gas desulfurisation and for very interesting cooperation.

I appreciate the encouragement and support of Dr. Joseph H. Oxley at Battelle, and his initiation of very interesting plant visits.

Without the help of Mrs. Anna-Stina Tyréus it would not have been possible to meet the printing deadline of this thesis.

I would like to thank my friens and colleagues at the Lund Institute and at Battelle for constituting a stimulating companionship. I would especially like to thank Mr Jonas Klingspor and Mr Lars-Ingvar O. Nilsson for participating in my work.

A large number of companies have contributed to this thesis; Tennessee Valley Authority, Jernkontoret and the steel works, Supra, EKA, Flakt Industri AB, Climax Molybdenum, and Tanaka Kikinyoku Kogyo. I would especially like to mention Dr Sune Bengtsson, Flakt, Dr Bob Ference, Climax, Mr Gunnar Modig, Supra, Mr Sven-Olof Rosby, Flakt, Mr George Schuisky, Fagersta AB and chairman of the NO_x committee, and Mr Lennart Östling, EKA, for stimulating discussions.

NOTATION

A mass-transfer area, m^{-1}

C concentration, mol m^{-3}

C p/100, Pa

D diffusion coefficient, $m^2 s^{-1}$

E enhancement factor (factor by which the absorption rate is increased by reaction)

H Henry's law constant, Pa m^3 mol^{-1}

k rate constant for reaction in liquid, s^{-1}

k mass-transfer coefficient for the gas side, mol m^{-2} Pa^{-1} s^{-1}

k physical mass-transfer coefficient in the liquid, m s^{-1}

N mass-transfer rate, mol m^{-2} s^{-1}

N number of mass-transfer units (rate constant multiplied by the gas residence time at final thickness of solids)

p partial pressure, Pa

t time, s

T temperature, K

Subscripts

G gas

i general value

V interfacial area of jets per unit volume occupied by jets

XG X in the gas phase

XL X in the liquid where X is D (=N_2O_4) or i (=general value)

Superscripts

o value in absence of chemical reaction

Greek Symbols

α stoichiometric ratio

δ reaction order

η removal efficiency

θ gas residence time, s

κ rate constant

ξ degree of oxidation, ie. NO_2/NO_x

ψ parameter, defined in Appendix VI

REFERENCES

1. Danckwerts, P.V., "Gas-Liquid Reactions", McGraw-Hill, New York 1970

2. van Krevelen, D.W. and Hoftijzer, P.J., "Rec. Trav. Chem.", 67, 563 (1948)

3. Brian, P.L.T., Hurley, I.F. and Hasseltine, E.H., "AIChE Journal", 7 (2), 226 (1961)

4. Hastings, C., "Approximations for Digital Computers", Princeton University Press, Princeton 1955

5. Wilhelmsson, J.-E., Master's thesis, Dept. of Chem. Eng., Lund Inst. of Techn., 1981

6. Kays, W.M. and Bjorkland, I.S., ASME paper 56-A-71 (1956)

7. Kramers, H., Blind, M.P.P. and Snoeck, E., "Chem. Eng. Sci." 14, 115 (1961)

8. Wendel, M.M. and Pigford, R.L., "AIChE Journal", 4, 249 (1958)

9. Dekker, W.A., Snoeck, E. and Kramers, H., "Chem. Eng. Sci." 11, 61 (1959)

10. Corriveau, C.E., Master's thesis, Univ. Calif., Berkley, 1971

11. Gerstacker, "Chem. Eng. Sci." 14, 124 (1961)

12. Kameoka, Y. and Pigford, R.L., "Ind. Eng. Chem., Fundam." 16, 163-169 (1977)

13. Caudle, P.G. and Denbigh, K.G., "Trans. Faraday Soc." 47, 39 (1953)

14. Komiyama H. and Inoue, H., "Chem. Eng. Sci." 35, 154-161 (1980)

15. Rohsenow W.M. and Hartnett, J.P., "Handbook of Heat Transfer", pp 4·72 - 4·75, McGraw-Hill, New York (1973)

16. Ringbakken, R., Lie, O. and Medell, G.T., Norsk Hydro, R.C., Porsgrunn, Norway, PTE/74/22 (1974)

Shorter Communication
ON THE ENHANCEMENT FACTOR FOR INSTANTANEOUS IRREVERSIBLE GAS/LIQUID REACTIONS

By H. T. KARLSSON and I. BJERLE
Department of Chemical Engineering, Lund Institute of Technology, Sweden

An explicit expression for the enhancement factor in instantaneous irreversible gas/liquid reactions is derived for the penetration theory. The equation proposed is accurate within 5% for $E_i \geq 2$ and $10^{-2} \leq D_B/D_A \leq 10^3$.

INTRODUCTION

When a dissolved gas diffuses into a quiescent liquid and reacts instantaneously and irreversibly with a dissolved reactant, the factor by which the rate of absorption is increased by reaction (the enhancement factor) can be described by

$$E_i = 1/\mathrm{erf}(\sigma) \tag{1}$$

where σ is taken from

$$q\sqrt{r} = \frac{1-\mathrm{erf}(\sigma/\sqrt{r})}{\mathrm{erf}(\sigma)\exp[\sigma^2(1-1/r)]} \tag{2}$$

and

$$r = D_B/D_A \tag{3}$$

$$q = C_{BL}/(b\,C_{Ai}) \tag{4}$$

The relation between E_i, q and r has been obtained analytically by Danckwerts[1] and others.

Since σ cannot be derived explicitly from equation (2), E_i must be obtained graphically or through iteration. Not only the procedure itself is intricate but difficulties arise when the group $\sigma/\sqrt{r}$ is large since $\mathrm{erf}(\sigma/\sqrt{r})$ approaches unity under the condition mentioned. However, some approximations are available; for example, when q is rather large, Astarita[2] showed that equations (1) and (2) can be simplified to

$$E_i \simeq 1/\sqrt{r} + q\sqrt{r} \tag{5}$$

Brian *et al*[3] suggested another formula

$$E_i \simeq 1 + q\sqrt{r} \tag{6}$$

which is obtained for values of r that are close to unity. Pearson[4] gives a slightly more complicated approximation

$$E_i \simeq 1/\sqrt{r} + q\sqrt{r} + \frac{\pi}{6}\frac{r-1}{q\sqrt{r^3}} \tag{7}$$

that can be derived for large values of $q\sqrt{r}$ when $r > 1$, and large values of $q\sqrt{r^3}$ when $r < 1$.

The approximation commonly used is equation (5), which works satisfactorily for evaluating experimental data even when E_i is as small as 5. Some examples are absorption of carbon dioxide in monoethanolamine (Emmert *et al*[5]), of hydrogen sulphide in hydroxide solutions (Astarita *et al*[6]) and of carbon dioxide in hydroxide solutions (Nijsing *et al*[7]). In all cases described, the value of r did not diverge considerably from unity and actually r ranged from 0.5 to 2.5. This rendency of r to attain values close to unity is often the case for many absorption systems of practical importance. However, in some cases the ratio r can diverge considerably from unity. For example, in biological systems where small molecules are absorbed and react with a large species, r will be much smaller than unity and, in the case where haemoglobin takes up oxygen, r will have a magnitude of 10^{-2}. The opposite occurs when a gas with a high molecular weight is absorbed and reacts with a low-molecular weight reactant.

In this paper an explicit expression is derived from equations (1) and (2). This is valid for a range of r that covers all practical cases. The problem is limited to $E_i \geq 2$, which will reduce the difficulties considerably. In general, E_i values smaller than 2 are hardly of practical importance, except in some cases where the liquid-side reactant has a very low concentration.

AN EXPLICIT EXPRESSION

From equation (1) the largest σ value is about 0.47 when $E_i = 2$; for all E_i values larger than 2, σ will be smaller. By expanding $\mathrm{erf}(\sigma)$ in a power series it can be shown that

$$\mathrm{erf}(\sigma) \simeq (2/\sqrt{\pi})\,\sigma \tag{8}$$

is an acceptable approximation for $\sigma \leq 0.47$. A maximum deviation of about 7% occurs when $\sigma = 0.47$. The exponential factor is rewritten in the following way

$$\exp[\sigma^2(1-1/r)] \simeq f\exp(-\sigma^2/r) \tag{9}$$

where

$$f = \exp(\sigma_0{}^2) \tag{10}$$

It is assumed that σ_0 is a value that can be estimated by

0046–9858/80/020138–03 $02.00/0
© Institution of Chemical Engineers

combining equations (1), (6) and (8).

$$\sigma_0 = \frac{\sqrt{\pi}}{2(1+q\sqrt{r})} \tag{11}$$

Equation (6) has been used instead of equation (5) to avoid unrealistic estimations of σ_0 for small r values. This is based on a comparison of the result in f using both of the equations.

Let $\sigma/\sqrt{r}$ be denoted by x. Then the following expression can be obtained by inserting the approximations in (2)

$$(2/\sqrt{\pi})xqrf \simeq [1-\mathrm{erf}(x)]\exp(x^2) \tag{12}$$

When $r<1$, it is not possible to find even a fairly complicated approximation through series expansion. Therefore a class of approximations of erf, suggested by Hastings[8], is studied

$$\mathrm{erf}(x) \simeq 1-exp(-x^2)\sum_{i=1}^{n}\frac{A_i}{(1+B_i x)^n} \tag{13}$$

If erf in equation (12) is replaced by Hastings formula, the following simplification is achieved

$$(2/\sqrt{\pi})xqrf \simeq \sum_{i=1}^{n}\frac{A_i}{(1+B_i x)^n} \tag{14}$$

Hastings confined his study to $n \geq 3$, which keeps the error low, but in this investigation n is set at one giving an expression that is as simple as possible.

$$(2/\sqrt{\pi})xqrf \simeq 1/[1+(2/\sqrt{\pi})x] \tag{15}$$

By rearranging equation (15)

$$\sigma \simeq \delta[-1+\sqrt{(1+\zeta/f)}] \tag{16}$$

where

$$\delta = \sqrt{(\pi r)}/4 \tag{17}$$

and

$$\zeta = 4/qr \tag{18}$$

From a practical point of view it is better to use an approximation formula for erf in equation (1). For $E_i \geq 2$, equation (1) can be written

$$E_i \simeq \frac{\sqrt{\pi}}{2\sin\sin(\sigma)} \tag{19}$$

with very high accuracy.

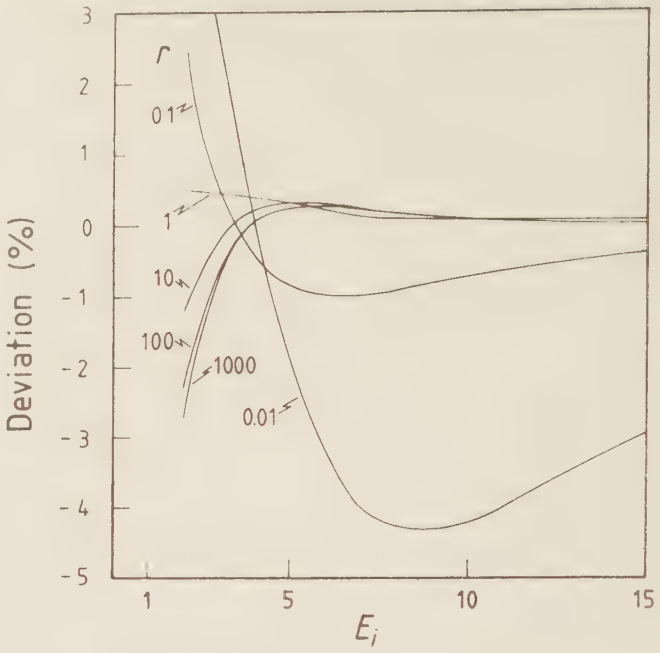

Figure 1. The deviation as a function of E_i for the approximation proposed when compared with the exact solution. For $r = 10^{-2}$ the curve goes through 5% at $E_i = 2$, which is not shown in the figure.

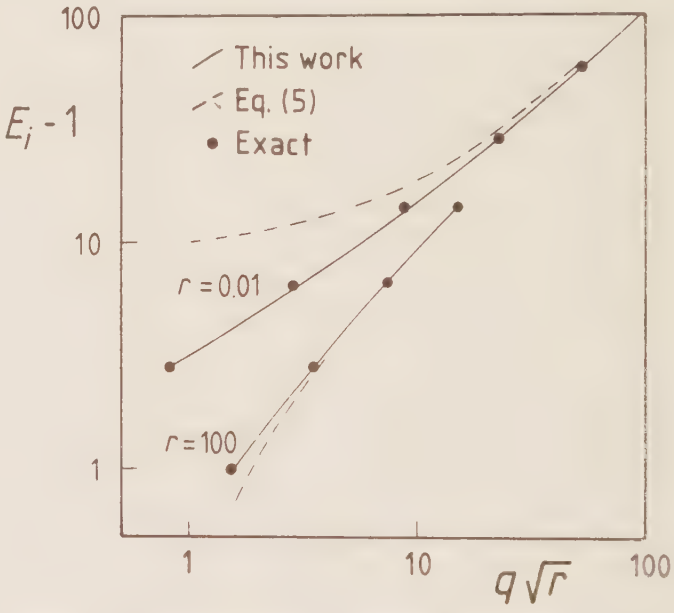

Figure 2. $E_i - 1$ as a function of $q\sqrt{r}$, for the approximation proposed, the exact solution and the approximation commonly used.

DISCUSSION

No more than 5% error in E_i was obtained when comparing equations (2) and (16), for values of r ranging from 10^{-2} to 10^3 and this range can be considered to cover all practical situations. The deviation, marked with a minus for underestimations, is shown in Figure 1.

In Figure 2, $E_i - 1$ is displayed as a function of $q\sqrt{r}$ for $r = 10^{-2}$ and $r = 10^2$, using the approximation proposed here. As can be seen, the exact solution ends up very close to these curves. For comparison, equation (5) has been included for the same values of r. It can be concluded then from the figure that when $E_i > 100$, equation (5) can be used in all practical cases and furthermore, equation (6) will be the diagonal in the diagram. Equation (7) should be used very carefully for small $q\sqrt{r}$ values, and it is not recommended under the conditions mentioned.

Application to Evaluation

In the examples previously described[5-7], equation (5) was used to evaluate constants and to verify that the reactions studied were instantaneous. This was accomplished, in principle, by plotting E_i as a function of C_{BL}, and obtaining a straight line indicated that the equation was applicable. The E_i values were estimated as the actual

mass-transfer rate divided by the mass-transfer rate in absence of a liquid-side reactant.

The combination of equations (1) and (16) can be utilized in the same way if some further simplifications are introduced. First, the factor f is assumed to be close to unity and second equation (8) is used. The following relationship can then be obtained

$$\frac{(E_i\sqrt{r})^2}{1+E_i\sqrt{r}} \simeq qr \tag{20}$$

If the left-hand side of equation (20) is plotted as a function of C_{BL}, a straight line will be the result. The error in E_i is no more than 8% for $E_i \geqslant 5$ and $10^{-2} \leqslant r \leqslant 10^3$.

CONCLUSIONS

For the penetration theory, the enhancement factor for irreversible instantaneous reactions can be estimated from

$$E_i \simeq \frac{\sqrt{\pi}}{2\sin\sin^{-1}\{\delta[-1+\sqrt{(1+\zeta f)}]\}} \tag{21}$$

where

$$\delta = \sqrt{(\pi r)}/4 \tag{17}$$

$$\zeta = 4/qr \tag{18}$$

$$f = \exp\left[\left(\frac{\sqrt{\pi}}{2(1+q\sqrt{r})}\right)^2\right] \tag{22}$$

The deviation from the exact implicit expression is no more than 5% for $E_i \geqslant 2$ and $10^{-2} \leqslant r \leqslant 10^3$.

SYMBOLS USED

A_i constant, equation (14)
B_i constant, equation (14)
b Number of moles of reactant reacting with each mole of gas
C_{Ai} Concentration of dissolved gas at the interface (mole m^{-3})
C_{BL} concentration of reactant in the bulk of liquid (mole m^{-3})
D_A diffusivity of dissolved gas ($m^2\ s^{-1}$)
D_B diffusivity of reactant ($m^2\ s^{-1}$)
E_i factor by which rate of absorption is increased by reaction
f equation (10)
n constant, equation (14)
q equation (4)
r equation (3)
x $= \sigma_i\sqrt{r}$

Greek symbols

δ equation (17)
ζ equation (18)
σ equation (2)
σ_0 approximate value for σ

REFERENCES

1. Danckwerts, P. V., 1950 *Trans Faraday Soc* 46 : 712.
2. Astarita, G., 1967, *Mass Transfer with Chemical Reaction*, p. 57 (Elsevier, Amsterdam).
3. Brain, P. L. T., Hurley, J. F. and Hasseltine, E. H., 1961, *AIChE J* 7 : 226.
4. Pearson, J. R. A., 1963, *Appl Sci Res, Sect A*, 11 : 321.
5. Emmert, R. E. and Pigford, R. L., 1962, *AIChE J* 8(2) : 171.
6. Astarita, G. and Gioia, F., 1964, *Chem Eng Sci*, 19 : 963
7. Nijsing, R. R. A. T. O., Hendriksz, R. H. and Kramer, H., 1959, *Chem Eng Sci*, 10 : 88.
8. Hastings, C., 1955, *Approximations for Digital Computers*, p. 167 (Princeton University Press, Princeton, USA).
9. Karlsson, H. T. and Bjerle, I., *Comp & Chem Eng* (in press).

ADDRESSES

Correspondence in connection with this paper should be addressed to Hans Karlsson, c/o Division of Chemical Technology, Department of Chemical Engineering, Chemical Center, Lund Institute of Technology, P.O.B. 740, S–220 07 Lund 7, Sweden.

The manuscript of this paper was received 24 July 1979 and accepted for publication 10 September 1979.

Computers and Chemical Engineering, Vol. 4, pp. 67–68
© Pergamon Press Ltd. 1980. Printed in Great Britain

A SIMPLE APPROXIMATION OF THE ERROR FUNCTION

H. T. KARLSSON* and I. BJERLE

Division of Chemical Technology, Department of Chemical Engineering, Chemical Center, Lund Institute of Technology, P.O.B. 740, S-220 07 Lund 7, Sweden

(*Received* 20 *February* 1979)

Abstract—A very simple approximation formula of the error function, with sufficient accuracy for engineering calculations, is proposed in this investigation. The presented form is compared with some of the less sophisticated approximations available in the literature. Aspects such as mnemonic form, computation time, accuracy and ease of inversion are considered.

The error function, defined as:

$$\text{erf}(x) = \frac{2}{\sqrt{(\pi)}} \int_0^x e^{-z^2} dz \qquad (1)$$

often appears in connection with chemical engineering problems. Some examples are:

- Transient diffusion and simultaneous chemical reaction in heterogenous systems (Dankwerts[1])
- Flow in pipes and packed beds (Sherwood[2])
- Chromatography and ion exchange (Sherwood[2]).

For manual calculations tabulated values can be used, and for computer calculations some approximations are available. If the calculations have to be repeated many times, they can be very time consuming. Problems also arise when the inverse has to be found.

LITERATURE DATA

Approximation of the error function is a well worked territory. For instance, Strecok[3] gives an approximation formula, containing about forty tabulated constants, resulting in an absolute error of less than 10^{-22}. The purpose of this investigation however, is to investigate some less sophisticated approximations for engineering calculations.

Hastings[4] suggested six expressions, of which the simplest are:

$$\text{erf}(x) \simeq 1 - (a_1 t + a_2 t^2 + a_3 t^3) e^{-x^2} \qquad (2)$$

where

$$t = 1/(1 + a_4 x)$$

and

$$\text{erf}(x) \simeq 1 - (1 + a_1 x + a_2 x^2 + a_3 x^3 + a_4 x^4)^{-4}. \qquad (3)$$

The absolute error is shown to be less than 2×10^{-5} and 5×10^{-4}, respectively. The inverse of erf can not be found easily in an explicit form from any of these formulae.

The approximation:

$$\text{erf}(x) \simeq 1 - 2\{1 + (a_1 + a_2 x)^{a_3}\}^{a_4} \qquad (4)$$

was obtained by Burr[5]. As can be seen, it is easy to find the inverse from this latter form.

The constants appearing in the formulae given, are shown in the table.

Table 1. The constants used in the approximate formulae adapted from the literature

EQUATION	a_1	a_2	a_3	a_4
(2)	0.3480242	-0.0958798		
(3)	0.278393			
(4)	0.196854			

PRESENT APPROXIMATION

A very simple approximation of erf is proposed in this paper. It has partly a theoretical and partly an empirical base. It reads:

$$\text{erf}(x) \simeq \begin{cases} \dfrac{2}{\sqrt{(\pi)}} \sin \sin (x) & 0 \le x \le 1 \\ \sin (x^{2/3}) & 1 \le x \le 2 \\ 1 & 2 \le x \le \infty. \end{cases} \qquad (5)$$

Equation (5) is accurate with a relative deviation of less than 0.7%. The deviation, marked with a minus for underestimations, is shown in Fig. 1 for values of x between 0 and 2. For comparison Eqs. (2)–(4) are included. The "exact" values were taken from the "Handbook of Mathematical Functions"[6]. The relative computing time, for $1 \le x \le 2$, was estimated to be 1, 2.2, 3.2 and 3.4 for Eqs. (5), (4), (3) and (2), respectively. For the range $0 \le x \le 1$, the figures are 1, 1.7, 2.4 and 2.6.

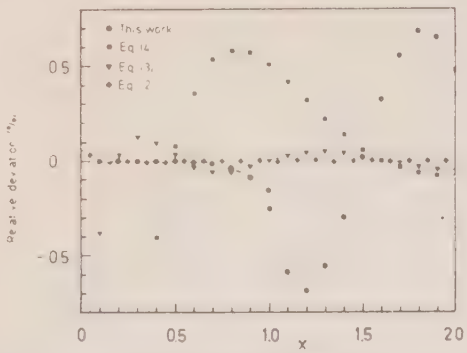

Fig. 1. The error obtained using approximative formulae for the error function. The relative deviation is defined as the percentage error in the observed Y values, compared with tabulated values.

*Author to whom correspondence should be directed.

THE INVERSE OF erf

The inverse form of Eq. (5) is:

$$\operatorname{erf}^{-1}(Y) \simeq \begin{cases} \arcsin \arcsin \left(\dfrac{Y\sqrt{(\pi)}}{2} \right) & 0 \le Y \le 0.84 \\ (\arcsin (Y))^{1.5} & 0.84 \le Y \le 0.995. \end{cases} \quad (6)$$

The deviation from the tabulated values is shown in Fig. 2. As can be seen, the deviation for erf^{-1} is much higher than for erf. At $x = 1.25$ the error reaches 2% and at $x = 2$ the error is about -10%. By adding the term $1.5(|x - 1.25|)^3 - 0.025$, in the range $1 \le x \le 2$, to the calculated x values, it is possible to obtain a deviation of less than $\pm 0.5\%$. This is shown in the figure.

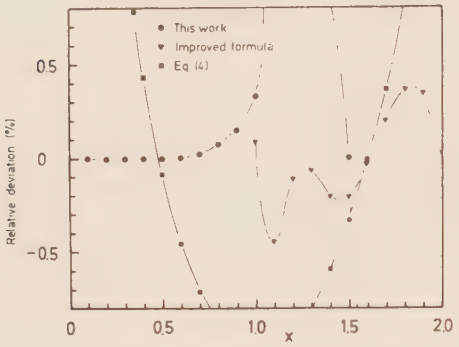

Fig. 2. The error obtained using approximate formulae for the inverse of the error function. The relative deviation is defined as the percentage error in the observed x values, compared with tabulated values.

For comparison Eq. (4) is included. The deviation decreases from $+\infty$, at $x = 0$, to -1%, at $x = 1$, and then increases to about 2%, at $x = 2$.

CONCLUSIONS

The approximation of erf, developed in this investigation, has the following properties:

- The formula is very easy to remember
- The resulting deviation is acceptable in connection with engineering calculations
- It is possible to find an explicit form of the inverse
- The deviation is rather high for the inverse at large arguments. This effect can be eliminated by introducing an empirical term as proposed
- The time consumption for calculation is low, and the usage is very simple.

REFERENCES

1. P. V. Dankwerts, *Gas-Liquid Reactions*. McGraw-Hill, New York (1970).
2. T. K. Sherwood, R. L. Pigford & C. R. Wilke, *Mass Transfer*. McGraw-Hill, New York (1975).
3. A. J. Strecok, On the calculation of the inverse of the error function. *Mathematics of Computation* **22**, 144–58 (1968).
4. C. Hastings, *Approximations for Digital Computers*, pp. 167, 185 Princeton University Press, Princeton (1955).
5. I. W. Burr, A useful approximation to the normal distribution function, with applications to simulation, *Technometrics* **9**, 647–51 (1967).
6. M. Abramowitz & I. A. Stegun, *Handbook of Mathematical Functions With Formulas, Graphs, and Mathematical Tables*, pp. 310–1 U.S. Dep. of Com., Washington (1964).

Chemical Engineering Science Vol. 35, pp. 1005–1007
Pergamon Press Ltd., 1980. Printed in Great Britain

Shorter Communications

A general explicit enhancement factor for irreversible gas–liquid reactions with gas-side resistance

(*Received* 26 *April* 1979)

Based on the classical implicit tanh-expression for the enhancement factor in gas–liquid reactions, an explicit expression was developed. The problem was treated from the view point of a second order reaction and based on the film theory. The deviation obtained is no more than 5%, if $E_i \geq 2$. It was concluded that the equation proposed is as accurate as the implicit expression, when compared to numerical solutions shown elsewhere.

In the second step, the implicit interfacial concentration was eliminated, in the case where gas-side resistance occurs. The general equation is expressed in terms of three dimensionless parameters, and has an accuracy of about 20%. Maximum deviation occurs at maximum gas-side resistance, in the middle of the transit region. However, a deviation as high as 30% can be obtained under special circumstances if $E < 3$.

Although the deviation in E is sometimes high, no more than 5% deviation in the mass-transfer rate will be the result for an arbitrary degree of gas-side resistance, if $E_i \geq 2$. This is due to the decrease of the enhancement-factor effect on the mass-transfer rate with increasing gas-side resistance.

The equation holds for a pseudo first-order and instantaneous reaction, along with the intervening transit region. Further development showed the equation to be valid for other reaction orders, and for the Higbie model.

INTRODUCTION

It is well known that the reaction rate, for many gas–liquid reactions of great practical importance, can be described with an expression of the form

$$-r_A = kC_A^m C_B^n \quad (\text{mole/m}^3\,\text{s}) \tag{1}$$

where A and B denote the gas and liquid reactants, respectively. In the case where no reaction occurs in the liquid bulk, $p_{AL} = 0$, the mass-transfer rate, for the gas and liquid side, can be described by

$$N_A = k_{AG}(p_{AG} - p_{Ai}) = Ek^0_{AL}p_{Ai}/H_A \quad (\text{mole/m}^2\,\text{s}). \tag{2}$$

No general analytical solution has been reported for the enhancement factor, E. However, an approximative expression has been adopted, both for the film and penetration theory. The equation reads, in the case of a second order reaction ($n = m = 1$)

$$E = \frac{\gamma\cdot([E_i - E]/[E_i - 1])}{\tanh\{\gamma\sqrt{([E_i - E]/[E_i - 1])}\}} \tag{3}$$

where

$$\gamma = \frac{\sqrt{(D_{AL}kC_{BL})}}{k^0_{AL}}. \tag{4}$$

For the film theory

$$E_i = 1 + \frac{D_{BL}C_{BL}H_A}{D_{AL}bp_{Ai}}. \tag{5}$$

Krevelen and Hoftizer[1] obtained eqn (3) for the film theory through a simplified method. They showed that the agreement with numerical solutions was within a few percent. However, the comparison was confined to three values, but Brian *et al.*[2] stated that the deviation from the true film theory is no more than 8%. From the result of Brian *et al.*[2], Dankwerts[3] concluded that eqn (3) can be used for the penetration theory and the Higbie model, with an error of less than 10%, if $D_{AL}/D_{BL} < 1$. In that case, E_i can be obtained, when $E_i \gg 1$, by multiplying eqn (5) by $s = \sqrt{(D_{AL}/D_{BL})}$. For further treatment of the subject, the reader is referred to the books of Astarita[4] and Dankwerts[3].

The use of the presented set of equations involves two main problems. First, eqn (3) does not allow E to be obtained explicitly. Second, in the case where gas-side resistance is involved, the concentration of A at the interface is given implicitly. Only for the limiting cases, pseudo first-order and instantaneous reactions, can these problems be simply solved. In the intervening transit region, iteration techniques are needed.

PROPOSED SIMPLIFICATION OF E

The aim of this investigation was to develop a general explicit enhancement factor that accounts for the gas-side resistance. The problem was first treated from the view point of a second order reaction, $n = m = 1$, and based on the film theory.

Liquid-side resistance

When the gas-bulk concentration is equal to the interfacial concentration, no implicit concentration appears in E. The problem therefore was reduced to finding an explicit expression for E derived from eqn (3). It was empirically found that eqn (3) can be approximated by the simple expression

$$E = \frac{(\gamma^{-3/2} + E_i^{-3/2})^{-2/3}}{\tanh(\gamma^{-3/2} + E_i^{-3/2})^{-2/3}} \tag{6}$$

where

$$E_i = 1 + f_2 \tag{7}$$

$$f_2 = \frac{D_{BL}C_{BL}H_A}{D_{AL}bp_{AG}}. \tag{8}$$

The approximation is accurate within 5%, if $E_i \geq 2$. When $E_i < 2$ and $\gamma \gg E_i$ a somewhat higher deviation will be the result. About 30% is the maximum, at $E_i = 1$ and $\gamma \gg E_i$. This situation is very seldom of practical importance. It was concluded, from the numerical solutions by Krevelen and Hoftijzer[1], that eqns (3) and (6) are approximately equally accurate. In the figure a comparison of the two expressions is displayed for three values of E_i. The values of E_i used were taken from the numerical solutions. The points shown in the figure correspond to those where Krevelen and Hoftijzer[1] obtained E numerically.

From eqn (6) the following conclusion can be drawn. When $E \geq 3$, the tanh-term can be dropped. Note, this is not the case for eqn (3). From this follows that also γ and E_i can be found explicitly.

Gas- and liquid-side resistance

By defining a dimensionless parameter as

$$f_1 = H_A k_{AG}/k^0_{AL}, \tag{9}$$

eqn (2) can be written as

$$p_{AG}/p_{Ai} = (f_1 + E)/f_1. \tag{10}$$

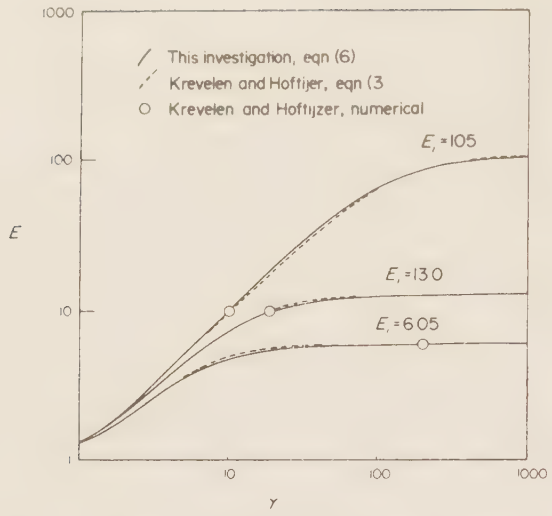

Fig. 1. The enhancement factor for the film theory, according to various solutions.

The instantaneous enhancement factor is

$$E_i = 1 + (f_1 + E)f_2/f_1. \tag{11}$$

A new dimensionless parameter can be defined

$$f_3 = f_1/f_2. \tag{12}$$

It should be noted that $f_3 \geq 1$. When the numerical value of $f_3 < 1$, physical considerations lead to $f_3 = 1$.

To obtain an explicit expression for E_i, involving f_1, f_3 and γ only, the following harmonic mean value was introduced

$$E = (1/\gamma + 1/E_i)^{-1}. \tag{13}$$

Elimination of E in eqns (11) and (13) leads to

$$E_i = \alpha + \sqrt{(\alpha^2 + \beta)} \tag{14}$$

where

$$\alpha = 0.5(1 + f_1/f_3 + \gamma/f_3 - \gamma) \tag{15}$$

$$\beta = \gamma(1 + f_1/f_3). \tag{16}$$

When used together with eqn (6), E can be obtained to an accuracy of about 20% if $E \geq 3$. The maximum deviation occurs with maximum gas-side resistance and $E_i \approx \gamma$. As the liquid-side resistance increases or E_i differs from γ, the deviation decreases. Although eqn (13) does not well describe the behaviour of E for $E < 3$, it was found that in connection with the other equations, no more than 30% deviation occurs in the predicted E, eqn (6).

The mass-transfer rate, in terms of dimensionless parameters, takes the following form

$$N_A = \eta k_{AG} p_{AG} \quad (\text{mole/m}^2\,\text{s}) \tag{17}$$

where

$$\eta = E/(f_1 + E). \tag{18}$$

It should be noted that only the deviation in the mass-transfer rate is of importance for design purposes, not the deviation in E. As can be seen from eqn (18), the influence of the enhancement factor decreases with increasing gas-side resistance. Therefore, still no more than 5% deviation occurs in the predicted mass-transfer rate, even if the deviation in E is as high as 20%.

EXTENSIONS

Reaction order

The developed formulae can be extended to 1-, nth-order reactions by defining the reaction parameter as

$$\gamma = \frac{\sqrt{(kC_{Bl}^n D_{AL})}}{k_{AL}^0}. \tag{19}$$

If the gas-side resistance is negligible, the relations can also be used for m-, nth-order reactions. The reaction parameter is then

$$\gamma = \frac{\sqrt{(kC_{BL}^n C_{Ai}^{m-1} D_{AL})}}{k_{AL}^0}. \tag{20}$$

As a simple approach, eqn (6) takes the following form

$$E = \frac{(\gamma^{-x} + E_i^{-x})^{-1/x}}{\tanh(\gamma^{-x} + E_i^{-x})^{-1/x}}. \tag{21}$$

The relationship was investigated for $0.5 \leq m \leq 4$, and the best exponent found was

$$x = 1/2 + 1/m. \tag{22}$$

Penetration theory

As earlier mentioned, eqn (3) has been adopted both for the film and penetration theory. Therefore the Higbie model is applicable if E_i is multiplied by s, in the case of no gas-side resistance. In the general case, eqns (15) and (16) are modified to

$$\alpha = 0.5(s + sf_1/f_3 + s\gamma/f_3 - \gamma) \tag{23}$$

$$\beta = s\gamma(1 + f_1/f_3) \tag{24}$$

with the restriction $f_3/s \geq 1$.

Limiting cases

The following limiting cases can be derived, with no approximations involved.

- Pseudo first-order reaction.

$$\eta = \gamma/(f_1 + \gamma) \tag{25}$$

$$1 \ll \gamma \ll E_i.$$

- Instantaneous reaction.

$$\eta = E_m/(f_1 + E_m) \tag{26}$$

$$E_i \ll \gamma.$$

For the film theory

$$E_m = (f_1 + f_3)/(f_3 - 1). \tag{27}$$

For the Higbie model

$$E_m = (f_1 + f_3)/(f_3/s - 1). \tag{28}$$

Application to evaluation

When evaluating the rate constant from experiments, second order reactions are generally treated as pseudo first-order reactions. This because the rate constant then can be obtained as the intercept in a log–log plot. However, eqn (6) allows data to be evaluated in the same way, in the transit region. When $E \geq 3$, the tanh-term in eqn (6) can be dropped, whereby

$$\left\{\left(\frac{N_A H_A}{k_{AL}^0 p_{Ai}}\right)^{-3/2} + E_i^{-3/2}\right\}^{-2/3} = \gamma. \tag{29}$$

The rate constant can simply be evaluated from this expression as described.

Division of Chemical Technology
Dept. of Chemical Engineering
Chemical Center
Lund Institute of Technology
P.O. Box 740, S-220 07 Lund 7
Sweden

H. T. KARLSSON
I. BJERLE

REFERENCES

[1] van Krevelen D. W. and Hofijzer P. J., *Rec. Trav. Chim.* 1948 **67** 563.
[2] Brian P. L. T., Hurley J. F. and Hasseltine E. H., *A.I.Ch.E.J.* 1961 **7**(2) 226.
[3] Dankwerts P. V., *Gas–Liquid Reactions*. McGraw-Hill, New York 1970.
[4] Astarita G., *Mass Transfer with Chemical Reaction*. Elsevier, Amsterdam 1967.

NOTATION

A gas reactant
b stoichiometric coefficient
B liquid reactant
C_A concentration of A in the liquid, mole/m^3
C_{Ai} concentration of A at the interface, mole/m^3
C_{AL} concentration of A in the bulk liquid, mole/m^3
C_B concentration of B, mole/m^3
C_{BL} concentration of B in the bulk liquid, mole/m^3
D_{AL} diffusion coefficient of A in the liquid, m^2/s
D_{BL} diffusion coefficient of B in the liquid, m^2/s
H_A Henry's law constant, Pa m^3/mole
k reaction rate constant, (mole/m^3)$^{1-m-n}$/s
k_{AG} mass-transfer coefficient for the gas side, mole/m^2 Pa s
k^0_{AL} physical mass-transfer coefficient in the liquid, m/s
m reaction order in A
n reaction order in B
N_A mass-transfer rate, mole/m^2 s
p_{Ai} partial pressure of A at the interface, Pa
p_{AG} partial pressure of A in the bulk gas, Pa
p_{Ai} $= H_A C_{AL}$, Pa
r_A reaction rate, mole/m^3 s
x exponent in eqn (20)

Dimensionless parameters

α eqns (15) and (23)
β eqns (16) and (24)
γ reaction parameter, eqns (4), (19) and (20)
η eqns (18), (25) and (26)
E $= k_{AL}/k^0_{AL}$, enhancement factor
E_i enhancement factor for instantaneous reaction
E_m asymptote of E with gas side resistance
f_1 eqn (9)
f_2 eqn (8)
f_3 eqn (12)
s $= \sqrt{(D_{AL}/D_{BL})}$

IV

Adsorption of Hydrochloric Acid on Solid Slaked Lime for Flue Gas Clean Up

By Hans T. Karlsson, Jonas Klingspor and Ingemar Bjerle

Department of Chemical Engineering
Lund Institute of Technology

Abstract – The reaction between hydrochloric acid and solid slaked lime was investigated by passing simulated flue gas through a fixed bed reactor. The influence of CO_2 and H_2O present in the flue gas was studied, as well as the influence of the reaction temperature in the range 423 to 673 K. The reaction was found to be of first order with respect to the two reactants. Expressions to account for the temperature and the CO_2 and H_2O concentrations were derived from the experimental data. Based on the test runs a model was developed for prediction of the removal efficiency in a process concept including injection of lime in a flue gas duct and capture of the solids, along with the fly ash, in a bag-house filter.

INTRODUCTION

Hydrochloric acid is quantitatively a modest air pollutant compared to sulfur dioxide, nitrogen oxides, and particulate matter. Nevertheless, it is indeed an undesirable species in the atmosphere due to its high solubility and corrosive nature. Emissions of HCl occur mainly from chlorination processes and incineration of refuse. The concentration in a flue gas may vary from a few hundred to several thousand ppm; refuse with a high content of PVC contributes to high concentrations of HCl. Emission regulations for HCl vary widely from one country to another. For instance, in West Germany the emission standard is 65 ppm for combustion units. Some countries may require the best technology available, or what is reasonable from an economic point of view.

A conceivable option for control of HCl is dry removal with slaked lime to form a product consisting of solid calcium chloride. When an HCl laden flue gas is contacted with slaked lime, the following reaction takes place:

$$2HCl + Ca(OH)_2 \rightarrow CaCl_2 + 2H_2O$$

The reaction can be regarded as irreversible since the equilibrium is strongly shifted to the right (1). One of the simplest designs possible for such a process may be injection of lime into the flue gas duct and a subsequent capture in a baghouse filter in which reaction with HCl takes place. This approach also provides simultaneous removal of fly ash.

The present study was undertaken to obtain kinetic data for the reaction between HCl and solid slaked lime. Experiments were performed in a small fixed bed reactor under controlled conditions and a typical flue gas was simulated by mixing gases from cylinders. Based on the test runs, a method was developed to interpret the data for the suggested process approach utilizing a baghouse filter.

EXPERIMENTAL

The lime utilized in the experiments was of Limhamn type, a technical quality with 90 percent $Ca(OH)_2$ by weight. Beside $Ca(OH)_2$, the lime contains a number of other species such as silica and magnesium compounds. It is hard to predict how much of these impurities react with HCl,

and how fast these reactions are compared with the reaction with $Ca(OH)_2$. The problem can be circumvented by assuming that the lime consists of 100 percent $Ca(OH)_2$. This leads to a slightly lower apparent conversion of lime than the actual. However, the approach is the best option from an engineering point o view, since "lumped" data are obtained which do not have to be recalculated when used for design. Table 1 summarizes the properties of the lime used.

A total of 20 experiments were performed utilizing the experimental conditions shown in table 2. Each test run lasted for 10 to 20 hours, depending on actual reaction temperature and how much information was required from the breakthrough curves.

TABLE 1. PROPERTIES OF SLAKED LIME FROM LIMHAMN

BET-surface		14.4 m^2/g
Bulk density		600 kg/m^3
Particle diameter		99.5 % < 0.2 mm 97.5 % < 0.09 mm
Constituents:	$Ca(OH)_2$	90.0 %
	$CaCO_3$	2.5 %
	$MgO/Mg(OH)_2$	1.0 %
	K_2SO_4/Na_2SO_4	0.5 %
	SiO_2 $Ca\text{-}SiO_2/Al_2O_3/Fe_2O_3$	6.0 %

TABLE 2. EXPERIMENTAL CONDITIONS

Reaction temperature	423 - 673 K
Concentration of HCl	630 ppm
Concentration of CO_2	0 - 8 %
Concentration of H_2O	0 - 10 %
Bed mass of lime	1.56 g
Superficial gas velocity	$6.40 \cdot 10^{-2}$ m/s

Apparatus

The equipment used in this study consisted of a gas manifold, a reactor and an analysis system, as shown in Figure 1. Simulated flue gas was obtained by mixing gases from cylinders in appropriate amounts using calibrated rotameters. Water was added by a pump to a thermally controlled preheater, in which the water was evaporated on ceramic beads. The bed of slaked lime was supported on a coarse glass plate in a vertical fixed bed reactor, and heated by an electrical resistance furnace. The gas was passed through the reactor from the top to react HCl with the lime and then dispersed in a cooled water absorber to remove virtually all of the HCl remaining in the flue gas.

Analysis

The concentration of HCl in the simulated flue gas was determined indirectly by measuring the conductivity of the liquid in the cooled water absorber with a probe and recording the signal on a strip chart recorder. After calibration it was possible to determine the HCl concentration from the slope of the curve obtained on the strip chart.

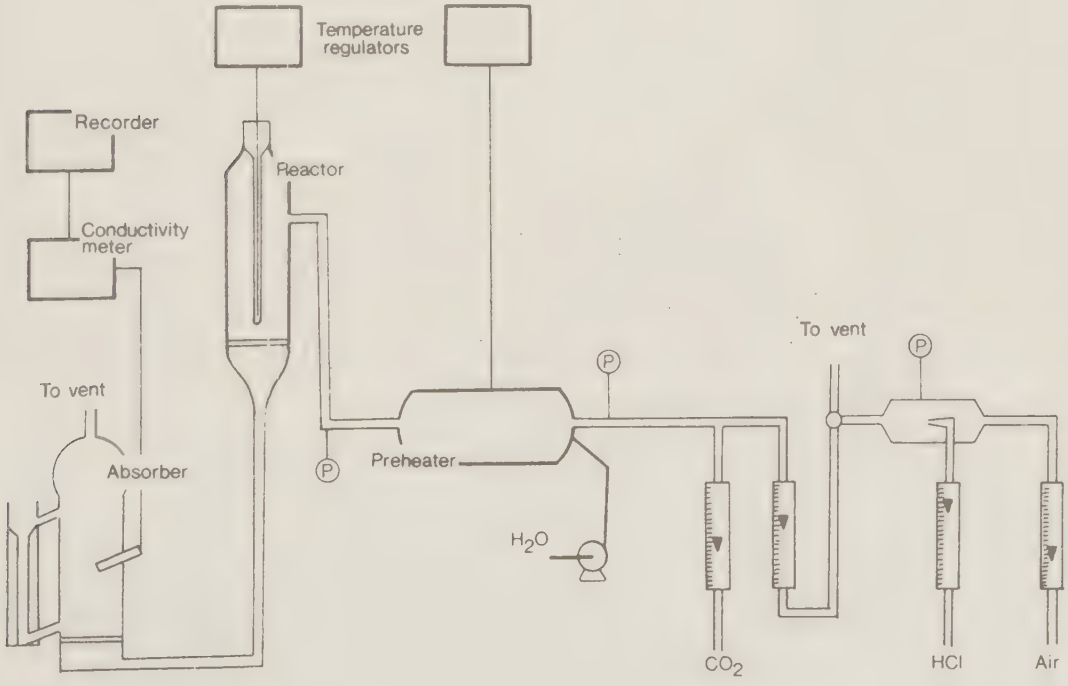

FIGURE 1. SCHEMATIC DIAGRAM OF EXPERIMENTAL APPARATUS

To verify the analysis, the amount of chloride captured in the slaked lime bed was analyzed by applying a method based on titration. The method includes dissolution of the bed in nitric acid, neutralization with sodium bicarbonate, and titration with silver nitrate solution using chromate ion as an indicator.

EXPERIMENTAL RESULTS

The first test runs exhibited a very low utilization of the lime at 1 percent breakthrough. It was suspected that the low utilization was due to a poor flow pattern caused by the extremely small lime particles which have a high tendency to become adhesive and stick together. In order to avoid the poor flow pattern, the lime was mixed with quartz sand. The lime utilization was then determined at 1 percent breakthrough as a function of the weight ratio of sand to lime (D) using the same amount of lime in all runs. H_2O and CO_2 were not added to the flue gas and the reaction temperature was set at 523 K. The result is shown in Figure 2; the asymptotic behaviour indicates that it is possible to eliminate the poor flow pattern provided that the D value is large enough. Due to practical limitations, the further test runs were performed with a D value of 20. Although this may not be the best option from a scientific point of view, it nevertheless is a feasible engineering approach.

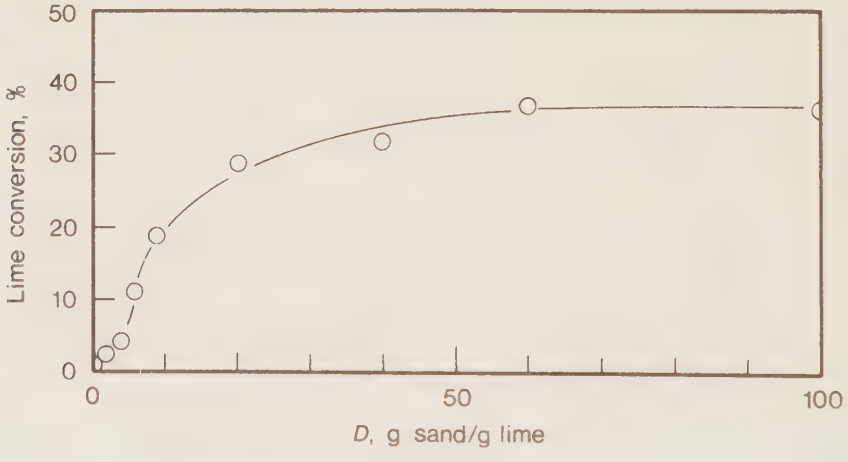

FIGURE 2. LIME CONVERSION AT 1 PERCENT BREAKTHROUGH OF HCl AS A FUNCTION OF THE DEGREE OF DILUTION OF THE LIME WITH SAND; 523 K REACTION TEMPERATURE

The conversion of lime at 1 percent breakthrough is plotted in Figure 3 as a function of temperature, with percent CO_2 and H_2O in the flue gas as parameters. The figure clearly shows the effect when CO_2 and/or H_2O are added. The reaction rate is strongly suppressed as a result of the presence of these species in the flue gas, especially at high temperatures. From the experiments it was found that the amount lime available for reaction with HCl was very close to 55 percent, independent of the composition of the flue gas. This was determined by continuing the test runs until complete penetration of HCl, that is when the reaction was complete.

EVALUATION OF THE EXPERIMENTS

Evaluation of the data was based on the conservation equation for fixed bed adsorption in the presence of a single adsorbate:

$$\varepsilon \frac{\partial C}{\partial t} + V_o \frac{\partial C}{\partial x} + \rho_B \frac{\partial q}{\partial t} = 0 \qquad (1)$$

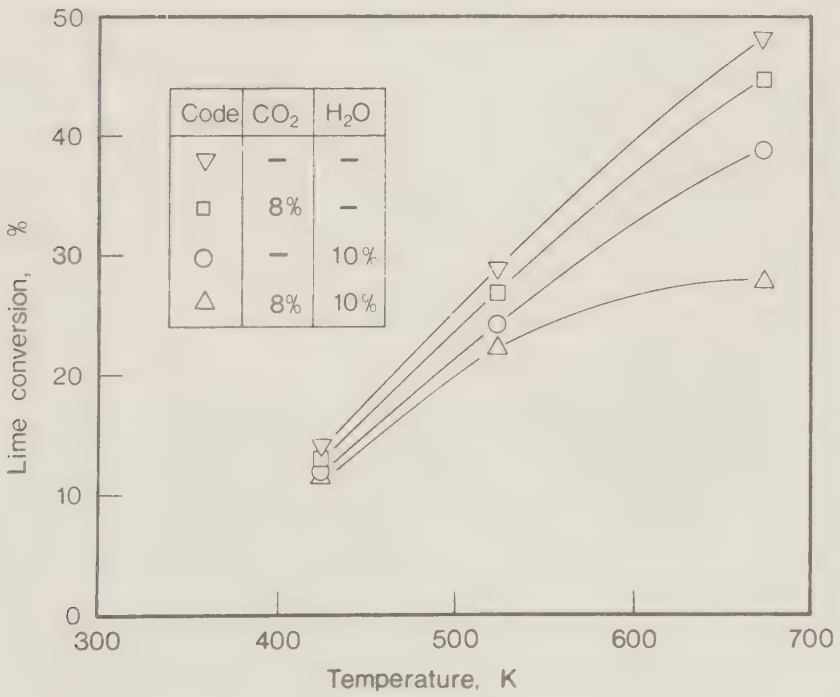

FIGURE 3. LIME CONVERSION AT 1 PERCENT BREAKTHROUGH OF HCl AS A FUNCTION OF TEMPERATURE AT DIFFERENT GAS COMPOSITIONS

The model assumes that the reaction is first order with respect to HCl and first order with respect to the number of moles of lime available for reaction per unit bed volume. For such an approach, the rate equation for the solid phase is:

$$\rho_B \frac{\partial q}{\partial t} = k\, C\left(1 - \frac{q}{q_o}\right) \qquad (2)$$

The boundary conditions are:

$$\begin{cases} x = 0 & (t > 0) \\ C = C_o \\ q = q_o \end{cases} \qquad \begin{cases} t = 0 & (x > 0) \\ C = 0 \\ q = 0 \end{cases}$$

Equation (1) and (2) can be solved by applying a constant pattern approach. The principle is based on the assumption that the width of the concentration front tends toward a constant value as the wave moves through the bed or solids. The solution has been given by Chi et al. (2), among others:

$$\ln\left(\frac{X}{1 - X}\right) = N(\tau - 1) \qquad (3)$$

where

$$N = k\theta \qquad (4)$$

Here k is the rate constant, θ is the bed volume at D = 0 divided by the actual volumetric gas flow, X is the fraction of HCl penetrated, and τ is the actual time divided by the time at which X = 0.5. Although a lumped kinetic model was used, it can be inferred by study of the experimental conditions that the system is, in fact, reaction rate limited. The small particle size of lime utilized, does not provide any external or internal diffusion resistances to mass transfer.

Data from the breakthrough curves are plotted in Figure 4 utilizing the parameters of Equation (3), in the cases where no CO_2 or H_2O were present. The plotted data indicate that the suggested model applies to the studied reaction system. Therefore, the rate constant can be evaluated as the slope, N, in Figure 4 for $D \geq 60$, divided by θ.

Temperature Dependency

The temperature dependency was determined for a D value of 20, by plotting experimental data at 423, 523, and 673 K similar to that shown in Figure 4. The N values, obtained as slopes in these plots for $X \leq 0.5$, were adjusted by multiplying by a factor to obtain the asymtotic values corresponding to proper flow pattern ($D \geq 60$). The factor was determined from Figure 4 as the ratio of the slope for D = 60 to the slope for D = 20. This approach assumes that the temperature dependency is the same for D values of 20 and 60. The reaction rate constant was then calculated at the three temperatures utilizing Equation (4), to give the results listed in Table 3. The rate constant increased too rapidly with the temperature to be fitted by an Arrhenius plot. Therefore the temperature dependency data were fitted by the following exponential equation:

$$k_o = 111 \exp\left[(T/554)^4\right] \qquad (s^{-1}) \qquad (5)$$

where T is the temperature in K; the subscript o indicates that no H_2O or CO_2 are present. Equation 5 fits the data points within half a percent.

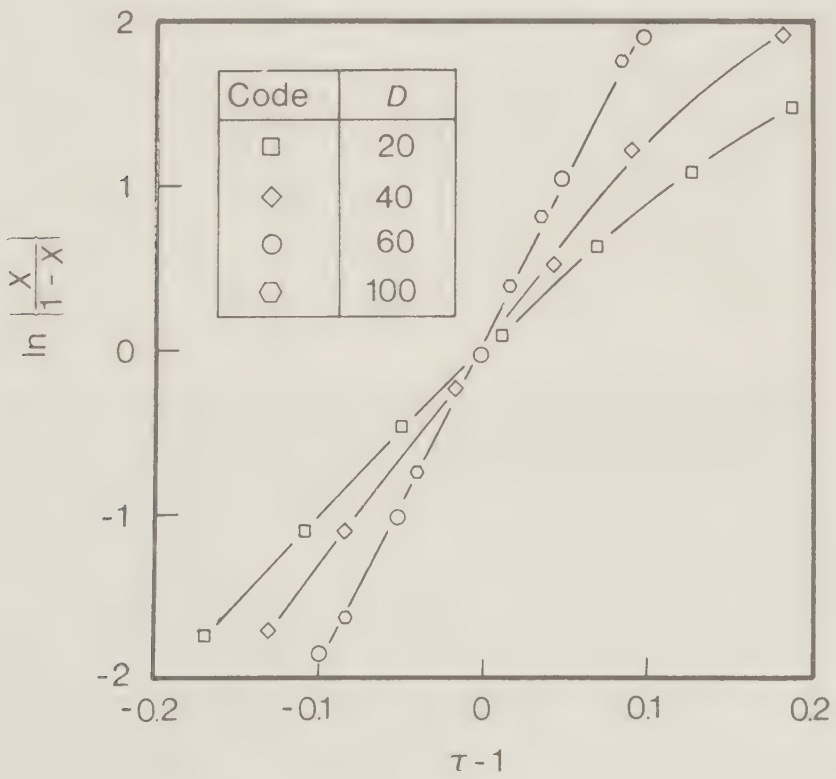

FIGURE 4. PLOT OF EQUATION (3) FOR 523 K BREAKTHROUGH CURVES IN THE ABSENCE OF CO_2 and H_2O

Influence of CO_2 and H_2O

The reduction in the reaction rate when CO_2 and/or H_2O are present in the flue gas was calculated in a way similar to that described for the temperature dependency. The parameter N from Equation (4) was determined for the test runs with CO_2 and/or H_2O at D = 20 and 523 K. The reduction in the rate (E), defined as the reaction rate in the presence of CO_2 and/or H_2O divided by the reaction rate in the absence of these species, was calculated by dividing by the N value for D = 20 in Figure 4. The same procedure was repeated at 423 and 573 K. The results are shown in Table 3. The data represent a limited number of experiments; however, the concentrations given are representative for typical flue gases. A relationship of a Langmuir type is suggested for calculation of E at other conditions:

$$E = k/k_o = (1 + \gamma_{H_2O}\, Y_{H_2O})^{-1}\ (1 + \gamma_{CO_2}\, Y_{CO_2})^{-1} \qquad (6)$$

where Y_{H_2O} and Y_{CO_2} are the mole fractions of H_2O and CO_2 present in the flue gas, respectively. The dimensionless parameter γ depends on the properties of the system. The experimental data indicated γ to have the same temperature dependency for both gases, namely:

$$\ln(\gamma_T/\gamma_{523}) = 0.014T - 7.3 \qquad (7)$$

where $(\gamma_{523})_{CO_2} = 0.95$ and $(\gamma_{523})_{H_2O} = 1.73$. The temperature is in K. Equations (6) and (7) describe the experimental values in Table 3 with an accuracy of about 5 percent. It is to be noted that Equation (6) is not a proven relationship, merely a convenient interpolation formula to calculate a factor for correcting the rate constant.

TABLE 3. TEMPERATURE DEPENDENCY OF THE RATE CONSTANT, AND REDUCTION IN REACTION RATE DUE TO THE PRESENCE OF CO_2 (8%) and H_2O (10%)

T (K)	423	523	673
$k_o(s^{-1})$	156	246	984
E_{CO_2}	0.98	0.93	0.65
E_{H_2O}	0.95	0.85	0.41
E_{CO_2,H_2O}	0.94	0.80	0.24

APPLICATION TO BAGHOUSE FILTERS

Concept and Modes of Operation

The simplest way of contacting lime with an HCl laden flue gas is by injection into the flue gas duct and subsequent capture of the solids in a baghouse filter. The method is of principal importance since minimal add on costs are posed for flue gases which require control of particulates along with the HCl. Lime and fly ash may simply be removed in the baghouse filter simultaneously.

When the lime is injected into the ductwork, reaction with HCl may occur during transport of the lime to the baghouse filter and when the solids are captured on the filter cloth. Reaction may then continue until the bags are cleaned and the solids are removed from the cloth to be collected in the fly ash bin.

There are two feasible modes of operating the process concept. The first assumes that the lime is continuously injected into the flue gas stream at a given stoichiometric ratio with respect to HCl. When the solids have been captured on the filter cloth, a homogeneous cake with continuously increasing thickness is formed. In the second mode of operation, all the lime used for a cycle is injected into the ductwork at the beginning of a cycle to precoat the filter cloth. The filter cake is then retained on the cloth for the entire cycle to remove the HCl. There is also a possibility of combining the two methods by precoating the bags with some of the sorbent and continuously injecting the remainder into the ductwork.

Reaction During Transport

The conversion of HCl during transport of lime from the injection point to the filter cloth can be estimated from the design equation for a plug flow reactor:

$$t_t = -\int_{C_o}^{C} \frac{dC}{k\,C\,(1-\frac{q}{q_o})f} \qquad (8)$$

where f is the molar concentration of lime in the flue gas divided by the molar concentration that lime would have in a packed bed and t_t is the transport time.

Assuming equimolar conditions at the injection point:

$$\frac{q}{q_o} + \frac{C}{C_o} = 1 \qquad (9)$$

which corresponds to the case in which lime is continuously injected into the ductwork. Substituting this condition into the rate equation, it is possible to integrate Equation (8). The fraction conversion of HCl then is:

$$\eta = [(kft_t)^{-1} + 1]^{-1} \qquad (10)$$

Under normal operation conditions, i.e. $f \sim 10^{-6}$ and $t_t < 5$ s, it can be shown from Equation (10) that the conversion of HCl is much less than 1 percent. A relationship similar to Equation (10) can be derived for other stoichiometric conditions; using this relationship under realistic stoichiometric conditions it can be shown that the conversion of lime is also much less than 1 percent in this case. For simplicity the conversion during transport then can be neglected when the lime is continuously injected. On the other hand, if the lime is used to precoat the filter, large amounts are injected into the ductwork during a very short time period. Although there may be a noticeable drop in the HCl concentration during the short period, the overall removal of HCl is very small; there is not enough HCl available during the short injection period to consume any substantial amount of lime. Thus, the reaction during transport can be neglected in all cases. This conclusion is helpful when deriving the overall removal efficiency of HCl, as described in the forthcoming sections.

Continuous Injection Model

The continuous injection model assumes that a filter cake that increases in thickness is formed on the cloth by lime supplied from an HCl laden flue gas passing through the cake. It is further assumed that the lime is evenly distributed on the cloth. Reaction between HCl and lime starts as soon as the lime has been added to the surface, and the reaction is terminated when the filter cloth is cleaned, i.e. all the unreacted lime is assumed to be removed at the end of each cycle. The procedure is then repeated.

The problem can be regarded as one dimensional with the origin at the surface where lime is added. The conservation equation is:

$$\varepsilon \frac{\partial C}{\partial t} + V_o \frac{\partial C}{\partial x} + \rho_B \frac{\partial q}{\partial t} = 0 \qquad (1)$$

and the rate equation for the present reaction system has been proven to be:

$$\rho_B \frac{\partial q}{\partial t} = kC\left(1 - \frac{q}{q_o}\right) \qquad (2)$$

If one cycle is studied, starting with a clean filter and ending with a cleaning procedure, then the following boundary conditions are pertinent:

$$\begin{cases} x = 0 \\ C = C_o \\ q = 0 \end{cases} \qquad \begin{cases} t = 0 \\ C = C_o \\ q = 0 \end{cases}$$

The equations can be solved by applying a constant pattern approach. It is assumed that each point on the concentration curve of HCl moves out from the cloth with the same velocity as the interface where lime is added. Then the following linear transformation can be used to convert the partial differential equations into two ordinary differential equations:

$$x = \upsilon t \qquad (11)$$

The velocity of the interface, υ, can be calculated from:

$$\frac{V_o}{\upsilon} = \frac{\Lambda}{\alpha} \qquad (12)$$

where:

$$\Lambda = \frac{q_o \rho_B}{C_o} \qquad (13)$$

and α is the stoichiometric ratio. Elimination of x in the conservation equation, and considering that $V_o/\upsilon \gg 1$, the following simplification is obtained:

$$\frac{dC}{dq} = -\alpha \frac{C_o}{q_o} \qquad (14)$$

With the use of either one of the boundary conditions, Equation (14) can be integrated to give:

$$q = q_o(1 - C/C_o)/\alpha \qquad (15)$$

Elimination of q in the rate equation leads to an ordinary differential equation of the following form:

$$\frac{dC}{dt} = - \frac{k}{\Lambda} [C(\alpha-1) + C^2/C_o] \qquad (16)$$

Separation of the variables and integrating, using the second boundary condition, lead to:

$$\frac{C}{C_o} = \frac{\alpha - 1}{\alpha \exp[k(\alpha-1)\ t/\Lambda] - 1} \qquad (17)$$

The overall removal efficiency of HCl is obtained by integrating over one cycle:

$$\eta = 1 - \frac{1}{t_f} \int_0^{t_f} \frac{C}{C_o}\, dt \qquad (18)$$

If the final thickness of the filter cake is x_f, the t_f value is obtained from Equation (11). By inserting Equation (17) in the definition of η and integrating, the following expression is obtained:

$$\boxed{\eta = \alpha - \alpha \ln \left\{ \frac{\alpha \exp[N(1-1/\alpha)] - 1}{\alpha - 1} \right\} /N} \qquad (19)$$

where

$$N = (k\ x_f/V_o) \qquad (20)$$

It should be noted that Equations (4) and (20) are both equal by definition; in both cases x_f/V_o is the bulk volume of lime charged during each cycle divided by the actual gas flow.

Equation (19) is not valid for $\alpha \equiv 1$. However, by expanding the exponential factor in a power series it can be shown that all terms of order two and higher vanish when $\alpha \to 1$. Thereby:

$$\boxed{\eta = 1 - \ln(1 + N)/N} \qquad (21)$$

Precoating Model

The precoating model assumes that all lime required for one cycle is injected instantaneously into the ductwork, with subsequent instantaneous coating of the filter cloth. It is further assumed that the filter cake is evenly distributed on the cloth and poses no tendency to channeling. The reaction starts when all the lime has been captured on the cloth and proceeds until the bags are cleaned.

The model is similar to the one used for evaluation of the kinetic data. Thus, the concentration distribution may be obtained from Equation (3):

$$\frac{C}{C_o} = \frac{1}{1 + \exp[N(1 - \tau)]} \tag{22}$$

The concentration is expressed as a function of a dimensionless time variable. The time for a cycle may in this case be obtained from (considering the definition $\tau = t/t_{\alpha=1}$):

$$\tau_f \alpha = 1 \tag{23}$$

Calculation of the removal efficiency, using Equation (18) with t replaced by τ leads to:

$$\eta = \alpha \ln \left\{ \frac{1 + \exp[N]}{1 + \exp[N(1 - 1/\alpha)]} \right\} / N \tag{24}$$

Discussion about the Models

To precoat the filter cloth is the most attractive option when considering reaction rate aspects. The presence of lime at the beginning of each cycle means that it starts with a high removal of HCl. If a set value for the overall removal efficiency is established, the pressure drop and/or lime consumption can be reduced considerably when switching from continuous injection of lime to a precoated filter. Since the pressure drop and lime consumption increase with increasing N and α values respectively, this statement can simply be verified by comparing Equations (19) and (24). This situation is illustrated in Figure 5 for $\alpha = 1.5$ and two different removal efficiencies.

On the other hand, if the pressure drop and the lime consumption have been established on acceptable levels, a considerably greater removal efficiency can be achieved if the filter is precoated. By switching from continuous injection to precoating, the removal can be increased from 95 percent to more than 99 percent.

The drawbacks, utilizing the precoat approach, are high risk of channeling, need of separate chambers to make it possible for some bags at a time to be precoated, risk to obtain an uneven distribution of the lime on the cloth and interaction with the removal of fly ash.

If the lime is continuously injected into the flue gas, it is concievable to presume that an even distribution of the lime can be obtained. If there is any tendency to channeling of the gas, the lime removed from the flue gas will effectively fill up the channels. On the other hand, channeling is more difficult to control for a precoated filter since there is no dispersed lime in the gas phase. Thus, any nonhomogeneousness in the cake of solids will remain for the entire cycle.

It may be possible to obtain an optimal strategy by precoating the bags with some of the sorbent and by continuously injecting the remainder into the ductwork. This may eliminate channeling effects and provides a higher removal than in the case of continuous injection.

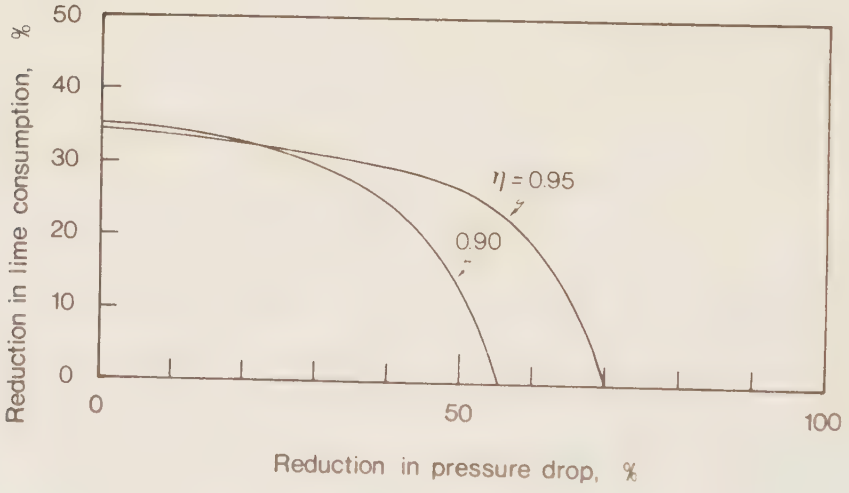

FIGURE 5. REDUCTION IN PRESSURE DROP AND/OR LIME CONSUMPTION WHEN SWITCHING FROM CONTINUOUS INJECTION TO PRECOATED BAGS AT α=1.5 AND TWO OVERALL REMOVAL EFFICIENCIES. THE PRESSURE DROP OVER THE CAKE IS ASSUMED TO OBEY $\Delta p=C_1N$ AND $\Delta p=C_1N/2$ FOR PRECOATED FILTER CLOTH AND CONTINUOUS INJECTION, RESPECTIVELY. LIME CONSUMPTION IS CALCULATED FROM α.

The models are based on the assumption that all unreacted lime is removed at the end of each cycle, i.e. when the bags are cleaned. This situation is desirable, and also possible to obtain, when treating a "clean" flue gas with no particulate matters present. However, when fly ash has to be removed along with the HCl, it is desirable to retain a homogeneous cake of solids on the cloth after each cleaning procedure. It is actually this cake that acts as a filter to separate the fly ash particles from the flue gas. Thus, only the outer part of the filter cake is removed when the bags are cleaned. It is possible to control this procedure to a large extent with the present know-how of baghouse filter technology. However, a small exchange will inevitably occur. Small amounts of unreacted lime in the removed solids will be exchanged with reacted lime in the retained cake adjacent to the cloth, due to backmixing during the short cleaning period. Although this exchange may be very small, the removal of HCl will increase considerably. From this it follows that the continuous injection model predicts conservative values for the removal efficiency. If channeling is not a problem, the same is true for the precoating model.

Remarks on Governing Parameters

The stoichiometric ratio α is defined from:

$$\frac{\alpha}{1.1} = \frac{\text{moles of lime injected}}{\text{moles of HCl in the flue gas}} \qquad (25)$$

Moles of lime injected refers to the apparent value, i.e. the number of moles of lime calculated from the mass of lime assuming that all the lime exists as $Ca(OH)_2$ with no impurities. The factor 1.1 is explained by the fact that the fraction lime available for reaction is approximateley 0.55 and that the stoichiometric coefficient is 2. This makes the definition specific to the present type of lime used. However, the definition may be modified to allow the data to be used for other lime qualities. In this case the factor 1.1 has to be adjusted proportionally to the fraction lime available for reaction, and the fraction $Ca(OH)_2$ in relation to inert solids (refers to Table 1).

The parameter N should be used at the standard state, where no fly ash or inert solids are present and the bulk density is 600 kg/m^3. This because the rate constant was determined at these conditions. From

a practical point of view, the problem can be circumvented by calculating x_f as the actual final thickness of the filter cake adjusted to the standard state.

Engineering Considerations

It is desirable to operate the process at a high temperature since the reaction rate increases with increasing temperature. However, there is an upper limit of operating temperature depending on the cloth material chosen for the baghouse. The highest temperatures can be resisted by a glass fiber based material operating at about 550 K. Teflon based filter cloths have an upper limit of about 530 K. A large combustion facility utilizing an air preheater generates a flue gas with a temperature of about 420 K, while in the absence of an air preheater the temperature may vary from 500 to 600 K.

The superficial gas velocity through the filter cloth is often referred to as the air to cloth ratio. Most practical applications use the narrow window of operation of 0.010 to 0.035 m/s. Too high a velocity will give an unacceptably high pressure drop and may adversely affect the removal of solids. For the process concept described here, it is especially important to choose a baghouse system that provides high velocity, in order to prevent lime being separated from the flue gas by gravitation rather than being captured on the filter cloth. In this context the particle size of the lime plays a very important role. This phenomenon is critical since the gas is retarded two to three orders of magnitude as it is led from the ductwork into the dust collector and through the filter cloth.

Large particles separated from the flue gas by gravitation pass through the system without being reacted with HCl. This contributes to a low utilization of lime. In general, small particles are formed during slaking of the lime. However, it is expensive to further refine the lime if this should be necessary.

Waste Disposal

The baghouse filter cake obtained from the described process concept consists of fly ash, calcium chloride and unreacted slaked lime. The latter component may correspond to more than 50 percent

of the feed of fresh lime. It was found that the product can undergo physical and/or chemical processes so that further lime can be reacted with HCl. However, the rate of these processes is very slow, especially at ambient temperatures. It should be possible to increase the lime utilization by recycling part of the filter cake with an intervening storage of lime. However, there is a limit to the amount that can be recycled because fly ash will build up in the system.

A possible way to utilize the unreacted lime is to dissolve the calcium chloride in water to obtain a concentrated calcium chloride solution; the lime and fly ash can be separated from the solution in a filter system and then be sent to a lime/limestone based SO_2 scrubber system. The fly ash will not build up in an SO_2 scrubber since a bleedoff occurs in the scrubber loop, and the presence of fly ash is acceptable in many system designs. If the concentrated calcium chloride solution can be used for melting ice and snow on roads, environmental impacts caused by the solid waste may be minimized. Also, the process cost is reduced considerably since waste disposal is expected to be very expensive.

Not only is the calcium chloride easily dissolved in water, but it is also highly hygroscopic. If the filter cake has to be disposed of, a variety of considerations have to be accounted for, depending upon geographic and legislative situations. Open dumping is expected to be precluded in all cases, due to the risk of leaching and run off to surface and ground water. There are a number of other feasible options available, such as ocean dumping, mine filling in the case in which a solulbe product has been mined, and land disposal at a line-pond.

ACKNOWLEDGEMENT

The information contained in this paper is based on a study sponsored by Flakt Industri AB, Växjö, Sweden. The authors are grateful to Flakt for supporting this work.

NOTATION

C concentration of HCl in gas, mol/m^3

C_o inlet concentration of HCl in gas, mol/m^3

D weight ratio sand to lime

E reduction in reaction rate due to the influence of CO_2 and/or H_2O

f moles lime in flue gas per unit volume divided by moles lime in a packed bed per unit bed volume

k rate constant, s^{-1}

k_o rate constant; absence of CO_2 and H_2O, s^{-1}

N number of mass transfer units, Equations (4) and (20)

q moles HCl adsorbed on (reacted with) slaked lime, mol/kg

q_o moles HCl adsorbed on (reacted with) slaked lime at completed reaction, mol/kg

t time, s

t_f cycle time, s

t_t transport time, s

T temperature, K

V_o superficial gas velocity through filter cloth, m/s

x distance, m

x_f final thickness of filter cake at standard state, m

X fraction HCl penetrated

Y volume fraction of H_2O or CO_2 in flue gas

Greek Symbols

α stoichiometric ratio, 1.1·(moles of lime/moles of HCl)

γ Equation (7)

ε void fraction in packed bed of lime

η overall removal efficiency of HCl

θ bed volume at D=0 divided by actual gas flow, s

Λ number of times HCl can be upgraded by reaction with lime, Equation (13)

υ velocity of the interface (lime/gas) where lime is added by removal from the gas phase, m/s

ρ_B bulk density of slaked lime, kg/m^3

τ actual time divided by time at X=0.5 (or α=1)

τ_f cycle time in dimensionless form, Equation (23)

LITERATURE CITED

1. Barin, I., Knacke, O. "Thermochemical Properties of Inorganic Substances", Springer, Berlin 1973.

2. Chi, C.W., Wasan, D.T. AIChEJ, 16 (1), 23, 1979.

V

Int. J. Heat Mass Transfer. Vol. 23, pp. 355–361.
Pergamon Press Ltd. 1980. Printed in Great Britain.

AN EXPERIMENTAL INVESTIGATION OF MASS TRANSFER FROM A GAS FLOW TO LIQUID JETS

H. T. KARLSSON, S. ÅBERG and I. BJERLE
Division of Chemical Technology, Department of Chemical Engineering, Chemical Center, Lund Institute of Technology, P.O.B. 740, S-220 07 Lund 7, Sweden

(*Received* 20 *November* 1978 *and in revised form* 23 *April* 1979)

Abstract – The mass-transfer factor, for flow perpendicular to varying configurations of liquid jets, has been experimentally determined. For the range $10 \leq Re \leq 200$, the following dependency was obtained $j_d = 1.13\,Re^{-0.60}$ where the usual definition of j_d has been slightly modified. At $Re = 10$ the result lies about 30% above data for heat and mass transfer to a stationary cylinder placed normal to the flow. The deviation decreases with increasing Re number and for comparison, ten expressions from the literature were adapted. The deviation was discussed in terms of the laminar film generated parallel to the jets and the wake flow generated behind each jet. Obviously, one can predict approximately mass transfer to liquid jets placed normal to the flow by using an expression for a stationary cylinder under similar conditions. The result can be improved by correcting for the effect caused by the wake flow and the parallel film, together with a geometric factor. For this purpose a semi-empirical model is suggested.

NOMENCLATURE

- a, spacing between centre of two jets in flow direction [m];
- A, mass-transfer area [m^2];
- b, spacing between centre of two jets normal to flow direction [m];
- c, specific heat of fluid [J/kg K];
- d, jet diameter, cylinder diameter [m];
- D, diffusion coefficient in fluid [m^2/s];
- f, configuration factor;
- G, gas flow [m^3/s];
- h, heat-transfer coefficient [J/K m^2 s];
- j, heat- and mass-transfer factor;
- k, thermal conductivity of fluid [J/K m s];
- k, mass-transfer coefficient [m/s];
- l, spacing between centre of a jet and wall [m];
- m, constant;
- n, constant;
- p, partial pressure of sulphur dioxide [Pa];
- t, time [s];
- U, superficial velocity [m/s].

Subscripts

- d, mass transfer;
- e, without jets;
- h, heat transfer;
- in, inflow;
- j, with jets;
- out, outflow;
- p, specific heat at constant pressure.

Superscript

- *, residence time of liquid jets.

Greek symbols

- α, increase in heat- and mass-transfer rate due to the wake flow;
- ν, kinematic viscosity of fluid [m^2/s];
- ρ, density of fluid [kg/m^3].

Dimensionless groups

- Nu, $= hd/k$, Nusselt number;
- Pr, $= c_p \nu \rho / k$, Prandtl number;
- Re, $= dU/\nu$, Reynolds number;
- Sc, $= \nu/D$, Schmidt number;
- Sh, $= k_d d/D$, Sheerwood number;
- Tr, $= d^2/t^* \nu$, residence-time number.

INTRODUCTION

AN ATTRACTIVE alternative to conventional gas cleaners is the multi-jet absorber. Among its advantages are its good mass-transfer properties, extremely low pressure drop and lack of need for any separation equipment for the two phases. No packing is needed for holding the liquid and its contact time is very short, which is sometimes good from the viewpoint of selectivity. The multi-jet absorber can also be used for laboratory investigations. The principle of a multi-jet absorber is shown in Fig. 1.

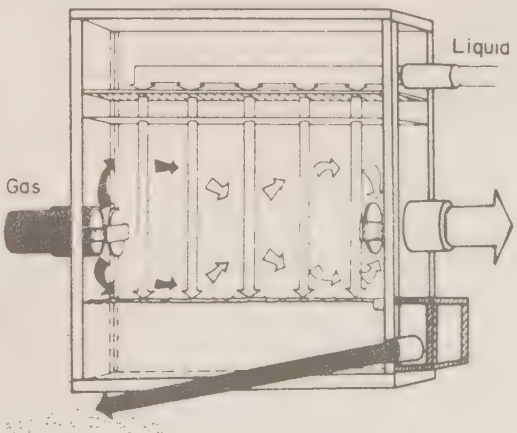

FIG. 1. The principle of a multi-jet absorber.

One of the main problems with the multi-jet absorber is to determine the mass-transfer coefficient, in the gas phase, for the liquid jets. Several important aspects are involved, such as the velocity of the perpendicular gas flow, the velocity of the liquid jets and the configuration of the jets.

Heat and mass transfer to a stationary cylinder can be shown to have similarities with mass transfer to liquid jets. In the literature it is possible to find mass- and heat-transfer factors, represented by an equation of the type

$$j = mRe^{-n} \tag{1}$$

For mass transfer, the following definition is conventional

$$j_d = \frac{Sh}{ReSc^{1/3}} \tag{2}$$

and for heat transfer

$$j_h = \frac{Nu}{RePr^{1/3}}. \tag{3}$$

In this investigation, the mass-transfer coefficient, for the gas phase, was experimentally determined for a gas flowing perpendicular to varying configurations of liquid jets. In the test runs sulphur dioxide was absorbed in a small multi-jet absorber, with sodium hydroxide as the scrubbing agent. The results were compared with data valid for flow perpendicular to a stationary cylinder. Based on this comparison, a general model for predicting mass transfer to liquid jets was proposed.

APPARATUS AND EXPERIMENTS

The absorber was 0.4 m long and 0.04 m wide, with jets about 0.08 m long. Generation of the jets was carried out with perforated steel plates. Air was passed, via a distributor, through the smallest cross-section.

The mass transfer was simulated by absorption of sulphur dioxide in a 0.2 M sodium-hydroxide solution. The air contained about 2000 vpm sulphur dioxide, and the reaction was infinitely fast at the interface, so the whole concentration distribution was located in the gas phase. The concentration in the gas was measured at the entrance to and the exit from the absorber, both in the presence and absence of jets, using a continuous IR-spectrophotometer. The mass-transfer coefficient was calculated using

$$k_d = \frac{G}{A}\left\{\ln\left(\frac{p_{in}}{p_{out}}\right)_j - \ln\left(\frac{p_{in}}{p_{out}}\right)_e\right\} \tag{4}$$

where G is the gas flow and A is the total mass-transfer area of the liquid jets. p_{in} and p_{out} are the partial pressure of sulphur dioxide in the entrance and exit flows, respectively. The subscripts j and e indicate measurements with and without jets in the absorber. Equation (4) assumes that the same amount is absorbed by the bottom surface with and without jets. This is a rather good approximation, because the contribution from the bottom surface is relatively small.

Three different kinds of jet configurations, as shown in Fig. 2, were examined. Ninety-five jets, with a diameter of 10^{-3} m, were used in all experiments. The absorber void fraction was >0.99 and the maximum velocity exceeded superficial velocity by less than 15% in the most extreme case.

The 0.08 m long jets had a mean velocity of 3 m/s, corresponding to a residence time of 0.027 s, if acceleration is taken into consideration.

The Re number ranged from 10 to 200, and was based upon the superficial velocity. At Re numbers higher than 200, a bending of the jets could be observed. At Re numbers below 10, it was difficult to analyze the gas concentration in the exit flow due to high absorption efficiency.

During the experiments the temperature was 30 ± 2°C. The diffusion coefficient for sulphur dioxide was calculated from Hirschfelder's equation to be 1.30×10^{-5} m^2/s at this temperature, corresponding to $Sc = 1.25$. Hirschfelder's equation can be found in any standard text treating the subject of diffusion. The value was checked using other equations and the same result was obtained.

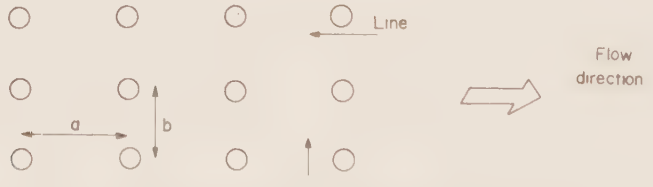

Config	a×10^3(m)	b×10^3(m)	Lines x rows	
1	35	∞	1	95
2	11.0	12 5	3	32
3	20.0	6.7	5	19

FIG. 2. The jet configurations investigated. For configuration 2, the middle line constitutes only 31 jets.

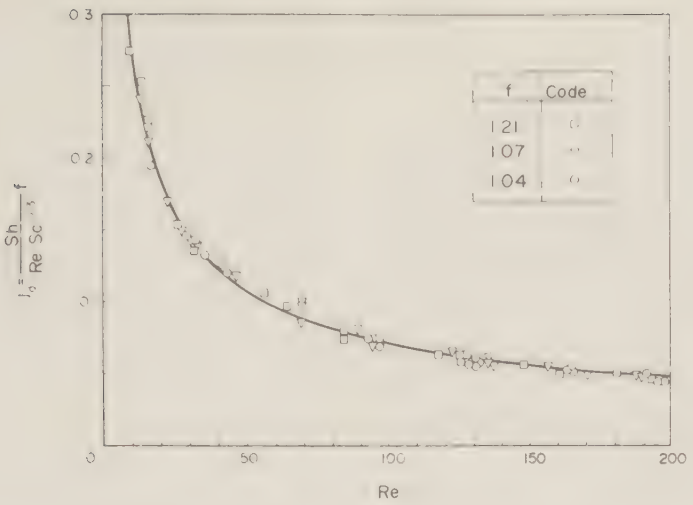

FIG. 3. A plot of the experimental data and the fitted curve. The mass-transfer factor as a function of the *Re* number.

EXPERIMENTAL RESULTS

Basic data, corresponding to 80 test runs, are plotted in Fig. 3. Some of the points in the figure are based on more than one run. By introducing a factor f, it was possible to represent data for all configurations with one relationship

$$j_d = 1.13\, Re^{-0.60} \tag{5}$$

where

$$j_d = \frac{Sh}{ReSc^{1/3}} f \tag{6}$$

and

$$f = (1 + d/a)^{3/4} \tag{7}$$

d and a are respectively the jet diameter and the spacing between the centre of two adjacent jets in the flow direction lines (see Fig. 2). The presented form of the mass-transfer factor is similar to that conventionally used for a single stationary cylinder, with the exception of the factor f. This factor is explained later on in the theoretical discussion.

LIQUID JETS COMPARED TO A SINGLE CYLINDER

In Fig. 4 equation (5) is compared with some data for heat and mass transfer adapted from the literature. The equations plotted are valid for flow perpendicular to a single tube, cylinder or wire. Furthermore, it has been assumed that heat and mass transfer are analogous, and therefore $j_d = j_h$. As can be seen, transfer to liquid jets in general is faster than to a stationary cylinder, and this effect is slightly enhanced with decreasing *Re* number. The difference observed is due to the film generated along the jets and the disturbance of the flow pattern by upstream jets which will affect

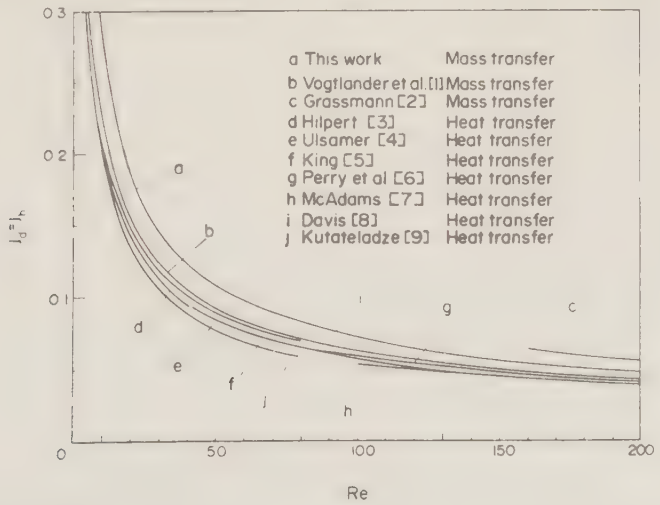

FIG. 4. A survey of heat- and mass-transfer data, for flow perpendicular to a cylinder, wire or tube. The mass-transfer factor as a function of the *Re* number.

the flow field of downstream jets. Parameters of importance for the latter phenomenon are mainly of geometric origin.

Geometric aspects

Johansson [10] investigated flow around a cylinder between two plates with $l/d = 5$, where l is the spacing between the major axis of the cylinder and the wall and d is the cylinder diameter. According to Johansson the wall effects are of no significance at $Re \geq 10$. Since $l/d \geq 6.6$ in this investigation, the influence of the walls on the flow around the jets was neglected. The same was true for adjacent lines of jets because $b/d \geq 6.6$, where b is the spacing between the centres of two jets normal to the flow direction.

When the superficial velocity was chosen as the basis for the Re number, j_d did not vary with b/d and this is in agreement with the previous discussion.

The jets placed in the same line are assumed to interact with each other in two ways. First an arbitrary jet is shadowing other jets downstream. According to Sissom *et al.* [11] it is possible, at $b/d > 1.5$, to increase the efficiency by increasing a/d. In this investigation a factor f was therefore introduced, and it was suggested that f should vary with a power of $(1 + d/a)$. According to Jakob [12] a similar factor is recommended, with the power of 1/2, for tubular heat-exchangers. In this investigation the best fit was obtained with the power 3/4, resulting in equation (7). With no shadowing it was assumed that $f \rightarrow 1$.

The second phenomenon is due to the wake flow generated behind each jet. The wake flow is assumed to prevail a certain distance after the jet, and thus affect downstream jets. It is expected that this phenomenon would be largely independent of the ratio a/d, since the wake length is much larger than a. Very little data is available for predicting this influence. However, some data have been given for heat transfer from bundles of tubes. According to Sissom *et al.*, the heat-transfer rate is increased by a factor $\alpha = 1.56$, if the bundle is 10 rows or more deep. However, it should be noted that the above mentioned α-factor is valid only for Re numbers from 500 to 20 000.

The film generated by the jets

The film generated along the jets enhances the mass-transfer rate. When there is no cross flow, this film is laminar. The phenomenon can be considered as a flow parallel to a cylinder or as a moving continuous cylinder and theories for both cases are similar. When a cross flow is introduced, a wake will be generated behind each jet, due to separation. For a smooth tube Johansson calculated the angle of separation by solving the Navier–Stokes equation. From his results the wake can be calculated to affect 22% of the whole cylinder surface at $Re = 10$ and to increase with increasing Re number. Schlichting [13] followed the same procedure by means of Blausius's series. In his case the wake affects 40% of the cylinder area, independent of the Re number. Probably small ripples on the jet surface are enough to decrease strongly the affected part.

The part corresponding to the wake therefore will give a turbulent film but this is difficult to take into account. However, with data taken from Bennet *et al.* [14] it can be shown that the mass-transfer rate for a laminar and turbulent film will have the same magnitude.

The Sh number depends on the Sc and Tr numbers, where

$$Tr = \frac{d^2}{t^* \nu} \tag{8}$$

d is the jet diameter, ν is the kinematic viscosity of the gas and t^* is the residence time of the liquid jets. The Sh number discussed here is a mean value. In Fig. 5, the group $Sh/Sc^{1/3}$ is displayed as a function of Tr according to various models. Experimental data from Bjerle *et al.* [15] have been included for comparison. The data are based on absorption of sulphur dioxide in a NaOH solution by means of a single laminar jet. Figure 5 is valid for $Sc = 1.25$, but from an investigation by Karnis *et al.* [16], it can be concluded that the group $Sh/Sc^{1/3}$ is almost independent of Sc, if common gases are utilized. Data for the models were taken from Eichhorn *et al.* [17] and Sherwood *et al.* [18] (model 1), Crank [19] (model 2), Karnis *et al.* [16]

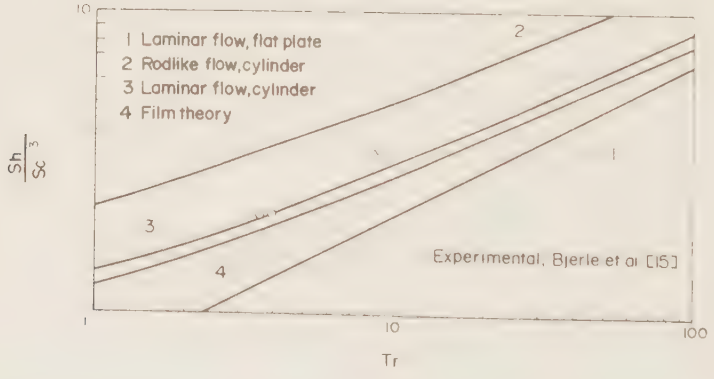

FIG. 5. The average Sh number for flow along a cylinder, or for a continuous moving cylinder, according to various models, at $Sc = 1.25$. $Sh/Sc^{1/3}$ as a function of the Tr number.

(model 3) and Sakiadis [20] (model 4).

In this investigation $Tr = 2.3$ was utilized in all test runs.

A GENERAL MODEL

The model proposed provides that the estimation of mass transfer to liquid jets can be based on a relationship valid for a stationary cylinder. In the following outline the data of Davis [8] have been chosen. The data can be described by

$$Sh/Sc^{1/3} = 0.86\, Re^{0.43} \qquad (9)$$

$$Re \leq 200.$$

Equation (9) thus describes mass transfer to a single jet, in the limiting case where the jet residence-time is infinite. In the general case equation (9) predicts a too small a value for a single jet, since the film generated by the jet enhances mass transfer, as previously mentioned.

The problem can be regarded as two perpendicular flows over a curved surface. For the hypothetical case where the surface is flat, the estimation can simply be carried out by utilizing the resultant of the Re numbers for the two flows. Since the flows over the curved surface are governed by one Re number and one Tr number, the difference in influence on mass transfer of these two numbers is not known. However, it was found from Fig. 6, that equation (9) can be used for estimation of the group $Sh/Sc^{1/3}$ for a single jet with no cross flow, by replacing the Re number with the Tr number multiplied by the constant 2.5. By applying the analogy with the flat surface, the estimation of mass transfer to a single jet with cross flow can be carried out, utilizing

$$Sh/Sc^{1/3} = 0.86\{\sqrt{[Re^2 + (2.5\, Tr)^2]}\}^{0.43}. \qquad (10)$$

A similar problem is that of a rotating cylinder with cross flow. Kays *et al.* [21] investigated this problem experimentally for three different values for the rotating Re-number. They suggested an equation analogous to equation (10). The constant corresponding to 2.5 in equation (10), was in their case obtained intuitively and not through a fit of the experimental data. However, by applying the method proposed here to the test runs by Kays *et al.*, a constant similar to that found by them intuitively was obtained.

Since equation (10) was developed for a single jet, the previous reasoning concerning the wake flow has to be taken into account, when a line of jets is considered. Comparing equations (5) and (10), for $f = 1$, an α-factor similar to that proposed by Sissom *et al.*, can be obtained. Equation (5) gave values larger by a factor ranging from 1.18 to 1.12. By utilizing a mean value, the final formula became

$$Sh/Sc^{1/3} = 0.98(Re^2 + 6.3\, Tr^2)^{0.215} f^{-1}. \qquad (11)$$

Limitations

For application to the design of a multi-jet absorber, certain limitations have to be set for preventing or minimizing the following effects;

(1) Liquid entrainment.
(2) Coalescence of the jets.
(3) Formation of drops instead of jets.
(4) Bending of the jets, due to the gas flow.
(5) High liquid recirculation ratio.

The following geometric limitations are recommended

$a/d,\ b/d \geq 3.5$
$0.5 \leq d \leq 2$ mm (suggested choice: 1 mm)
Jet length ≤ 0.15 m.

The parameters governing equation (11) should lie in the following ranges

$Re \leq 200$
$0.5 \leq Tr \leq 5$
$1 \leq f \leq 1.21$

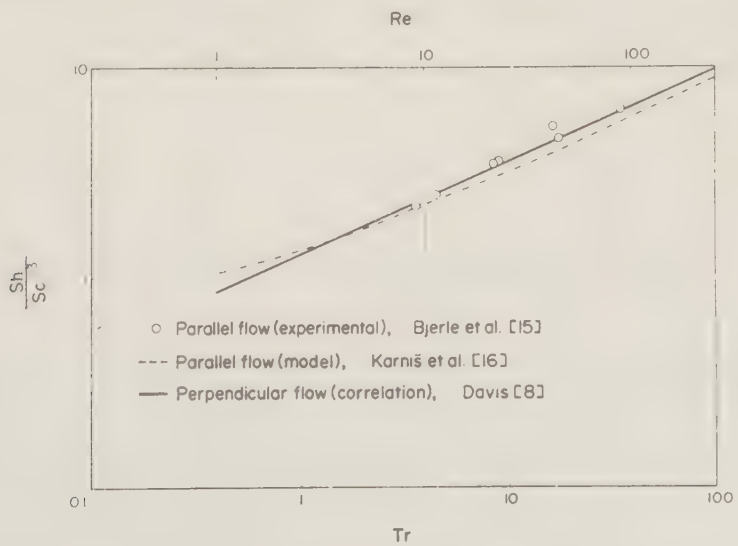

FIG. 6. $Sh/Sc^{1/3}$ as a function of the Re and Tr numbers, for flow perpendicular and parallel to a cylinder, respectively. The same equation can be used for parallel and perpendicular flow by putting $Re = 2.5\, Tr$.

Table 1. The k_dA value for various types of absorbers

TYPE OF ABSORBER	k_dA (1/s)	INVESTIGATOR
MULTI-JET ABSORBER	1 - 30	THIS WORK
PACKED TOWER	0.01 - 10	KWANTEN ET AL. [22]
PLATE TOWER	0.5 - 30	KWANTEN ET AL. [22]
SPRAY SCRUBBER	0.3 - 2	MEHTA ET AL. [23]
BUBBLE COLUMN	2 - 4	DANKWERTS [24]

The multi-jet absorber compared with commercial absorbers

In the table, the magnitude of the k_dA value for the multi-jet absorber is shown. As a comparison, data for different types of absorbers are included.

CONCLUSIONS

Mass transfer to liquid jets can be determined by the equation

$$Sh/Sc^{1/3} = 0.98(Re^2 + 6.3\,Tr^2)^{0.215} f^{-1} \quad (11)$$

Equation (11) is valid for

$$Re \leq 200 \quad f \leq 1.21 \quad b/d \geq 5$$

REFERENCES

1. P. H. Vogtländer and C. A. P. Bakker, An experimental study of mass transfer from a liquid flow to wires and gauzes, *Chem. Engng Sci.* **18,** 383–389 (1963).
2. P. Grassmann, Elektrochemiche Messung von Stoffübergangzahlen, *Chemie-Ingr-Tech.* **8**(33), 529–533 (1961).
3. R. Hilpert, Wärmeabgabe von geheizten Drähten and Rohren im Luftstrom, *Forsch. Geb. Ing Wes.* **4,** 215–224 (1933).
4. J. Ulsamer, Die Wärmeabgabe eines Drahtes oder Rohres an einen senkrecht zur Achse strömenden Gas – oder Flüssigkeitsstrom, *Forsch. Geb. Ing Wes.* **3,** 94–98 (1932).
5. W. J. King, The basic laws and data of heat transmission, *Mech. Engng* **54,** 410–414, 426 (1932).
6. R. H. Perry and C. H. Chilton, *Chemical Engineers Handbook*, 5th edn, pp. 10–13. McGraw-Hill, New York (1973).
7. W. H. McAdams, *Heat Transmission*, 3rd edn, p. 259. McGraw-Hill, New York.
8. A. H. Davis, Convective cooling of wires in streams of viscous liquids, *Phil. Mag.* **47,** 1057–1092 (1924).
9. S. S. Kutateladze, *Fundamentals of Heat Transfer*, 2nd edn, p. 247. Edward Arnold, New York (1963).
10. H. Johansson, A numerical solution of the flow around a circular cylinder between two parallel plates, Report no. 74-F-2, p. 32. Dept. of Chem. Engng, Lund Inst. of Techn. (1974).
11. L. E. Sissom and D. R. Pitts, *Elements of Transport Phenomena*, pp. 499–506. McGraw-Hill, New York (1972).
12. M. Jakob, *Heat Transfer*, Vol. 2, p. 254. John Wiley, New York (1949).
13. H. Schlichting, *Grenzschicht-Theorie*. 3rd edn, p. 145. G. Braun, Karlsruhe (1965).
14. C. O. Bennett and J. E. Myers, *Momentum, Heat, and Mass Transfer*, 2nd edn, pp. 333, 367. McGraw-Hill, New York (1974).
15. I. Bjerle, S. Bengtsson and K. Färnkvist, Absorption of SO_2 in $CaCO_3$-slurry in a laminar jet absorber, *Chem. Engng Sci.* **27,** 1853–1861 (1972).
16. J. Karnis and V. Pechoc, The thermal laminar boundary layer on a continuous cylinder, *Int. J. Heat Mass Transfer* **21,** 43–47 (1978).
17. R. Eichhorn, E. R. G. Eckert snd A. D. Anderson, An experimental study of nonuniform wall temperature on heat transfer in laminar and turbulent axisymmetric flow along a cylinder, *J. Heat Transfer* **82C,** 353 (1960).
18. T. K. Sherwood, R. L. Pigford and C. R. Wilke, *Mass Transfer*, p. 80. McGraw-Hill, New York (1975).
19. J. Crank, *The Mathematics of Diffusion*, 2nd edn, pp. 87–88. Clarendon Press, Oxford (1975).
20. B. C. Sakiadis, Boundary-layer behavior on continuous solid surfaces—III. The boundary layer on a continuous cylindrical surface, *A.I.Ch.E.Jl* **3,** 467–472 (1961).
21. W. M. Kays and I. S. Bjorklond, Heat transfer from a rotating cylinder with and without cross flow, ASME paper 56-A-71 (1956).
22. F. J. G. Kwanten and J. Huiskamp, *Gas Purification Processes for Air Pollution Controll* (edited by G. Nonhebel) 2nd edn, pp. 101–103. Newness–Butterworths, London (1972).
23. K. C. Mehta and M. M. Sharma, Mass transfer in spray columns, *Br. Chem. Engng* **15**(11), 1440–1444 (1970).
24. P. V. Dankwerts, *Gas–Liquid Reactions*, McGraw-Hill, New York (1970).

ETUDE EXPERIMENTALE DU TRANSFERT MASSIQUE ENTRE UN GAZ EN MOUVEMENT ET DES JETS LIQUIDES

Résumé — On a déterminé expérimentalement le coefficient de transfert massique pour des écoulements perpendiculaires à des jets liquides. Dans le domaine $10 < Re < 200$, on obtient la relation $j_d = 1{,}13\,Re^{-0.60}$ où la définition habituelle de j_d est légèrement modifiée. A $Re = 10$, les résultats sont de 30% supérieurs à ceux du transfert de chaleur et de masse à un cylindre fixe placé normalement à l'écoulement. L'écart décroit quand le nombre Re augmente et on adapte dix expressions antérieures. L'écart est discuté à partir du film laminaire généré et parallèle aux jets et du sillage formé derrière chaque jet. On peut prévoir approximativement le transfert massique pour des jets liquides perpendiculaires à l'écoulement, en utilisant une expression pour un cylindre fixe dans des conditions semblables. Le résultat peut être amélioré en le corrigeant des effets provoqués par le sillage et le film parallèle, à l'aide d'un facteur géométrique. On suggère un modèle semi-empirique.

EINE EXPERIMENTELLE UNTERSUCHUNG DES STOFFÜBERGANGS VON EINER GASSTRÖMUNG AN FLÜSSIGKEITSSTRAHLEN

Zusammenfassung—Stoffübergangszahlen für die Strömung normal zu unterschiedlichen Anordnungen von Flüssigkeitsstrahlen wurden experimentell untersucht. Für den Bereich $10 < Re < 200$ wurde die folgende Abhängigkeit $j_d = 1{,}13\,Re^{-0.60}$ erhalten, wobei die übliche Definition von j_d leicht modifiziert wurde. Bei $Re = 10$ liegt das Ergebnis etwa 30% über Werten für Wärme- und Stoffübergang an einem ruhenden Zylinder, der normal zur Strömung angeordnet ist. Die Abweichung nimmt mit zunehmender *Re*-Zahl ab, und zum Vergleich wurden 10 Beziehungen aus der Literatur herangezogen. Die Abweichung wurde hinsichtlich des parallel zu den Strahlen erzeugten laminaren Films und der hinter jedem Strahl erzeugten Nachlaufströmung diskutiert. Offensichtlich kann man näherungsweise den Dtoffübergang an Flüssigkeitsstrahlen vorhersagen, die normal zur Strömung angeordnet sind, indem man einen Ausdruck für stationäre Zylinder unter ähnlichen Bedingungen verwendet. Das Ergebnis kann verbessert werden durch Korrektur für den Einfluß der Nachlaufströmung und des parallelen Films sowie durch einen geometrischen Faktor. Zu diesem Zweck wird ein halb-empirisches Modell vorgeschlagen.

ЭКСПЕРИМЕНТАЛЬНОЕ ИССЛЕДОВАНИЕ МАССОПЕРЕНОСА ОТ ПОТОКА ГАЗА К СТРУЯМ ЖИДКОСТИ

Аннотация — Экспериментально определен коэффициент массопереноса для потока газа, направленного перпендикулярно струям жидкости переменной конфигурации. Для диапазона значений числа Рейнольдса $10 \leq Re \leq 200$ получена следующая зависимость $j_d = 1{,}13\,Re^{-0.60}$ где общепринятое определение j_d несколько модифицировано. При $Re = 10$ получаемый результат на 30% выше данных для неподвижного цилиндра, расположенного перпендикулярно направлению потока. С увеличением числа *Re* это расхождение уменьшается. Для сравнения использованы десять зависимостей, взятых из опубликованных источников. Расхождение в значениях объясняется наличием ламинарной пленки, образующейся параллельно струям, и следным течением, индуцированным каждой струей. Перенос массы к струям жидкости, направленным перпендикулярно потоку, вероятно, можно приближенно рассчитать с помощью выражения для неподвижного цилиндра в аналогичных условиях. Более точный результат можно получить за счёт введения поправки на влияние течения в следе и в параллельной пленке, а также введения геометрического фактора. Для этой цели предложена полуэмпирическая модель.

VI

Absorption of NO and NO_2 in a H_2O_2 Solution Using a Multi-Jet Absorber

By Hans T. Karlsson and Ingemar Bjerle

Department of Chemical Engineering
Lund Institute of Technology

Abstract – A new type of laboratory reactor - the multi-jet absorber - for investigation of gas-liquid reactions has been demonstrated. The absorber was used to determine the kinetics for absorption of nitrogen tetroxide into water, and the evaluated data were shown to agree well with data from 8 investigations presented in the literature.

The reactor has well-defined mass transfer properties and is suitable for the evaluation of reaction mechanisms and kinetic data. A straightforward integral method was developed for evaluation of the rate constant and the reaction order from a straight-line plot. The multi-jet absorber has also properties similar to full scale absorbers which makes it suitable for direct scale up.

The simultaneous absorption of NO and NO_2 in a H_2O_2 solution was extensively studied. Three gaseous species react with H_2O_2, ie. NO, N_2O_4 and N_2O_3, and the reaction products are water and nitric acid. The rate constant was determined for the first species, as well as the influence of the nitric acid strength on the absorption rate. The rate limiting steps for N_2O_4 and N_2O_3 were found to be the hydrolytic reactions; kinetic data were determined. Nitric acid has a slight influence on the hydrolysis of the latter species.

When considering cost data, H_2O_2 has a very limited application for scrubbing of NO_x. The reactant is very expensive and it will add unacceptably to the operating cost. Only small units are feasible, in which case the only alternative may be a high capital investment.

The removal efficiency of NO_x in a reasonably sized scrubber is low. Hence, there are probably no, or very limited, practical applications of wet scrubbing of NO_x with H_2O_2.

TABLE OF CONTENTS

	Page
INTRODUCTION	1
OBJECTIVE AND SCOPE	1
APPARATUS	1
General	1
Description of the Multi-Jet Absorber	2
Experimental Set-Up	2
Mass Transfer Properties of the Multi-Jet Absorber	4
Liquid Side	4
Gas Side	4
Interfacial Area	5
Mass Transfer Tests; Absorption of NO_2 in Water	5
Theory	5
Experimental	8
ABSORPTION OF NO_2 IN A H_2O_2 SOLUTION	9
Theory	9
Experimental	13
ABSORPTION OF NO IN H_2O_2 SOLUTION	15
Theory	15
Experimental	16
SIMULTANEOUS ABSORPTION OF NO AND NO_2	18
Theory	18
Experimental	20
Extension of the Mathematical Treatment	22
INFLUENCE OF NITRIC ACID ON ABSORPTION OF NO_x IN A H_2O_2 SOLUTION	22
Background	22
Experimental	23
Absorption of NO	23
Absorption of NO_2	24
Simultaneous Absorption of NO and NO_2	25
ENGINEERING ANALYSIS	27
Economy	27
CONCLUSIONS	28
NOTATION	29
ACKNOWLEDGEMENT	31
REFERENCES	31
APPENDIX	

INTRODUCTION

The use of wet scrubbing for control of NO_x is in general limited by the inert nature of the gaseous species represented by NO_x. Especially when NO_x consists of mainly NO, the problem is exacerbated. There is a limited number of liquid reactants available for the scrubbing of NO. A feasible option is H_2O_2. This reactant has desirable properties since the main products when reacting NO_x with H_2O_2 are water and nitric acid. The product solution can be recovered as a useful byproduct; the application has potential use in the scrubbing of nitric acid tail gas.

OBJECTIVE AND SCOPE

The objective of the present study was to experimentally investigate wet scrubbing of NO_x (NO and NO_2) utilizing a solution of H_2O_2. The investigation was focused on the low range concentration of NO_x. Experiments were performed in a laboratory absorber to establish the reaction mechanism and to obtain kinetic data. The information was used in an engineering analysis of feasible applications of NO_x control.

APPARATUS

General

The absorption experiments were performed in a multi-jet absorber, which is a new type of laboratory reactor. The principle, as shown in Figure 1, is based on the features of the well-known laminar jet absorber, i.e. well-defined mass transfer properties. However, a large number of jets is utilized rather than a single one. Such an approach offers a design where the gas is contacted with the liquid in a plug flow pattern. Thus, parameters as mass transfer interfacial area and gas residence time can be set at values similar to those of full scale absorbers. This feature provides direct scale-up, which is of importance when complex reaction systems are studied, in which case the kinetic data are hard to evaluate.

Shah (1) pointed out that two different types of laboratory absorbers exist. The first type has well-defined mass transfer properties and is suitable for the evaluation of reaction mechanisms and of kinetic

data. The second type has properties similar to full scale absorbers and is suitable for direct scale-up. The multi-jet absorber was constructed in order to combine these two properties. If experiments are performed in the multi-jet absorber, useful information is obtained even if the reaction mechanism is too complex to outline.

Description of the Multi-Jet Absorber

The absorber was 0.4 m long and 0.04 m wide, with jets 0.14 m long. Generation of the jets was carried out with a perforated steel plate, and gas was passed through the reactor in a cross-flow pattern.

A total of 497 jets, with a diameter of 10^{-3} m, were used in all experiments. The corresponding absorber void fraction was 0.97.

The jets had a mean velocity of about 1.4 m/s, corresponding to a residence time of 0.1 s if acceleration is taken into consideration. The gas velocity ranged from 0.014 to 0.070 m/s.

Experimental Set-Up

The whole experimental set-up is displayed in Figure 2. Simulated tail gas was obtained by mixing gases from cylinders. The nitrogen cylinder valve was adjusted to obtain the desired gas residence time in the absorber, and the NO and/or NO_2 valves were adjusted to obtain the set readings of the NO and NO_2 analyzers at the inlet of the reactor. No oxygen was present in the gas to prevent NO from being oxidized to NO_2 in

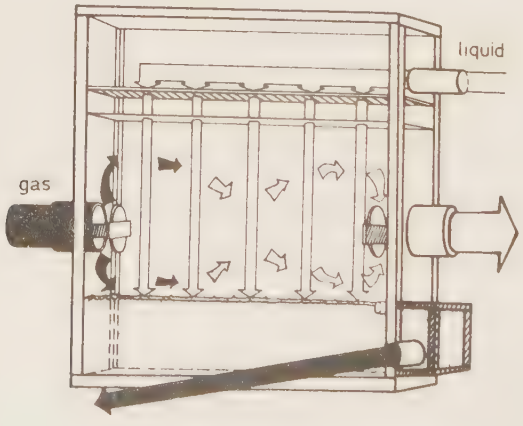

FIGURE 1. THE PRINCIPLE OF A MULTI-JET ABSORBER

the gas phase. Gas samples were continuously withdrawn from the outlet or inlet of the reactor for analyses of NO and NO_2. The analyzers were a Uras 2T® for IR detection of NO and a Limas® for UV detection of NO_2. The instruments were calibrated using a standard gas containing 5000 ± 250 ppm NO_x in nitrogen; the NO_2 amounted to 61 mole percent of the oxides of nitrogen. The nonlinearity of the instruments was taken into consideration by mixing standard gas with nitrogen by means of a Wösthoff M10® gas mixing pump in the following proportions: 10/0, 9/1, 8/2, . . . 1/9, and 0/10.

A system of two liquid tanks was used to supply scrubbing liquor to the absorber. The lower (40 l) main storage tank was equipped with a heat exchanger to obtain isothermal conditions. A large amount of liquid was pumped to a tank placed 1.5 m above the absorber and the overflow was returned to the lower tank. A small stream was taken from the upper tank, via a valve and a rotameter, to the absorber. The effluent from the absorber was dumped into the 40-liter tank. By this design it was possible to control the liquid flow rate very accurately.

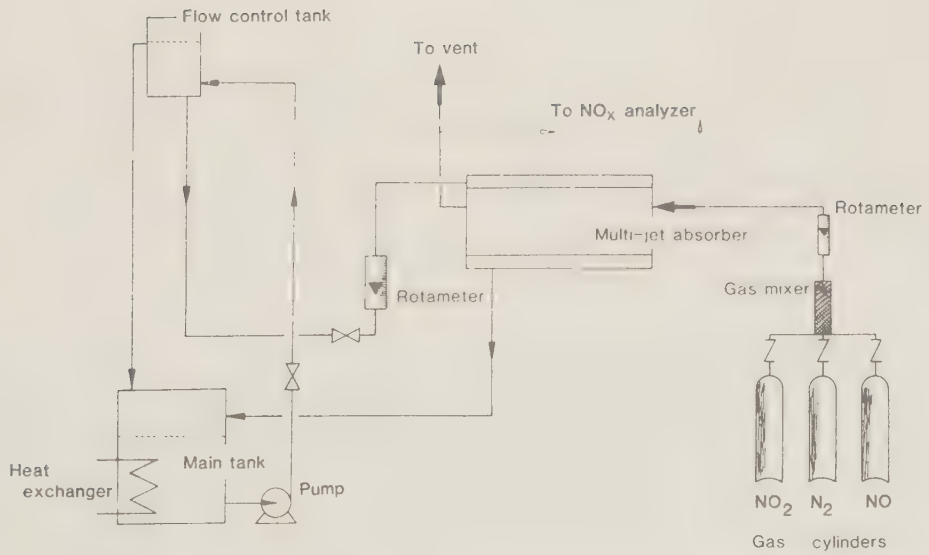

FIGURE 2. SCHEMATIC OF THE APPARATUS

Mass Transfer Properties of the Multi-Jet Absorber

Liquid Side

The liquid side mass transfer coefficient without chemical reaction may be estimated from the penetration theory. It is assumed that the liquid jets constitute a quiescent phase with ideal geometry. Then the following expression is valid:

$$k^{o}_{iL} = \sqrt{\frac{4D_{iL}}{\pi t^{*}}} \qquad (1)$$

where t^{*} is the residence time of the liquid jets and D_{iL} is the diffusion coefficient for the absorbed species (i).

Gas Side

The mass transfer coefficient in the gas phase is more complex, since both the motion of the jets and the perpendicular gas flow generate boundary layers. The problem has previously been discussed (2), and the following relationship is recommended in that study:

$$Sh/Sc^{1/3} = 0.98\ [Re^{2} + 6.3\,Tr^{2}]^{0.215}\ f^{-1} \qquad (2)$$

where

$$f = (1 + d/a)^{3/4} \qquad (3)$$

and Sh, Sc, and Re are the Sherwood, Schmidt and Reynolds number, respectively. The dimensionless group Tr depends on the diameter of the jets and the residence time of the jets. Equation (2) has the following limitations:

$$Re \leq 200 \qquad f \leq 1.21 \qquad b/d \geq 5$$

where d and b are respectively, the jet diameter and the spacing between the center of two jets normal to the flow direction. The configuration factor depends on the ratio of the jet diameter and the spacing between the center of two jets in the flow direction.

Interfacial Area

The interfacial mass transfer area of the jets is 112 m^2/m^3 when using the present configuration and diameter of the jets. In addition, the liquid in the bottom of the absorber contributes with a 7 percent increase, giving a total of 120 m^2/m^3. However, the mass transfer properties of the lquid in the bottom of the absorber is dissimilar to the mass transfer properties of the jets. Only in the limiting case in which the gas phase resistance is negligible and the reaction is of m:th-order type, the two interfacial areas can be added without introducing any error. This is the case for many reaction systems and in the general case, the error is not great since the bottom surface only contributes with 7 percent.

Mass Transfer Tests; Absorption of NO_2 in Water

In order to outline the applicability of the multi-jet absorber in evaluating kinetic data for gas-liquid reactions, some absorption experiments were performed. The reaction of NO_2 with water was considered appropriate since this system has been thoroughly outlined in the literature.

Theory

Absorption of NO_2 in water can be represented by the following set of formulae:

$$2\,NO_2 \rightleftarrows N_2O_4 \qquad (a)$$

$$N_2O_4 + H_2O \rightarrow HNO_3 + HNO_2 \qquad (b)$$

$$3\,HNO_2 \rightarrow HNO_3 + H_2O + 2\,NO \qquad (c)$$

Reaction (a) is instantaneous and occurs in the gas phase. Thus, the relationship between NO_2, denoted by A, and N_2O_4, denoted by D, is given by:

$$K_I = \frac{P_{DG}}{P_{AG}^2} \qquad (4)$$

After physical dissolution, N_2O_4 reacts with water according to a pseudo-first order reaction (b). In accordance with the penetration theory, the absorption rate of NO_2 is given by:

$$N_A = 2\,N_D = 2\sqrt{k_D\,D_{DL}}\;p_{DG}/H_D \qquad (5)$$

Evaluation of data from the multi-jet absorber can be performed by adopting a plug flow reactor model:

$$-\frac{d\,p^*_{AG}}{dt} = N_A\,A_V\,R\,T_G \qquad (6)$$

where

$$p^*_{AG} = p_{AG} + 2\,p_{DG} \qquad (7)$$

Combination of Equations (4) through (7) leads to:

$$-\frac{d\,p_{AG}}{dt} = 2\sqrt{k_D\,D_{DL}}\;K_I\,A_V\,R\,T_G\,H_D^{-1}\,\frac{p_{AG}^2}{(1 + 4\,K_I\,p_{AG})} \qquad (8)$$

with the following boundary condition:

$$\begin{cases} t = 0 \\ p_{AG} = (p_{AG})_o \end{cases}$$

The variables of Equation (8) can be separated and the integrated result is:

$$\frac{p_{AG}^{-1} - (p_{AG})_o^{-1} + 4\,K_I \ln\left[(p_{AG})_o/p_{AG}\right]}{2\,K_I\,A_V\,R\,T_G} = H_D^{-1}\sqrt{k_D\,D_{DL}}\;\theta \qquad (9)$$

The partial pressure of NO_2 appearing in Equation (9) corresponds to the reactor outlet value, where the gas contact time is equal θ.

Data for the present reaction system are often presented in form of the parameter $H_D^{-1}\sqrt{(k_D\,D_{DL})}$, which can be obtained from Equation (9) by plotting the left hand side as a function of the gas residence time (θ).

Equation (9) is valid only under certain assumptions. Firstly the penetration theory is pertinent since liquid jets are applied. Equation (9) assumes that $k\,t^* >> 1$ for the penetration theory. Most studies have revealed the rate constant to be at least 250 s^{-1} at 20 ^oC. Since

the present value of t* is about 0.1 s, the condition given above can be considered to be fulfilled. Secondly, if NO is formed by decomposition according to reaction (c), and transported back to the gas phase, the absorption of NO_2 is enhanced by formation of N_2O_3. This can be inferred because N_2O_3 is in turn absorbed and reacts with water. However, reaction (c) is slow and the liquid residence time in a multi-jet absorber is short. Therefore only small amounts of NO are expected in the gas phase. According to the gas phase analyses of NO in the test runs, the concentration was in fact negligible.

Thirdly, other absorption mechanisms then the the one considered here are feasible. If the gas phase concentration of NO_2 is lowered under a certain level, there will not exist any appreciable amount of N_2O_4. Then NO_2 is dissolved into the liquid phase where it undergoes a second order reaction with water; the tetroxide acts as an intermediate. In this case the absorption rate is proportional to the 3/2 power of the partial pressure of NO_2. If the gas phase concentration of NO_2 is decreased further down, NO_2 is dissolved into the liquid phase and transported into the bulk liquid, where it undergoes a very slow reaction with water. Under these circumstances, the absorption rate shows a linear dependency with respect to NO_2. However, from data by Komiyama and Inoue (3) it can be deducted that the mechanism assumed in the present study is valid down to about 200 ppm NO_2.

A fourth assumption includes negligible resistance to mass transfer in the gas phase. This is always valid for low concentrations of NO_2 due to the equilibrium reaction (a) in the gas phase. Since the reactive species (N_2O_4) has a much lower concentration than NO_2 in the gas phase, the latter component will enhance mass transfer of N_2O_4 in the gas phase. Equation (2) can be used to calculate the mass transfer coefficient for the gas phase in order to check the statement of negligible resistance to mass transfer. The mass transfer rate can be written:

$$N_A = 2\, k_{DG}\, \Delta p_{DG} + k_{AG}\, \Delta p_{AG} \qquad (10)$$

where Δ_p denotes the difference in partial pressure across the gas film. By combining Equations (5) and (10), and using literature data for the kinetic rate constant, the influence of mass transfer in the gas phase can be estimated. It was found in all cases that the concentrations of N_2O_4 and NO_2 dropped much less than 1 percent across the gas film. Thus, the resistance to mass transfer in the gas phase can be neglected.

Experimental

A total of 30 test runs were performed. The inlet concentration of $NO_2 + 2\,N_2O_4$ was varied from 500 to 1,100 Pa (5,000 to 11,000 ppm). The gas residence time was screened from 9 to about 25 s. The temperature was controlled at $20 \pm 1\ ^{o}C$.

Figure 3 shows a plot of the data using Equation (9) with the left-hand side replaced by the symbol ψ. The equilibrium constant was calculated using the following equation given by Nonhebel (4):

$$K_I = 6.98 \cdot 10^{-15} \exp\left(\frac{6866}{T}\right) \qquad (11)$$

The data points represent three different concentration ranges of $NO_2 + 2\,N_2O_4$. As may be noted, no significant difference exists between high and low NO_2 concentration, which suggests that the model is applicable with fair accuracy. The concentration of $NO_2 + 2\,N_2O_4$ was always greater than 800 ppm.

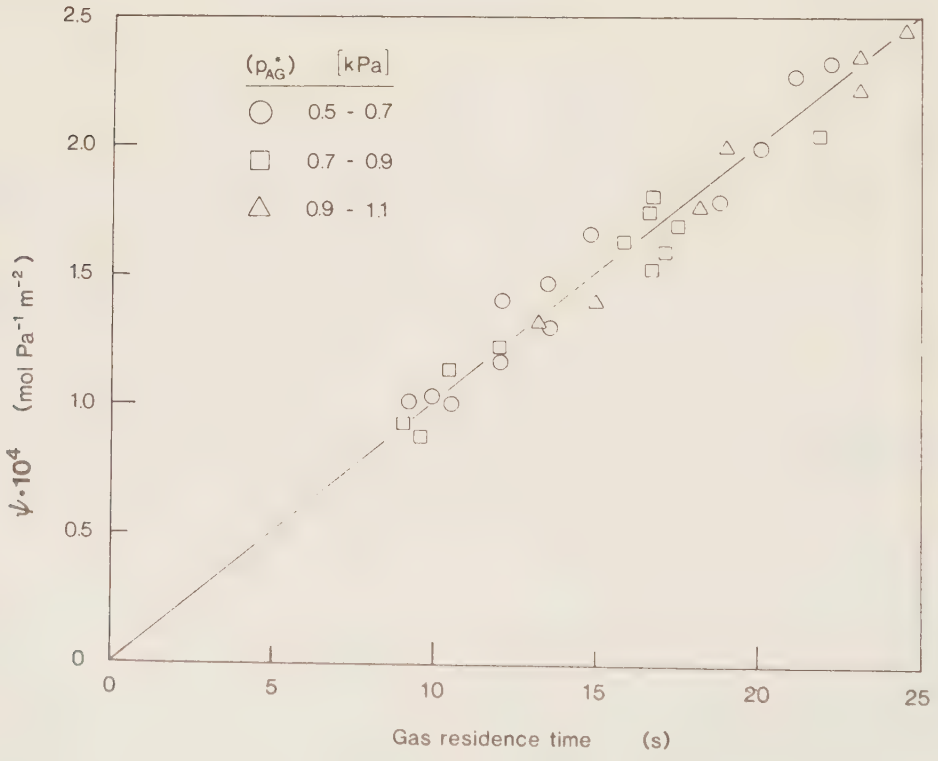

FIGURE 3. PLOT OF EQUATION (9); LEFT-HAND SIDE (ψ) AS A FUNCTION OF GAS RESIDENCE TIME.

The straight line corresponds to a least-square fit, and the slope is given in table 1, along with data from other investigations. In conclusion, data are obtained from the multi-jet absorber with fair accuracy. As can be seen, data from nine studies vary a factor three.

TABLE 1. KINETIC DATA FOR THE REACTION BETWEEN NITROGEN TETROXIDE AND WATER AT 20 °C

Investigation (Reference)	$H_D^{-1} \sqrt{(k_D D_{DL})} * 10^5$ (mol $Pa^{-1} s^{-1} m^{-2}$)
Present study	1.0
Kramers et al. (5)	0.77
Wendel & Pigford (6)	0.53*
Decker et al. (7)	1.0*
Corriveau (8)	0.52*
Gerstacker (9)	0.9 - 1.0*
Kameoka & Pigford (10)	0.63*
Caudle & Denbigh (11)	1.0*
Kamiyama & Inoue (3)	1.58**

* Adjusted from 25 to 20 °C by temperature dependency given by Nonhebel (4); 10 percent decrease.

** Adjusted from 15 to 20 °C as above.

ABSORPTION OF NO_2 IN A H_2O_2 SOLUTION

Theory

When NO_2 is absorbed into a solution of H_2O_2, the following overall reaction is pertinent:

$$2\,NO_2 + H_2O_2 \rightarrow 2\,HNO_3 \qquad (d)$$

If it is N_2O_4 that is the reactive species, formed from the instantaneous gas phase reaction (a), the absorption rate can be written:

$$N_A = 2 k_{DL}^{o} E p_{DG} H_D^{-1} \tag{12}$$

As previously pointed out, there is no resistance to mass transfer in the gas phase.

Assuming an m:th -order reaction with respect to N_2O_4 and n:th-order with respect to H_2O_2, the enhancement factor is:

$$E = \gamma \tag{13}$$

where

$$\gamma = \frac{\sqrt{\left\{\frac{2}{m+1} k_D C_{BL}^{n} C_{Di}^{m-1} D_{DL}\right\}}}{k_{DL}^{o}} \tag{14}$$

provided:

$$1 << \gamma << E_i \tag{15}$$

where

$$E_i \simeq 1 + \frac{2 C_{BL}}{C_{Di}} \sqrt{\left\{D_{BL}/D_{DL}\right\}} \tag{16}$$

If the concentration of NO_2 in the gas phase is sufficiently low, we may put $p_{AG}^{*} \simeq p_{AG}$. This simplification gives the following expression for the governing differential equation:

$$-\frac{d p_{AG}}{dt} = R T_G A_V N_A \tag{17}$$

Considering the relationship between NO_2 and N_2O_4 in the gas phase:

$$p_{DG} = K_I p_{AG}^{2} \tag{4a}$$

and Henry's law:

$$p_{DG} = H_D C_{Di} \tag{18}$$

the following equation is obtained:

$$-\frac{d p_{AG}}{dt} = A_V R T_G 2 \sqrt{\left\{\frac{2}{m+1} k_D C_{BL}^{n} D_{DL}\right\}} (K_I/H_D)^{(m+1)/2} p_{AG}^{(m+1)} \tag{19}$$

By defining the following parameters:

$$\delta = m + 1 \tag{20}$$

$$\kappa = A_V R T_G \, 2\sqrt{\left[\frac{2}{m+1} k_D C_{BL}^{n} D_{DL}\right]} \; (K_I/H_D)^{(m+1)/2} \; 100^m \tag{21}$$

$$C = 10^{-2} p_{AG} \tag{22}$$

the following simplification is obtained:

$$-\frac{dC}{dt} = \kappa C^{\delta} \tag{23}$$

The pertinent boundary conditions are:

$$\begin{cases} t = 0 \\ C = C_o \end{cases} \qquad \begin{cases} t = \theta \\ C = C \end{cases}$$

The equation can be integrated to give:

$$\kappa = \frac{C_o^{1-\delta}}{\theta(1-\delta)} \left[1 - (C/C_o)^{1-\delta}\right] \tag{24}$$

This relation can be recognized as the design equation for a plug flow reactor with a δ:th-order irreversible reaction or a batch reactor with the same reaction; constant volume is necessary in both cases. The equation is thus of principal importance since it appears in many instances besides the multi-jet absorber. There is no simple method available for the evaluation of the "rate constant" (κ) and the "reaction order" (δ). For instance, various δ values can be assumed and then $\kappa\theta$ is plotted as a function of θ. A straight line indicates that the assumed δ value was an appropriate choice. However, poor planning of the experiments and/or improper treatment of the data may give a straight line for different δ values. A numerical method can also be used. By assuming various δ values, a mean value of κ can be estimated from all experiments as a function of δ. The true reaction order is reflected in minimal standard deviation with respect to κ. Again, poor planning of the experiments may cause uncertainty in the evaluation.

It would be beneficial to find a graphic method by which δ and κ could be evaluated from a straight-line plot. Such a method readily shows trends and deviations in the δ value. Scattered points which are

obviously in error can be easily noticed and eliminated from the evaluation. The simplest way of finding such a method is by approximating Equation (24) by a relationship of the following form:

$$B = A f(\delta) + g(\kappa) \tag{25}$$

where B and A depend on the experimental conditions, ie. C, C_o and θ. The two functions, f and g, depend on δ and κ respectively. By plotting B as a function of A, the reaction order is obtained from the slope, and the rate constant from the intercept.

From several attempts, the following forms emerged as the simplest and most workable:

$$f(\delta) = \delta \tag{26}$$

$$g(\kappa) = \ln \kappa \tag{27}$$

Thus:

$$B = A\delta + \ln \kappa \tag{25a}$$

To determine the properties of B and A, a collocation type of method can be applied. Rohsenow and Hartnett (12) show how to use the collocation method to find approximate solutions to differential equations. As will be shown here, the method can also be used to approximate a nonlinear equation.

Since there are two parameters to determine (A and B), two collocation points are required. Thus, Equation (25a) has to fulfil the properties of Equation (24) in $[\delta_1, \kappa(\delta_1)]$ and $[\delta_2, \kappa(\delta_2)]$, where:

$$\kappa(\delta_i) = \frac{C_o^{1-\delta_i}}{\theta(1-\delta_i)} \left[1 - (C/C_o)^{1-\delta_i}\right] \tag{28}$$

Hence:

$$A = \frac{\ln [\kappa(\delta_2)/\kappa(\delta_1)]}{\delta_1 - \delta_2} \tag{29}$$

$$B = \frac{\delta_2 \ln [\kappa(\delta_1)] - \delta_1 \ln [\kappa(\delta_2)]}{\delta_2 - \delta_1} \tag{30}$$

These are the general expressions of A and B. If reasonable δ values are considered, a specific explicit expression of Equation (25a) can be obtained. By putting $\delta_1 = 0$ and $\delta_2 = 2$, Equations (25a) and (28) through (30) degenerate into:

$$\ln [(C_o - C)/\theta] = \delta \ln [\sqrt{ (C_o C)}] + \ln [\kappa] \qquad (30)$$

The approximation has the following properties:

- The error in κ is no more than 2 percent if $C/C_o \geq 0.5$ and $0 \leq \delta \leq 2$. By expanding the validity to $0 \leq \delta \leq 3$, the ratio C/C_o must be greater than 0.7 to obtain less than 2 percent error. However, if $C/C_o < 0.5$, the error is still not great.

- When the true δ value coincides with one of the collocation points, Equation (28) is exact; if the δ value is reasonably close to one of the collocation points, the accuracy is sufficient.

From the last property, it can be inferred that the true reaction order can be obtained with a high accuracy even if the conversion is great (small C/C_o value). This because one of the original collocation points can be replaced by the evaluated value of δ. Thus, an iterative procedure is followed.

Experimental

A total of 16 test runs were performed in the multi-jet absorber, using a scrubbing solution with 1 percent by weight of H_2O_2. The gas residence time was screened from 7 to 23 s, and the temperature was kept at 20 ^oC. The inlet concentration of NO_2 was varied from 2000 to 1000 ppm, to ensure $p^*_{AG} \simeq p_{AG}$. The approximation is valid with a deviation of less than 4 percent at 2000 ppm, and the error drops rapidly as the gas is exhausted with respect to NO_2; the overall error is negligible. The concentration of NO_2 was never below 400 ppm at the outlet of the multi-jet absorber.

The result is plotted in Figure 4 as the removal of NO_2 as a function of the gas residence time. The data have been replotted in Figure 5, utilizing the parameters of Equation (30). A least-square fit gave a slope that deviated from two by less than 1 percent. The straigt

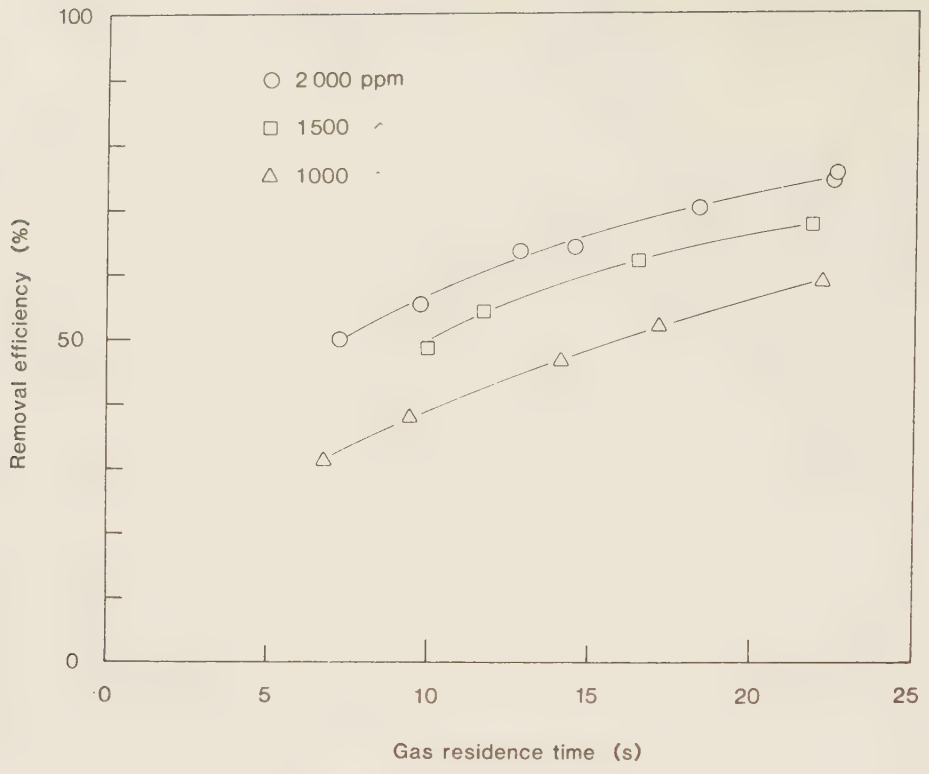

FIGURE 4. REMOVED NO_2 IN A 1 PERCENT H_2O_2 SOLUTION AS A FUNCTION OF GAS RESIDENCE TIME AT 20 °C.

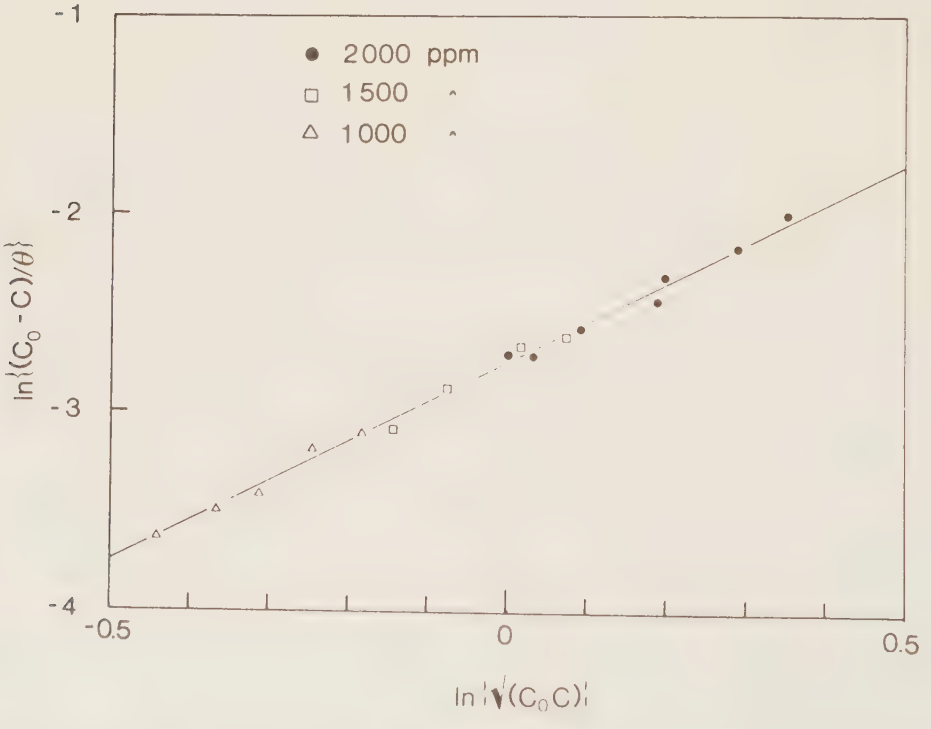

FIGURE 5. PLOT FOR EVALUATION OF KINETIC DATA FOR ABSORPTION OF NO_2 IN A 1 PERCENT H_2O_2 SOLUTION AT 20 °C.

line in the figure corresponds to a (very slightly) modified least-square fit were $\delta \equiv 2$. The reaction order with respect to N_2O_4 thus is unity, which can be obtained from Equation (20). Moreover, κ can be evaluated from the intercept. In turn, the following value can be obtained from Equation (21) by inserting κ and physical constants:

$$\sqrt{(k_D C_{BL}^n D_{DL})} H_D^{-1} = 1.0 \cdot 10^{-5} \text{ [mol Pa}^{-1} \text{ s}^{-1} \text{ m}^{-2}\text{]}$$

This value is the same as the one obtained for pure water.

In conclusion, H_2O_2 has no enhancing effect on the absorption rate for NO_2, ie. $n = 0$. Secondly, the reaction order with respect to N_2O_4 is unity. Thus, the following reaction mechanism can be established:

$$2\,NO_2 \rightleftarrows N_2O_4 \qquad \text{(a)}$$

$$N_2O_4 + H_2O \rightarrow HNO_2 + HNO_3 \qquad \text{(b)}$$

$$HNO_2 + H_2O_2 \rightarrow HNO_3 + H_2O \qquad \text{(c)}$$

ABSORPTION OF NO IN H_2O_2 SOLUTION

Theory

According to Baveja et al. (13), NO can be absorbed into a solution of H_2O_2, where the following reaction occurs:

$$2\,NO + 3\,H_2O_2 \rightarrow 2\,HNO_3 + 2\,H_2O \qquad \text{(f)}$$

The reaction was found to be of first order with respect to the two reactants, suggesting the following rate limiting step:

$$NO + H_2O_2 \rightarrow NO_2 + H_2O \qquad \text{(g)}$$

The second order rate constant was fitted by the following relationship:

$$\ln k_E = 22.6 - 6900/T \text{ [m}^3 \text{ mol}^{-1} \text{ s}^{-1}\text{]} \qquad (31)$$

which is valid for $288 \leq T \leq 303$ K, and up to 2 percent by weight of H_2O_2.

It should be pointed out that Baveja et al. performed their experiments at very high concentrations of NO, actually too high to be pertinent to practical applications; the gas phase concentration of NO was varied from 7 to 25 percent by volume.

The absorption rate of NO can be written:

$$N_E = \sqrt{(k_E C_{BL} D_{EL})}\, p_{EG} H_E^{-1} \qquad (32)$$

if negligible resistance to mass transfer in the gas phase can be assumed. Moreover, a pseudo-first order reaction is assumed, ie. Condition (15) must be fulfilled.

The differential equation can be written:

$$-\frac{d p_{EG}}{dt} = R T_G A_V \sqrt{(k_E C_{BL} D_{EL})}\, p_{EG} H_E^{-1} \qquad (33)$$

subject to:

$$\begin{cases} t = 0 \\ p_{EG} = (p_{EG})_o \end{cases} \qquad \begin{cases} t = \theta \\ p_{EG} = p_{EG} \end{cases}$$

Upon integration:

$$p_{EG} = (p_{EG})_o \exp\left[-\theta R T_G A_V \sqrt{(k_E C_{BL} D_{EL})}\, H_E^{-1}\right] \qquad (34)$$

Experimental

A limited number of experiments were performed to outline the applicability of the data by Baveja et al. at low NO concentrations. The data points are plotted in Figure 6, along with a theoretical prediction using Equation (34). Solubility data and the diffusion constant were taken from the International Critical Table (14) and Sherwood et al. (15), respectively.

The agreement between the experiments and the data by Baveja et al. is excellent. The applicability of the rate constant, Equation (31), is thus extended considerably with respect to the NO concentration. The present data points correspond to an inlet concentration of 2000 ppm which means that the range is extended about 35 times giving validity from 0.2 to 25 percent by volume of NO.

The present analysis was based on the assumption that $E = \gamma$, ie. $1 << \gamma << E_i$, and negligible resistance to mass transfer in the gas phase. The first assumption can be checked by combining Equations (1) and (14):

$$\gamma = \sqrt{\left(\frac{\pi}{4} k_E C_{BL} t^*\right)} \qquad (34)$$

By inserting the values at the pertinent conditions used in the experiments, the γ value is 3.0. Although this is not much greater than unity, it is in fact sufficient. From a practical point of view, the condition $1 << \gamma$ may be exchanged by $3 \leq \gamma$. The penetration theory predicts a 2 percent higher value when using the exact solution at $\gamma = 3.0$ rather than the approximate ($E = \gamma$).

The limiting value of E for an instantaneous reaction can be calculated from Equation (16) to be $E_i \simeq 1.4 \cdot 10^5$. Thus $\gamma << E_i$.

The influence of gas phase resistance to mass transfer may be analyzed in the following way. If it is assumed that the partial pressure of NO drops from p_{EG} to p_{Ei} over the gas film, the following relationship can be used:

$$N_E = k_{EG} (p_{EG} - p_{Ei}) = \sqrt{(k_E C_{BL} D_{EL})} H_E^{-1} p_{Ei} \qquad (35)$$

Upon rearrangement:

$$\frac{p_{EG}}{p_{Ei}} = 1 + \frac{\sqrt{(k_E C_{BL} D_{EL})}}{H_E k_{EG}} \qquad (36)$$

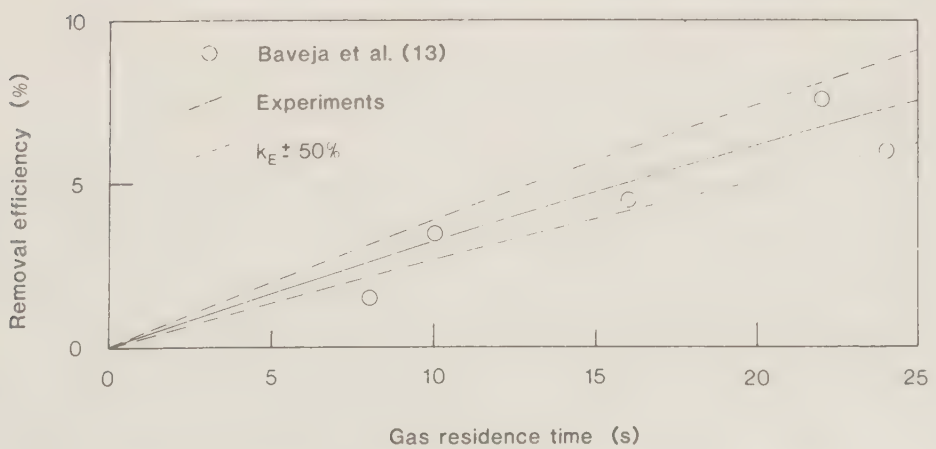

FIGURE 6. REMOVED NO IN A 1 PERCENT H_2O_2 SOLUTION AS A FUNCTION OF GAS RESIDENCE TIME AT 20 °C.

Thus, negligible resistance to mass transfer in the gas phase exists when:

$$\frac{\sqrt{(k_E C_{BL} D_{EL})}}{H_E k_{EG}} << 1 \qquad (37)$$

The value for k_{EG} can be calculated from Equation (2) as:

$$k_{EG} = Sh \frac{D_{EG}}{d R T_G} \qquad (38)$$

Considering a gas residence time ranging from 10 to 25 s, the following values can be obtained:

$$8.1 \cdot 10^{-4} < \frac{\sqrt{(k_E C_{BL} D_{EL})}}{H_E k_{EG}} < 1.2 \cdot 10^{-3}$$

Thus, Condition (37) is fulfilled.

SIMULTANEOUS ABSORPTION OF NO AND NO_2

Theory

When a mixture of NO and NO_2 is absorbed into an aqueous solution, a rather complex series of reaction has to be considered. Reactive species are generated by the following two instantaneous gas phase reactions:

$$2\,NO_2 \rightleftarrows N_2O_4 \qquad (a)$$

$$NO + NO_2 \rightleftarrows N_2O_3 \qquad (h)$$

According to the classical analysis, these two oxides of nitrogen are absorbed into the water, where they react to form nitric and nitrous acids. In the presence of H_2O_2, the monoxide also reacts. Hence, the overall gas-liquid reactions:

$$N_2O_4 + H_2O_2 \rightarrow 2\,HNO_3 \qquad (d)$$

$$N_2O_3 + 2\,H_2O_2 \rightarrow 2\,HNO_3 \qquad (i)$$

$$2\,NO + 3\,H_2O_2 \rightarrow 2\,HNO_3 + 2\,H_2O \qquad (f)$$

If N_2O_3 is denoted by F, the absorption rate of NO_2 and NO can be derived similar to previous outlinings:

$$N_A = 2 H_D^{-1} \sqrt{(k_D D_{DL})} K_I p_{AG}^2 + H_F^{-1} \sqrt{(k_F D_{FL})} K_{II} p_{AG} p_{EG} \quad (39)$$

$$N_E = H_E^{-1} \sqrt{(k_E C_{BL} D_{EL})} p_{EG} + H_F^{-1} \sqrt{(k_F D_{FL})} K_{II} p_{AG} p_{EG} \quad (40)$$

Here K_{II} is the equilibrium constant for reaction (h), and the following relation has been given by Nonhebel (4):

$$K_{II} = 6.53\ 10^{-13} \exp(\frac{4740}{T}) \quad (41)$$

The governing differential equations are:

$$-\frac{d p_{AG}^*}{dt} = R T_G A_V N_A \quad (42)$$

$$-\frac{d p_{EG}^*}{dt} = R T_G A_V N_E \quad (43)$$

where:

$$p_{AG}^* = p_{AG} + 2 p_{DG} \quad (44)$$

$$p_{EG}^* = p_{EG} + p_{FG} \quad (45)$$

If the NO_2 content is less than 1 percent by volume, $p_{EG}^* \simeq p_{EG}$ with high accuracy.

The pertinent boundary conditions can be written:

$$\begin{cases} t = 0 \\ p_{AG} = (p_{AG})_o \\ p_{EG} = (p_{EG})_o \end{cases}$$

By inspecting Equations (39) and (40), it is noted that the second terms represent the absorption of N_2O_3. It has been assumed that the rate limiting step is:

$$N_2O_3 + H_2O \rightarrow 2 HNO_2 \quad (j)$$

followed by oxidation of nitrous oxide to nitric acid by H_2O_2. Although reaction(j) appears frequently, not much quantitative information is published. It is also doubtful if the present straightforward abstraction is sufficient to describe the reaction system in an appropriate way. For instance, Komiyama and Inoue (3) pointed out that reaction (h) occurs in the liquid rather than in the gas phase. Thus, N_2O_3 is an intermediate in a second order gas-liquid reaction rather than a species transported from the gas into the liquid phase. Accordingly, Komiyama and Inoue (3) managed to fit experimental data to a 3/4 power dependency with respect to the product $C_{Ai}\, C_{Ei}$, rather than a linear dependency as predicted by Equations (39) and (40). However, the referred investigation was rather incomplete with respect to theoretical analyses, and it seems strange that a 3/4 dependency was obtained also when $C_{Ai} \neq C_{Ei}$.

Experimental

Absorption experiments were performed at 20 °C with 4000 ppm NO_x and a varying composition. The content of H_2O_2 in the scrubbing solution amounted to 1 percent by weight. The degree of oxidation, defined as:

$$\xi = \frac{p_{AG} + 2\, p_{DG} + p_{FG}}{p_{AG} + 2\, p_{DG} + p_{FG} + p_{EG}} \qquad (46)$$

was set at 0.25, 0.50 and 0.75. The data points are plotted in Figure 7, as removed NO_x as a function of gas residence time. The curves are simulated data obtained by solving, numerically, Equations (39) through (45). The displayed simulation corresponds to the optimum with respect to $H_F^{-1} \sqrt{(k_F\, D_{FL})}$, using the data points for ξ = 0.75 and 0.50. The mean difference between the experimental values of p_{AG} and p_{EG} and the simulations, was less than 2 percent at ξ = 0.75 and 0.50. The lower set of data points (ξ = 0.25) showed a mean deviation of about 7 percent.

The evaluated $H_F^{-1} \sqrt{(k_F\, D_{FL})}$ value is shown in Table 2, along with data from two other investigations. To evaluate the data by Komiyama & Inoue (3), solubility data given by Sherwood et al. (15) were used. As can be noted, the data almost cover a range of one order of magnitude. Since different experimental techniques were applied in all three cases, the broad range may reflect the uncertainty in the assumed reaction mechanism. In addition, if the rate limiting step for absorption

TABLE 2. KINETIC DATA FOR ABSORPTION OF N_2O_3 INTO AQUEOUS SOLUTION

Investigation (Reference)	$H_F^{-1} \sqrt{(k_F D_{FL})} * 10^5$ (mol $Pa^{-1} m^{-2} s^{-1}$)	Remarks
Komiyama & Inoue (3)	13.0	15 °C - Stirred vessel Slightly alkaline solution
This investigation	5.2	20 °C - Multi-jet absorber 1 % H_2O_2 solution
Sherwood et al. (15)	1.6	25 °C - Wetted speres Pure water

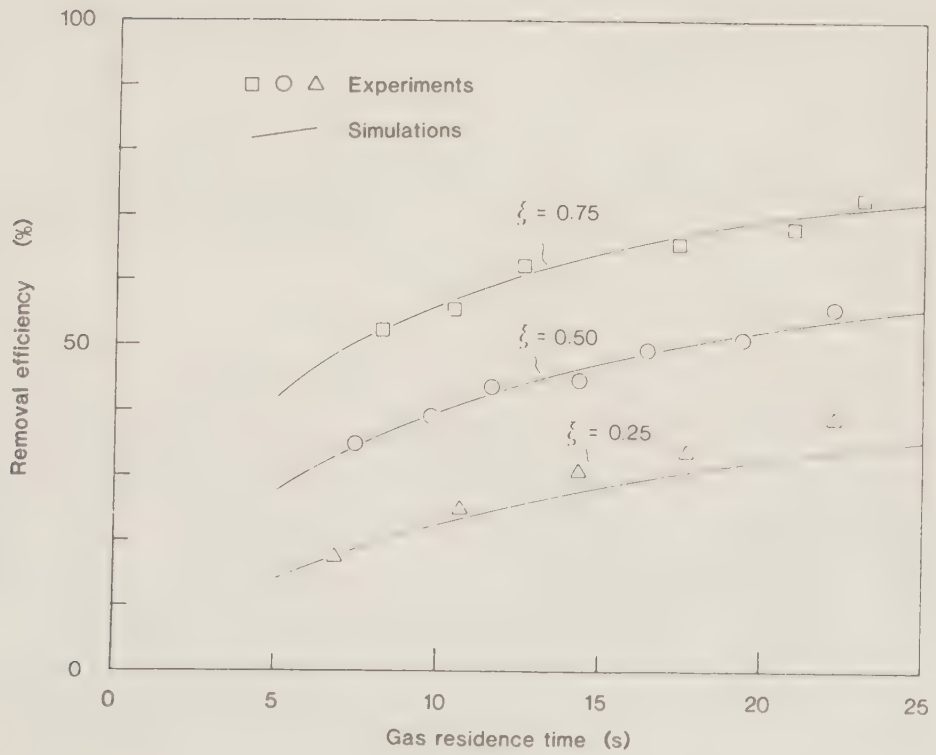

FIGURE 7. REMOVED NO_x IN A 1 PERCENT H_2O_2 SOLUTION AS A FUNCTION OF RESIDENCE TIME AT 20 °C.

of NO is:

$$NO + H_2O_2 \rightarrow NO_2 + H_2O \qquad (g)$$

the produced NO_2 may, or may not, interact with the other two absorbed species (ie. N_2O_4 and N_2O_3). However, from Figur 7 it appears that the overall result when simulating the suggested differential equations agree well with experimental data.

Extension of the Mathematical Treatment

Equations (39) through (45) are of principal importance since they describe the behavior of simultaneous absorption of NO and NO_2 in many types of solutions, eg. alkaline solutions and urea solutions. This assumes that the first term of the right-hand side of Equation (40) is dropped, ie. NO is not a reactive species. The set of equations can be solved numerically in order to simulate the depletion of NO and NO_2 along the absorber in the gas flow direction. This technique was used in the previous section to evaluate a constant from experimental data. Sherwood et al. (15) used the technique to demonstrate how the NO_x content of a gas is depleted in a packed tower.

Under certain assumptions, the two governing nonlinear differential equations can be solved analytically. This is shown in the appendix.

INFLUENCE OF NITRIC ACID ON ABSORPTION OF NO_x IN A H_2O_2 SOLUTION

Background

An implemented absorption process will include a scrubber loop where the concentration of reaction product (ie. nitric acid) is built up. The acceptable steady state level of nitric acid in the scrubbing liquor is determined from requirements on materials of construction, influence on NO_x removal, decomposition rate of H_2O_2 as a function of acid strength, and acceptable amount of unreacted H_2O_2 in the bleed stream.

Experimental

A series of experiments were made to outline the influence of HNO_3 on the absorption of NO_x in a H_2O_2 solution. The test runs were performed at 20 °C with 1 percent by weight of H_2O_2. The gas residence time was screened from 7 to 24 s.

Absorption of NO

Figure 8 shows the result of experiments with 2000 ppm NO, with the removal efficiency as a function of gas residence time. Nitric acid has a pronounced effect on the removal of NO. However, at 10 percent HNO_3 and above, no further increase in removal can be obtained. The data were evaluated from Equation (34) in terms of $H_E^{-1} \sqrt{(k_E C_{BL} D_{EL})}$ as a function of the acid strength, and plotted in Figure 9. It can be seen that the mass transfer rate is enhanced more than four times when at least 10 percent by weight of nitric acid is added to the scrubbing liquor. Since the rate constant appears under the square root sign, the rate constant increases a factor 20. It should be pointed out that the increase displayed in Figure 9 is specific to a solution containing 1 percent by weight of H_2O_2.

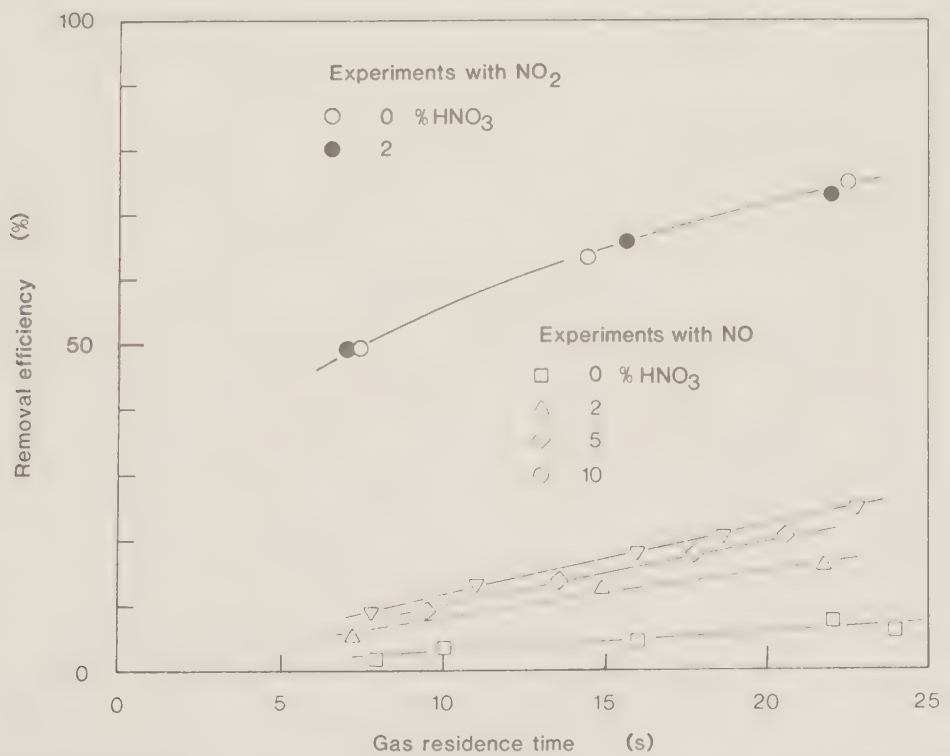

FIGURE 8. INFLUENCE OF HNO_3 IN SCRUBBING LIQUOR ON ABSORPTION OF NO AND NO_2, AT 20 °C.

No attempts have been made to outline the reaction mechanism in the presence of nitric acid. However, a feasible option is the following oxidation:

$$2\,NO + HNO_3 + H_2O \rightarrow 3\,HNO_2 \qquad (k)$$

This reaction is feasible since the presence of H_2O_2 will cause a rapid depletion of HNO_2:

$$HNO_2 + H_2O_2 \rightarrow HNO_3 + H_2O \qquad (1)$$

By combining these two reactions, the following overall reaction is obtained:

$$2\,NO + 3\,H_2O_2 \rightarrow 2\,HNO_3 + 2\,H_2O \qquad (f)$$

which is the same as the non-catalytic reaction between NO and H_2O_2.

Absorption of NO_2

Figure 8 indicates that nitric acid has no influence on the absorption rate of NO_2; a 2000 ppm inlet level was used. The reaction system was not investigated for concentrations of nitric acid above 2 percent by weight, since the most marked effect was noted below this value

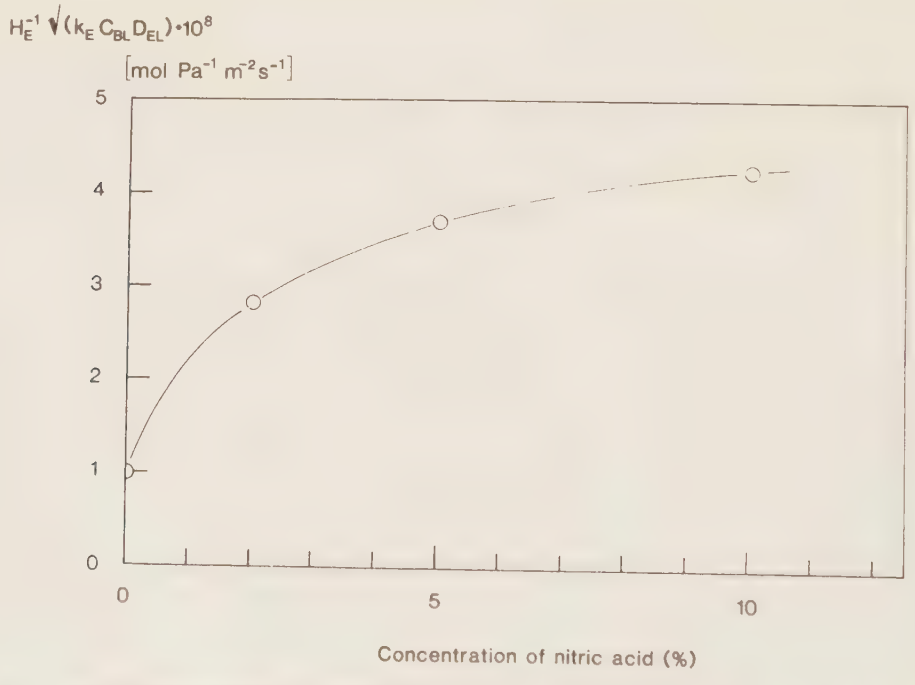

FIGURE 9. MASS TRANSFER COEFFICIENT FOR ABSORPTION OF NO IN A 1 PERCENT H_2O_2 SOLUTION, AS A FUNCTION OF HNO_3 CONCENTRATION.

when absorbing NO. Of course there will be small effects at very high concentrations of nitric acid, in terms of salting out effects on the N_2O_4 solubility and a decrease in the diffusion rate due to an increase in the viscosity.

Simultaneous Absorption of NO and NO_2

Figure 10 shows the removal efficiency of NO_x as a function of gas residence at different concentration levels of nitric acid. The experiments were performed using a gas with 2000 ppm NO and 2000 ppm NO_2. It was found that the enhancement of the absorption rate of the NO species was not sufficient to account for the increase in removal efficiency when the nitric acid concentration was increased.

The curves in Figure 10 correspond to simulations using Equations (39) through (45) in which case values of $H_F^{-1} \sqrt{(k_F D_{FL})}$ have been used according to the series shown in Table 3. Accordingly, values of $H_E^{-1} \sqrt{(k_E C_{BL} D_{EL})}$ have been used as given by Figure 9. The values in Table 3 were obtained from the best agreement between experiments and simulations.

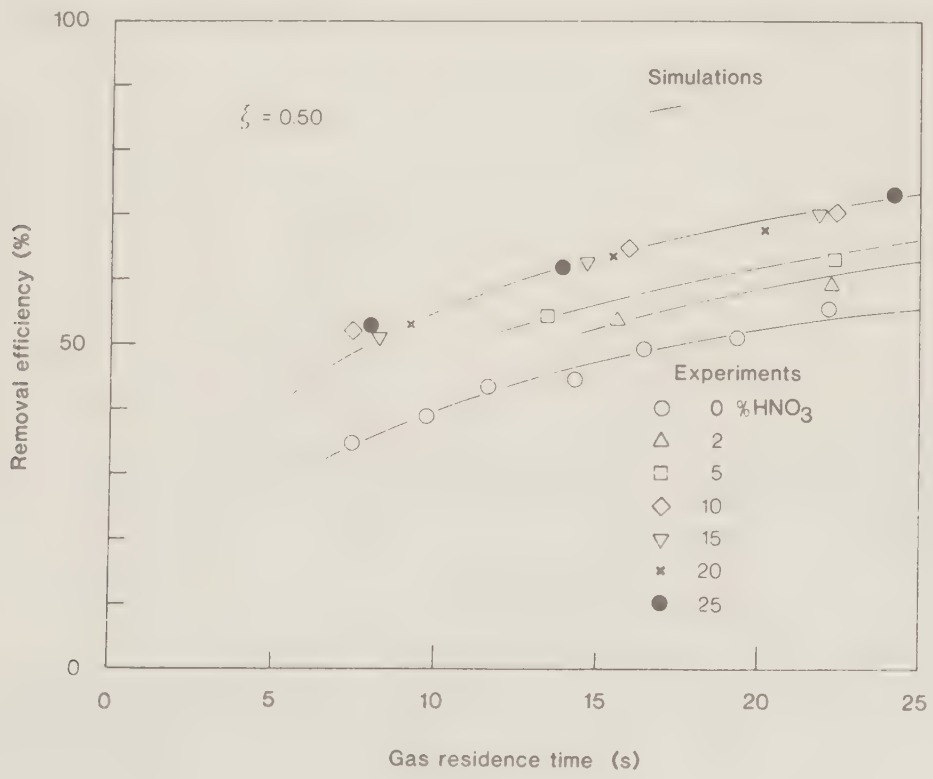

FIGURE 10. INFLUENCE OF ACID STRENGTH ON REMOVED NO_x IN A 1 PERCENT H_2O_2 SOLUTION AT 20 °C.

TABLE 3. INFLUENCE OF ACID STRENGTH ON KINETIC DATA FOR ABSORPTION OF N_2O_3 IN A 1 PERCENT SOLUTION OF H_2O_2

Concentration of HNO_3 (percent)	$H_F^{-1} \sqrt{(k_F D_{FL})} * 10^5$ (mol Pa^{-1} s^{-1} m^{-2})
0	5.2
2	6.5
5	7.8
≥ 10	13

A number of experiments were also performed at an oxidation degree of 0.25. The result of this set of data is shown in Figure 11 along with simulations using the same data and equations as were used for the simulations shown in Figure 10. At high acid concentrations, the data points are scattered, probably because entrained acid mist is interacting with the gas analyzers. This was not obtained at $\xi = 0.50$. Therefore, 50 percent of the data points for concentrations greater than 10 percent have been omitted. The agreement between simulations and experiments can be considered fair, in light of the deviation for $\xi = 0.25$ shown in Figure 7.

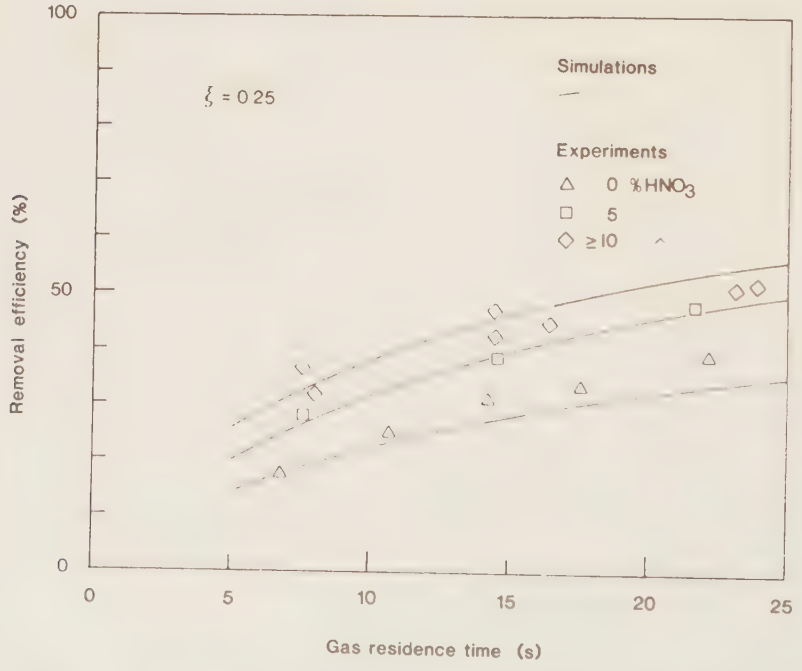

FIGURE 11. INFLUENCE OF ACID STRENGTH ON REMOVED NO_x IN A 1 PERCENT H_2O_2 SOLUTION AT 20 °C

ENGINEERING ANALYSIS

Depending on type of emission source, the concentration and composition of NO_x will vary considerably. Also, the presence of particulates and other gaseous species beside NO_x, and the large volumes of gas to be processed, present big enineering problems. As a first step, a basic analysis is required to outline if reasonable removal of NO_x can be achieved with H_2O_2 scrubbing. This analysis has to be carried out on the basis of pertinent compositions and concentrations of NO_x, encountered in practical situations.

Three different cases have been identified which should cover most of the practical applications:

- coal-fired power plant
- nitric acid plant
- steel pickling plant

The required tower height was in each case calculated, by means of Equations (42) and (43), using kinetic data for 10 percent HNO_3, 1 percent H_2O_2 and 20 ^oC. In addition, the gas phase oxidation:

$$2\,NO + O_2 \rightarrow 2\,NO_2 \qquad (m)$$

was taken into account. The third order rate constant for this reaction is given by Nonhebel (4):

$$k' = 2.17*10^{-11} \exp\left(\frac{1399}{T}\right) \; [Pa^{-2}\,s^{-1}] \qquad (47)$$

Table 4 shows typical data for the first two cases; data for the steel pickling plant have been chosen for a very favorable case. The calculated tower heights are also included in the table. The result indicates that H_2O_2 has a very limited (if any) application for wet scrubbing of NO_x.

Economy

The use of hydrogen peroxide as a liquid reactant is very costly, ie. more than $\$10^3$/ton (100 % H_2O_2). This is a comparatively very high cost for a chemical, used for environmental protection.

The stoichiometry depends on the composition of NO_x. Pure NO_2 requires 0.5 moles H_2O_2, pure NO requires 1.5 moles H_2O_2 and equimolar

absorption requires 1 mole H_2O_2 for each mole NO_x absorbed. In addition, an excess of H_2O_2 is consumed because large amounts are removed by the bleed stream. If the absorption is accomplished in a 1 percent H_2O_2 solution, and the nitric acid concentration is built up to about 2 percent in the scrubber loop, about 1 mole of unreacted H_2O_2 is removed by the bleed for each mole NO_x absorbed. Thirdly, H_2O_2 is easily decomposed into water and oxygen. However, the rate for this decomposition has not been determined.

TABLE 4. CASE STUDIES OF WET SCRUBBING OF NO_x with H_2O_2

Item	Coal-fired power plant	Nitric acid plant	Steel pickling plant
Inlet level of NO_x	750 ppm	1400 ppm	1000 ppm
Degree of oxidation (ξ)	10 %	25 %	50 %
Oxygen content	5 %	4 %	20 %
Required emission level	100 ppm	200 ppm	75 % removal
Interfacial area	50 m^{-1}	50 m^{-1}	150 m^{-1}
Superficial gas velocity	3 m/s	2 m/s	0.5 m/s
Required tower height	> 1 km	~ 0.5 km	26 m

CONCLUSIONS

The simultaneous absorption of NO and NO_2 in a H_2O_2 solution has been extensively studied. Three gaseous species react with H_2O_2, ie. NO, N_2O_4 and N_2O_3, and the reaction products are water and nitric acid.

When considering the cost, H_2O_2 has a very limited application for NO_x scrubbing. The reactant is very expensive and it will add unacceptably to the operating cost. Only very small units are feasible, in which case the only alternative may be a very high capital investment.

The removal efficiency of NO_x in a reasonably sized scrubber is low. Hence, there are probably no, or very limited, practical applications for scrubbing of NO_x with H_2O_2.

NOTATION

a spacing between center of two jets in flow direction, m

A mass-transfer area, m^{-1}

A parameter, Eq. (25)

b spacing between center of two jets normal to flow direction, m

B parameter. Eq. (25)

C concentration, mol m^{-3}

C p/100, Pa

d jet diameter, m

D diffusion coefficient, $m^2 s^{-1}$

E enhancement factor (factor by which the absorption rate is increased by reaction)

f configuration factor, Eq. (3)

H Henry's law constant, Pa m^3 mol^{-1}

k rate constant for reaction in gas phase, $Pa^{-2} s^{-1}$

k rate constant, for reaction in liquid, $(mol\ m^{-3})^{1-m-n} s^{-1}$

k mass-transfer coefficient for the gas side, mol m^{-2} Pa^{-1} s^{-1}

k physical mass-transfer coefficient in the liquid, $m\ s^{-1}$

K equilibrium constant, Pa^{-1}

m reaction order in gas side reactant

n reaction order in liquid side reactant

N mass-transfer rate, mol $m^{-2} s^{-1}$

p partial pressure, Pa

t time, s

T temperature, K

V velocity of gas, m/s

Subscripts

G gas
i general value
i interface
i instantaneous reaction
V interfacial area of jets per unit volume occupied by jets
I reaction (a)
II reaction (h)
o inlet (start) value
1 first collocation point
2 second collocation point

Species

XG X in the gas phase
Xi X at the interface
XL X in the liquid
where X is A (=NO_2), B (=H_2O_2), D (=N_2O_4),
E (=NO), F (=N_2O_3), and i (=general species)

Superscripts

o value in absence of chemical reaction
* residence time of liquid jet
* sum of A and 2 D, or E and F
' gas phase rate constant

Greek Symbols

γ reaction parameter, Eq, (14)
δ "reaction order", Eq. (20)
θ gas residence time, s
κ "rate contant", Eq. (21)
υ kinematic viscosity of gas, $m^2 s^{-1}$
ξ degree of oxidation, Eq. (46)
ψ left-hand side of Eq. (9)

Dimensionless Groups

Re = $d V/\nu$, Reynold's number

Sc = ν/D, Schmidt number

Sh = $R T k d/D$, Sherwood number

Tr = $d^2/t^*\nu$, residence-time number

ACKNOWLEDGEMENT

The authors are grateful to EKA and Supra AB for financial support.

REFERENCES

1. Y.T. Shah, "Gas-Liquid-Solid Reactor Design", p. 149. McGraw-Hill, New York (1979)
2. H.T. Karlsson and I. Bjerle, "Int. J. Heat Mass Transfer" 23. 355-361 (1980)
3. H. Komiyama and H. Inoue, "Chem, Eng. Sci." 35, 154-161 (1980)
4. G. Nonhebel, "Gas Purification Processes for Air Pollution Control", pp 164-187. Newnes - Butterworths, London (1972)
5. H. Kramers, M.P.P. Blind and E. Snoeck, "Chem. Eng. Sci." 14, 115 (1961)
6. M.M. Wendel and R.L. Pigford. "AIChE Journal" 4, 249 (1958)
7. W.A. Dekker. E. Snoeck and H. Kramers, "Chem. Eng. Sci." 11, 61 (1959)
8. C.E. Corriveau, Master's thesis, Univ. Calif., Berkely, 1971
9. Gerstacker, "Chem. Eng. Sci." 14, 124 (1961)
10. Y. Kameoka and R.L. Pigford, "Ind. Eng. Chem., Fundam." 16, 163-169 (1977)
11. P.G. Caudle and K.G. Denbigh, "Trans. Faraday Soc." 47, 39 (1953)
12. W.M. Rohsenow and J.P. Hartnett, "Handbook of Heat Transfer", pp 4·72 - 4·75, McGraw-Hill, New York (1973)
13. K.K. Baveja, D.S. Rao and M.K. Sarkar, "J. Chem. Eng. Jpn." 12, 322-325 (1979)
14. International Critical Table, Vol III, 1:st ed. (1928)
15. T.K. Sherwood, R.L. Pigford and C.R. Wilke, "Mass Transfer", McGraw-Hill, New York (1975)

APPENDIX

Absorption and simultaneous reaction of N_2O_3 and N_2O_4 in a plug-flow absorber

The governing equations are (39), (40), (42) and (43), if the term for absorption of NO is dropped. The following dimensionless notations are introduced:

variables

$$\tau = R\,T_G\,A_V\,H_F^{-1}\,\sqrt{(k_F\,D_{FL})}\;t \tag{A1}$$

$$\Phi = K_{II}\,p_{EG} \tag{A2}$$

$$\Lambda = K_{II}\,p_{AG} \tag{A3}$$

parameter

$$\beta = 2\,\frac{K_I\,H_F}{K_{II}\,H_D}\sqrt{\left(\frac{k_D\,D_{DL}}{k_F\,D_{FL}}\right)} \tag{A4}$$

If the problem is studied under the assumption of a relatively low range concentration of NO_2, it is possible to approximate p^*_{AG} with p_{AG}. If Equations (39) and (40) are inserted in (42) and (43), the following simplification is achieved:

$$-\frac{d\,\Lambda}{d\,\tau} = \beta\,\Lambda^2 + \Phi\,\Lambda \tag{A5}$$

$$-\frac{d\,\Phi}{d\,\tau} = \Phi\,\Lambda \tag{A6}$$

By eliminating τ, the two equations are condensed down to:

$$\frac{d\,\Lambda}{d\,\Phi} = \beta\,\frac{\Lambda}{\Phi} + 1 \tag{A7}$$

A new variable can be defined as:

$$\chi = \frac{\Lambda}{\Phi} \Rightarrow \begin{cases} \dfrac{\partial\,\chi}{\partial\,\Lambda} = \dfrac{1}{\Phi} \\ \dfrac{\partial\,\chi}{\partial\,\Phi} = -\dfrac{\Lambda}{\Phi^2} \end{cases} \tag{A8}$$

From this it can be inferred:

$$d\chi = \left(\frac{\partial \chi}{\partial \Lambda}\right) d\Lambda + \left(\frac{\partial \chi}{\partial \Phi}\right) d\Phi = \frac{1}{\Phi}\, d\Lambda - \frac{\Lambda}{\Phi^2}\, d\phi \qquad \text{(A9)}$$

By using Equation (A7) to eliminate Λ:

$$d\chi = \frac{1}{\Phi}(\beta\chi + 1)\, d\Phi - \chi \frac{1}{\Phi}\, d\Phi = [(\beta - 1)\chi + 1] \frac{d\Phi}{\Phi} \qquad \text{(A10)}$$

This equation is now separable, and can be integrated to give:

$$\int_{\Phi_o}^{\Phi} \frac{d\Phi}{\Phi} = \int_{\Lambda_o/\Phi_o}^{\Lambda/\Phi} \frac{d\chi}{(\beta-1)\chi + 1} \qquad \text{(A11)}$$

$\beta = 1$ (singularity)

When $\beta = 1$, Equation (A11) is simplified to:

$$\ln[\Phi/\Phi_o] = \Lambda/\Phi - \Lambda_o/\Phi_o \qquad \text{(A12)}$$

To obtain the time dependencies, Λ is inserted in Equation (A6):

$$\frac{d\Phi}{d\tau} = -\Phi^2 (\Lambda_o/\Phi_o + \ln[\Phi/\Phi_o]) \qquad \text{(A13)}$$

This equation can be solved by defining a new variable:

$$\Omega = \Lambda_o/\Phi_o + \ln[\Phi/\Phi_o] \qquad \text{(A14)}$$

The transformed equation becomes:

$$\frac{d\Omega}{d\tau} = -\Phi_o \Omega \exp(\Omega - \Lambda_o/\Phi_o) \qquad \text{(A15)}$$

The solution can be expressed in terms of the well-known exponential integral, defined as:

$$E_1(x) = \int_x^{\infty} \frac{\exp(-t)}{t}\, dt \qquad \text{(A16)}$$

The solution is:

$$\tau = - \exp(\Lambda_o/\Phi_o) \int_{\Omega_o}^{\Omega} \frac{\exp(-\Omega)}{\Omega} d\Omega = \exp(\Lambda_o/\Phi_o) [E_1(\Omega) - E_1(\Omega_o)] \quad (A17)$$

By elimination of all dummy variables:

$$\theta = \frac{H_F \exp[(p_{AG})_o/(p_{EG})_o]}{R T_G A_V \sqrt{(k_F D_{FL})}} \left\{ E_1\left\{(p_{AG})_o/(p_{EG})_o - \right.\right.$$

$$\left.\left. - \ln[p_{EG}/(p_{EG})_o]\right\} - E_1\left\{(p_{AG})_o/(p_{EG})_o\right\}\right\} \quad (A18)$$

$$p_{AG} = p_{EG} \left\{(p_{AG})_o/(p_{EG})_o + \ln[p_{EG}/(p_{EG})_o]\right\} \quad (A19)$$

$\beta \neq 1$ (general case)

In the general case, Equation (A11) can be written:

$$\ln\left[\frac{\Phi}{\Phi_o}\right] = \frac{1}{\beta-1} \ln\left[\frac{(\beta-1)\,\Lambda/\Phi + 1}{(\beta-1)\,\Lambda_o/\phi_o + 1}\right] \quad (A20)$$

By solving Λ explicitly and inserting the expression in Equation (A6), the following differential equation is obtained:

$$\frac{d\Phi}{d\tau} = - \Phi^2 \left\{[(\beta-1)\,\Lambda_o/\Phi_o + 1]\,(\Phi/\Phi_o)^{\beta-1} - 1\right\}/(\beta-1) \quad (A21)$$

By defining:

$$\zeta = [(\beta-1)\,\Lambda_o/\Phi_o + 1]\,\Phi_o^{1-\beta} \quad (A22)$$

and introducing a new variable:

$$\Gamma = \Phi^{-1} \quad (A23)$$

the transformed expression of Equation (A21) becomes:

$$(1-\beta)\frac{d\Gamma}{d\tau} = \zeta\,\Gamma^{1-\beta} - 1 \quad (A24)$$

This equation is separable, and can in its simplest form be written:

$$\tau = (1-\beta) \int_{\Gamma_o}^{\Gamma} \frac{d\Gamma}{\zeta \Gamma^{1-\beta} - 1} \qquad (A25)$$

By defining an integral function as:

$$T(a,b,c) = \int_0^a \frac{dx}{b x^c - 1} \qquad (A26)$$

and eliminating the dummy variables, the following result is obtained:

$$\theta = \frac{(1-\beta) H_F}{R T_G A_V \sqrt{(k_F D_{FL})}} \left\{ T(\Gamma, \zeta, 1-\beta) - T(\Gamma_o, \zeta, 1-\beta) \right\} \qquad (A27)$$

$$p_{AG} = p_{EG} \left\{ [(\beta-1)(p_{AG})_o / (p_{EG})_o + 1] [p_{EG} / (p_{EG})_o]^{\beta-1} - 1 \right\} / (\beta-1) \qquad (A28)$$

where:

$$\Gamma = [K_{II} p_{EG}]^{-1} \qquad (A29)$$

$$\Gamma_o = [K_{II} (p_{EG})_o]^{-1} \qquad (A30)$$

$$\zeta = [(\beta-1) (p_{AG})_o / (p_{EG})_o + 1] [K_{II} (p_{EG})_o]^{1-\beta} \qquad (A31)$$

$$\beta = 2 \frac{K_I H_F}{K_{II} H_F} \sqrt{\left(\frac{k_D D_{DL}}{k_F D_{FL}} \right)} \qquad (A32)$$

There exist a few special cases where the solution can be simplified:

1: $\zeta > 0$

The integral function is condensed to:

$$T'(a, c) = \int_0^a \frac{dx}{x^c - 1} \qquad (A33)$$

The solution is:

$$\theta = \zeta^{1/(1-\beta)} \frac{(1-\beta)\, H_F}{R\, T_G\, A_V \sqrt{(k_F\, D_{FL})}} \left[T'(\Gamma', 1-\beta) - T'(\Gamma'_o, 1-\beta)\right] \qquad \text{(A34)}$$

where:

$$\Gamma' = \Gamma\, \zeta^{1/(1-\beta)} \qquad \text{(A35)}$$

$$\Gamma'_o = \Gamma_o\, \zeta^{1/(1-\beta)} \qquad \text{(A36)}$$

2: $\beta < 1$ and $|\zeta\, \Gamma_o^{1-\beta}| < 1$

By using the following variable transformation:

$$\Gamma'' = \zeta\, \Gamma^{1-\beta} \qquad \text{(A37)}$$

the integral can be described by means of Gauss' hypergeometric function, which can be expressed in terms of a series: .

$$2F_1\,(a, b, c; x) = \sum_{n=0}^{\infty} \frac{(a)_n\, (b)_n}{(c)_n} \frac{x^n}{n!} \qquad \text{(A38)}$$

where $(a)_n$, $(b)_n$, and $(c)_n$ are so called Pochammer symbols, eg.:

$$(a)_n = a(a+1)\,(a+2).....(a+n-1) = \frac{(a+n-1)!}{(a-1)!} \qquad \text{(A39)}$$

The solution is:

$$\theta = \frac{(1-\beta)\, H_F}{R\, T_G\, A_V \sqrt{(k_F\, D_{FL})}} \left\{ (K_{II}\, p_{EG})^{-1}\; {}_2F_1\,[1,\, 1/(1-\beta),\, 1 + 1/(1-\beta);\right.$$

$$\left. \zeta\, \Gamma^{1-\beta}] - (K_{II} (p_{EG})_o)^{-1}\; {}_2F_1\,[1,\, 1/(1-\beta),\, 1 + 1/(1-\beta);\, \zeta\, \Gamma_o^{1-\beta}] \right\} \qquad \text{(A40)}$$

where ζ, Γ, and Γ_o are given by Equations (A31), (A29) and (A30), respectively.

VII

Reprinted from APCA JOURNAL, *Vol. 30, No. 6, June 1980*

Technical Aspects of Lime/Limestone Scrubbers for Coal-Fired Power Plants

Part I: Process Chemistry and Scrubber Systems

Hans T. Karlsson and Harvey S. Rosenberg
Battelle Columbus Laboratories

This 2-part article deals with the technical aspects of lime/limestone scrubbers for coal-fired power plants. Part I covers process chemistry and scrubber systems. Part II (next month) will cover instrumentation, particulate removal, and sludge disposal.

Figure 1 is a schematic diagram of a typical lime/limestone based flue gas desulfurization (FGD) system, a process consisting of conventional components and utilizing supposedly well-established technology. Due to its relative simplicity, lime/limestone scrubbing is widely used in order to meet the SO_2 emission standards in the U. S. and all over the world today. Over 60 coal-fired power plants will have applied this method in the U. S. by the end of 1979; about half the installations use lime and half use limestone as the reactant. Taking into account the planned FGD systems, the number will increase more than 200% by 1988. In Japan the situation is similar regarding the extent of utilization of the system, but in Western Europe only a small number of plants are operating. Although these statistics are factual, it is an exaggeration to state that the majority of the systems accomplish their purpose. Many unforeseen technical problems remain to be solved.

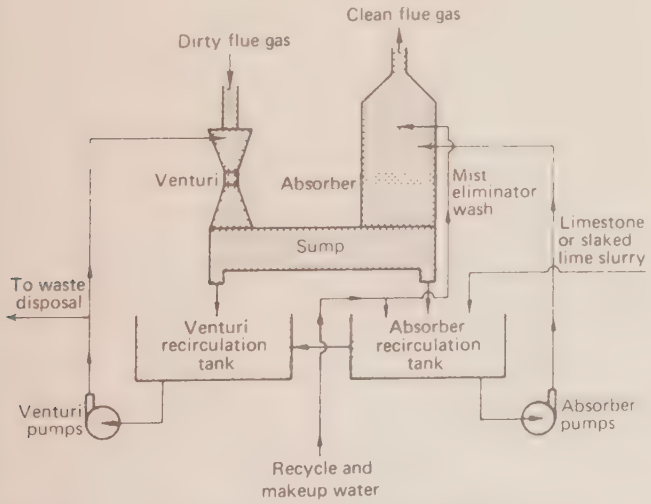

Figure 1. Typical flow sheet for a lime or limestone FGD system.

Before considering lime/limestone FGD systems to be commercially available, the following conditions must be met:[1]

- High removal efficiency to meet emission standards even when burning high sulfur and ash coal,
- High reliability on a commercial scale, to keep the expenses for repairing and maintenance low and to meet the emission standards over the long-term,
- Operation in a closed-loop mode, preventing discharge of process water to natural water systems.

Process Chemistry

The SO_2 removed in a lime/limestone based FGD system is converted to sulfite, generally represented by the overall reactions

$$SO_2 + CaCO_3 \rightarrow CaSO_3 + CO_2$$
$$SO_2 + Ca(OH)_2 \rightarrow CaSO_3 + H_2O$$

when using limestone and lime, respectively. Part of the sulfite is oxidized with the oxygen content in the flue gas to form sulfate

$$CaSO_3 + \tfrac{1}{2}O_2 \rightarrow CaSO_4$$

Although the overall reactions are simple, the chemistry is quite complex and not well defined. In a comprehensive theoretical and experimental study by Radian[2] it was established that 41 neutral and ionic species in solution and 7 solid components are of importance. Therefore, it can be inferred that the reaction rate and the influence of design and process variables on composition in this complicated three-phase system are almost impossible to determine. The complex chemistry may also explain why various studies have led to different conclusions.

When the slurry flows down through the absorber and contacts the SO_2-laden flue gas, SO_2 may react with 15 different basic species, corresponding to a hundredfold increase in the inlet concentration of dissolved lime or limestone. The choice between lime and limestone, the type of limestone, and method of calcining and slaking can influence the gas-liquid-solid reactions taking place in the absorber.

Copyright 1980-Air Pollution Control Association

In order to achieve optimum absorption of SO_2, it is necessary to understand the process chemistry. However, much of the present knowledge has been developed mainly on an empirical basis. Some important operational aspects that can be controlled by understanding the process chemistry are:

- Removal efficiency,
- Plugging and scaling,
- Reagent utilization,
- Corrosion.

High removal efficiency is governed by a high pH; a low pH decreases the reaction rate and increases the SO_2 back-pressure from the scrubber solution. On an empirical basis, it has been established that for lime systems the reactions are controlled when the pH is kept in the range of 6.9 to 8.9. For limestone, it is not possible to achieve pH values above 7.

Interest has also been focused on the effect of magnesium on the absorption rate. Since magnesium sulfite is about 300 times as soluble as calcium sulfite, the concentration of the former can build up on the scrubber loop. This considerably increases the amount of available basic species which, in turn, increases the removal efficiency. The source of magnesium can be as an additive, for instance the oxide or sulfate, but alternatively a lime type with a high magnesium content can be used (calcined dolomite). Small amounts of magnesium, on the order of 5% MgO, are enough to build up a magnesium to calcium ratio as high as 100 in the scrubbing liquor. The actual value is determined by the bleed-off from the absorber loop. If uncalcined dolomite is utilized, the absorption efficiency instead will be depressed due to the extremely slow dissolution rate of associated magnesium and calcium carbonates. Magnesium is not used as an additive in any commercial application at the present, but this type of system is being installed on a 670 MW power plant.[3] However, the magnesium content in the lime is considered in the choice of raw material and a specially selected lime with 3 to 9% MgO is being used in several installations.

The concentration of undissolved reactant in the absorber loop is of importance for the removal efficiency in the cases where the dissolution rate is the rate controlling step. Thus, an increased concentration, as well as a decreased particle size, will increase the absorption efficiency in these cases.

Scaling is a very complex phenomenon that depends on design parameters and process variables as well as process chemistry. Hard scale build up causes increased pressure drop and plugging in the equipment, and therefore, it is one of the main causes for shut downs. Three different types of scaling are commonly referred to:

- Carbonate scaling,
- Sulfite scaling,
- Sulfate scaling.

It has been found by experience that the former two types can be controlled to a large extent by keeping the pH well below 9. In practice, sulfite scaling seldom occurs in limestone scrubbing because the pH is lower and because sulfite supersaturates to such a degree that crystallization does not occur until the slurry reaches the reaction tank. However, sulfate scaling is much more difficult to control. Unlike sulfite, the decrease in pH down through the scrubber does not help hold sulfate in solution. Thus, if there is a considerable amount of sulfite oxidation in the scrubber, sulfate crystallization can occur. Since the oxidation rate of sulfite to sulfate increases with decreasing pH, it is not unreasonable to presume that sulfate scaling can also be prevented by adjusting the pH. However, this has never been proven to be the case.

Sulfate is continuously formed in the absorber loop and most of it precipitates in the holding tank. It has been found that sulfate can supersaturate to a factor of 1.4 before massive nucleation starts,[4] but deposition can still occur below 1.4. Therefore, the sulfate concentration should be kept below the saturation level to insure against spurious deposition. The saturation level is mainly dependent on the solids composition. If the degree of oxidation is below 20%, only mixed crystals of sulfite and sulfate will exist so that the slurry remains in an unsaturated state with respect to sulfate. This is however, difficult to control, especially for low sulfur coals or old boiler units with high excess air. Both cases give a relatively high oxygen to SO_2 ratio in the flue gas.

The ratio of sulfate to sulfite in an FGD system can be predicted to a certain extent from the method of fly ash removal, the pH of the scrubbing liquor, and the ratio of oxygen to SO_2 and the content of nitrogen oxides in the flue gas. Other factors are also of importance, such as presence of magnesium and chloride ions, so that it is difficult to prevent sulfate scaling by control of the sulfate concentration. In some cases carbide lime, a byproduct of acetylene generation from calcium carbide, is utilized as the scrubbing reagent. These systems are noteworthy for a lack of oxidation which permits them to operate in an unsaturated mode with respect to sulfate ion. It has been theorized that carbide lime contains an oxidation inhibitor which has not yet been identified.

An alternative method for sulfate scale prevention is to allow large amounts of gypsum to recirculate so that deposition starts on the crystals present instead of on scrubber surfaces. A solid gypsum concentration of 5% has been found to be sufficient for this purpose. One method utilized to achieve the desired 5% concentration of gypsum is forced oxidation. Fly ash also helps to prevent scaling by providing sites for deposition; according to a TVA study[5] a total solids content exceeding 10% causes crystallization of the sulfate on the solids. However, an increased solids content in the slurry loop makes it difficult to pump the high volumes of slurry required for high SO_2 removal, so that an upper limit of 15% is generally accepted. In most of the FGD systems in the U.S., a 7 to 15% solids content exists in the recirculating slurry, but in some cases values as low as 3% occur. In Japan, gypsum seed-crystals are sometimes added to the process to provide sites for sulfate nucleation.

The optimum solids level in the loop can only be predicted on an empirical basis, while the lime/limestone addition is determined theoretically by the stoichiometry; more reagent than is required by the stoichiometry has to be added. A high degree of utilization demands a small bleed-off from the slurry reaction tank which implies that there is a buildup of soluble as well as solid species in the loop. This has a positive effect for some soluble species such as magnesium, but a negative effect regarding chloride and other undesirable components. The maximum possible utilization can be determined from a material balance when the constraints, such as buildup of unwanted species and removal efficiency, are known. In most cases 75 to 90% of the lime/limestone is utilized, but a value as high as 98% has been reported for a limestone system installed on a utility boiler in Japan. In general, reagent utilization is higher for lime than for limestone.

Corrosion occurs at low pH, and in the presence of chloride ions the problem is exacerbated. During absorption of the SO_2, the pH of the scrubbing liquor is usually lowered to less than 7. The scrubbing liquors also contain chloride ions introduced from the coal and the water and lime or limestone used in making up the scrubbing slurries. Since water pollution regulations usually preclude dumping the scrubbing liquor, closed loop recirculation of the liquid results in considerable buildup of soluble chlorides and other contaminants. The resultant acid chloride solutions can be quite corrosive. The power industry generally expects 20 years or more of service from equipment, and concern has been expressed about the cor-

rosion failures that have occurred.

Stainless steel construction has been the choice for a number of absorbers. This construction requires the highest initial investment of the choices available, but has been selected by some with the belief that it will require less maintenance, and also less down time than other materials choices. Moreover, weld patching and replacement of new plates can be much easier and quicker than a reapplication of a lining (refer to Figure 2). It is recognized, however, that high chlorides can present a corrosion problem.

Figure 2. Corrosion of a stainless steel absorber wall

Lime vs. Limestone

The choice between lime and limestone is usually based on economic considerations. When utilizing lime, the expenses for calcination, transportation, and slaking must be considered. With regard to limestone, transportation and grinding are of importance. The cost for lime is much higher due to the calcination. The cost ratio of lime to limestone on a molar basis may vary from 2 to 4 depending on the transportation distance. Although the carbon dioxide in limestone contributes to an increase in the molecular weight, the costs for transportation and handling tends to be lower than for lime since it can be transported in open trucks.[6]

In the past, when few full-scale units were in operation, it was generally believed that less scaling and higher removal efficiency could be attained with lime rather than limestone. This, however, has never been definitely proven to be the case. The trend today is slowly turning towards utilization of limestone instead of the more expensive lime. Of the plants under construction or contracted in the U.S., twice as many are based on limestone than on lime. Very few, if any, lime systems are under consideration for projected plants.

Nevertheless, some differences between lime and limestone have been observed. The dissolution rate of limestone is much slower than for lime. Mass transfer data also indicate a greater liquid-side resistance for the former. Although it has not been proven, the faster dissolution rate of lime probably leads to better load-following capability. An unsaturated mode is somewhat easier to attain with lime, as well. More important than the previously mentioned factors is the fact that in some cases instability of pH has occurred with limestone due to the slow dissolution rate.

Scrubber Systems

Prescrubber

A prescrubber can have several functions such as removal of fly ash and chlorides and prevention of temperature surges in the absorber. Since most of the absorber types are inefficient in particulate removal, venturi scrubbers are used for this purpose. The simple construction seems to pose no unique problems regarding the fly ash; however, some wet/dry deposition can build up on the top surface. Soot blowers or upstream prequenching can possibly eliminate this problem. The latter approach may cause corrosion, however.

A separate scrubber stage for removal of chlorides is desirable. The chloride not only causes increased problems with scaling and corrosion in the main absorber, but also lowers the removal efficiency. Magnesium and chloride act in opposite directions regarding the scaling; the higher the magnesium content is, the more chloride can be accepted. If the chloride content is higher than 5000 ppm, in the absence of magnesium, subsaturation of sulfate is impossible to achieve. Corrosion problems can occur at a few hundred ppm of chloride if stainless steel is used in the construction.

In order to prevent the chloride from coming in contact with the absorber, a separate loop and purge stream is necessary for the prescrubber. While all Japanese processes utilize it, this technique is used in the U.S. in only a few installations.

Absorber

Because of the difficulty in controlling the scaling problem, the main consideration in absorber design/choice seems to center around the scaling potential. Despite this fact, a trade-off exists among many other factors, such as pressure drop, mass transfer properties, turndown ratio, particulate removal, and gas/liquid distribution properties.

The simpler an absorber is in design, the smaller the risk of scaling is. Consequently, marble beds, involving stacked solid balls, are not installed anymore; also, devices such as turbulent contact absorbers and mobile beds are unnecessarily complex. Spray towers without packing, with grid-type packing, or with rods may be the best alternatives. A very interesting new type is the Weir cross flow absorber, Figure 3.

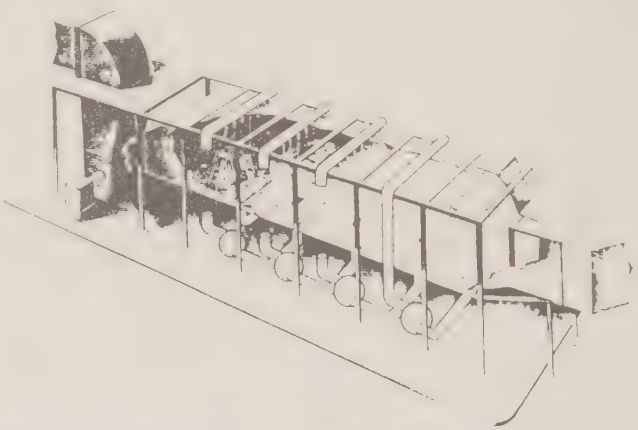

Figure 3. Schematic diagram of a Weir cross flow scrubber.

It is a horizontal vessel with no moving parts or packing involved, and can be regarded as an extension of the duct system. This simplicity may provide a very low scaling potential; however, the experience is limited to a commercial 170 MW test unit in operation for about one year. Some installations now under construction are expected to be in operation by late 1979/early 1980.[7]

The second important parameter is the pressure drop. A high pressure drop not only leads to a high power requirement, about 1% of the energy output of the electric generating system for 15 in. H_2O, but also to a high load on the induced draft fan which, combined with scaling and plugging, can cause fan failure.[8] The lowest pressure drop can be achieved in open vessels. For instance, the Weir scrubber displayed a pressure drop lower than 1.5 in. H_2O (at a gas velocity of 22 ft/sec). The venturi scrubber undoubtedly has the highest pressure drop; as much as 30 in. H_2O has been measured in a single unit.[7]

The mass transfer properties of the absorber are not of ut-

most importance; the removal efficiency is usually met, but in one installation in which this was not the case, the problem was simply solved through increasing the liquid flow rate. In general, very high liquid to gas flow ratios (L/G) exist in lime/limestone systems; the values are as high as 100 gal/10^3 ft^3 in some cases. This is in fact the order of magnitude necessary for countercurrent absorption in pure water, which indicates the relative slowness of the reactions. Consequently, the pump costs are high, with a power requirement of 1% of the energy output of the unit at an L/G of 75 gal/10^3 ft^3. However, a high L/G value is the simplest way to meet the SO_2 emission standard. In addition, scaling can be suppressed to a certain extent by circulating large amounts of liquid. Highest mass-transfer area is attained in a packed absorber, while venturis and open vessels generally provide a smaller area. The choice between cocurrent and countercurrent flow is of importance for limestone due to the slow dissolution rate of the reactant. A cocurrent absorber would require a much higher liquid flow rate than a countercurrent absorber to achieve the same SO_2 removal efficiency. This qualification, however, will be of minor importance in the choice between lime and limestone in the future, since other absorber designs are available.

The turndown ratio is limited only in a few types of absorbers, such as mobile beds and venturis with a fixed throat. If several parallel units are utilized, the problem can be avoided through the shutdown of one or more units at reduced boiler load.

High fly ash removal efficiency in the absorber is advantageous for several reasons; for instance, the particulate removal unit can be reduced in size, and the presence of fly ash helps prevent scaling. Most absorber types are poor in particulate removal. The most significant exceptions are the venturi and the mobile bed. In addition, it is claimed that the Weir scrubber achieves as high as 90% particulate removal.[3]

Proper gas/liquid distribution is in most cases connected with high pressure drop and scaling potential. An exception may be spray scrubbers with a short liquid contact time, like in the Weir scrubber, in which case the droplets do not extensively coalesce. A spray scrubber equipped with layers of rods or grids improves the distribution to a certain extent, but if many stages are utilized, poor distribution of the liquid is to be expected in the lower stages. Good distribution is offered by mobile bed and turbulent contact absorbers. In these types, compartments are included in order to keep the balls in position and thereby facilitate the distribution. In addition, since the volume of the gas in the absorber is much greater than the volume of the liquid, it can be inferred that it is the distribution of the liquid that is the critical factor in achieving good gas/liquid contact.

It is frequently stated that the liquid holdup is of great importance. This may be true in some exceptional cases, but in general it is of little importance. Firstly, the holdup does not vary significantly from one absorber type to another. Secondly, three conditions have to be met simultaneously for the holdup to be of significance. A low liquid to gas flow ratio, a high back pressure of SO_2 from the slurry, and significant reaction in the scrubber must exist.[9] All processes fail to meet the first condition, cocurrent processes with high removal efficiency fail to meet the second condition, and most limestone systems fail to meet the last condition.

Slurry Reaction Tank

The holding tank must be designed to allow added lime/limestone to mix properly, the reaction in the liquid from the scrubber to be complete, and the gypsum to precipitate. When the lime/limestone is added, proper mixing is a necessity to prevent bypassing of high pH liquor causing scaling in the scrubber. In practice, however, complete back mixing is hard to achieve. Therefore, a plug flow approach conveying the liquid smoothly as it is mixed is said to be preferred. In the cases where limestone is utilized, plug flow also aids in the completion of the reactions. In an investigation it was shown that the SO_2 removal efficiency was increased from 66 to 76% by changing from mixed flow to plug flow.[6]

A retention time of 5 to 10 min has been established to be the lower limit when considering the above mentioned factors. However, in practice much lower values are used to obtain a reasonably sized holding tank. The 5 to 10 min rule is hard to achieve, especially when high liquid flow rates are used.

References

1. H. S. Rosenberg, "How good is flue gas desulfurization?" *Hydrocarbon Processing* **57** (5): 132 (1978).
2. P. S. Lowell, "A Theoretical Description of the Limestone Injection-Wet Scrubbing Process," Vol. 1, PB-193029, National Technical Information Service, Springfield, VA, 1970.
3. J. C. Yarze and H. Hurwitz, "Scrubbing gas from high sulfur coal," *Electrical World* **190** (8): 76 (1978).
4. J. L. Phillips, "Precipitation Kinetics of $CaSO_4$-$2H_2O$," presented at Second International Lime/Limestone Wet-Scrubbing Symposium, New Orleans, LA, Nov. 1971.
5. A. V. Slack and J. D. Hatfield, "Removal of Sulfur Dioxide from Stack Gases by Scrubbing with Limestone Slurry: Operational Aspects of the Scaling Problem," presented at Second International Lime/Limestone Wet-Scrubbing Symposium, New Orleans, LA, Nov. 1971.
6. A. V. Slack and G. A. Hollinden, *Sulfur Dioxide Removal from Waste Gases*, Second Edition, Noyes Data Corporation, Park Ridge, NJ, 1975.
7. M. Smith and M. Melia, "EPA Utility FGD Survey: July-September 1979," EPA-600/7-79-022f, National Technical Information Service, Springfield, VA, Oct. 1979.
8. L. W. Nannen, R. E. West, and F. Krieth, "Removal of SO_2 from low sulfur coal combustion gases by limestone scrubbing," *JAPCA* **24**: 29 (1974).
9. P. V. Danckwerts, *Gas Liquid Reactions*, McGraw-Hill, New York, 1970.

Mr. Karlsson and Mr. Rosenberg are in the Chemical Process Development Section, Battelle Columbus Laboratories, 505 King Avenue, Columbus, OH 43201.

VIII

Reprinted from APCA JOURNAL, *Vol. 30, No. 7, July 1980*

Technical Aspects of Lime/Limestone Scrubbers for Coal-Fired Power Plants

Part II: Instrumentation and Technology

Hans T. Karlsson and Harvey S. Rosenberg
Battelle Columbus Laboratories

This is the conclusion of a 2-part article dealing with the technical aspects of lime/limestone scrubbers for coal-fired power plants. It covers instrumentation, particulate removal and sludge disposal. Part I (June JAPCA) covered process chemistry and scrubber systems.

Instrumentation

The monitoring of various process variables is justified due to the need for process control, checkup of operating conditions, and insuring that the SO_2 regulatory standard is met. Process control, i.e., rate of lime/limestone addition, can be based on pH sampling of the slurry, thus keeping the pH at a desirable level, or on a material balance based on the SO_2 inlet concentration in the flue gas.

The most common means of determining the gas flow is by measuring the pressure difference across part of the boiler system and calibrating on start up. Flow meters such as a pitot tube, hot-wire anemometer, etc. seem to be more troublesome, especially for the large flow rates that are involved in FGD systems, and are therefore not utilized frequently. The flow rate can be hard to specify due to possible gas leakage in dampers, heat exchangers, etc. Because of this, flow metering at different positions is desirable.

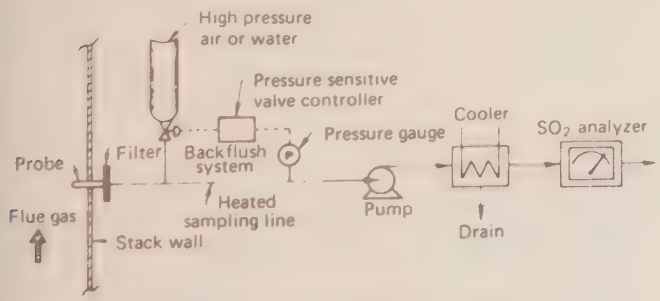

Figure 4. A successful sampling/monitoring system for SO_2.

Sampling SO_2 is a difficult problem for several reasons, due in part to the unspecified forms of sulfur species. The highly corrosive environment, which may vary from acidic to alkaline, and the presence of moisture, vapor, and entrained solids make it a delicate task. The SO_2 can be measured directly by a source/receiver system mounted on the duct system or the stack. Additional difficulties stem from the large dimensions.

Copyright 1980-Air Pollution Control Association

It is claimed that a properly designed sampling system is the most successful way to handle the problem (see Figure 4).[10] The gas is drawn via a heated system of a sampling probe, a filter, and a pump to a cooler. If the heating temperature is kept well above the flue gas temperature, no moisture or vapor will condense. Liquid in the sampling system will act as an absorbent for acidic species. The backflush system monitors the suction pressure of the pump continuously, and, when necessary, the probe and filter are backflushed with high pressure air or liquid. The gas is cooled to below the ambient temperature before the SO_2 concentration is measured, and part of the sample is allowed to pass through the drain to remove liquid. In this way, less than 1% of the SO_2 will be absorbed in the liquid.

Since the solids content is hard to predict, it may be necessary to measure the slurry concentration. One type of instrument that is considered is the nuclear density meter, which has been proven to work well, and has replaced a meter based on vibration in two cases. This type of checkup is most important for limestone systems due to the slow pH response. In general, use of the instrument is not widespread, and instead manual samples can be taken once or twice a day. Furthermore, a license is needed to handle the radioactivity.

The mist concentration/distribution in the flue gas is rather cumbersome to monitor; no simple and reliable method has been developed. To achieve good results, one must rely on microphotographic processes involving computerized evaluation of photos of the mist.[11]

Process Control

Lime/limestone addition is frequently based on a pH monitoring procedure. However, the method has been proven to be very unreliable. When the pH system does not follow boiler load fluctuations, pH instability occurs, possibly causing serious scaling problems. Shutdown of the FGD system can result. Two common reasons for failure of pH measuring systems are probe cracking and plugging of the sampling line. Development of new systems is underway. The pH probe should be located at the absorber effluent since changes in boiler load are first noted there. In order to avoid cracking of the probe, a small dip tank is suitable. A screened location in the scrubber, which is applied in some cases, is best.

In principle, feedback control based on the SO_2 concentration in the flue gas is as simple as pH sampling. The required addition of lime/limestone is specified by the measured

gas flow, the SO_2 inlet concentration, the desired outlet concentration based on the emission standard, and the stoichiometric ratio. Some problems need to be mentioned. At large boiler fluctuations, the response may not be fast enough. By setting one upper and one lower limit of the outlet concentration at which a considerable increase and decrease, respectively, in lime/limestone addition is initiated, the problem has been successfully solved.[12] Furthermore, high sulfur coals can cause an undesirably wide fluctuation in the SO_2 concentration. Since an absorber generally is designed for a fixed removal efficiency, the stoichiometric ratio has to be varied along with the fluctuation to maintain a fixed outlet concentration.

Additionally, a combination of two control methods is considered in some cases. For instance at Bruce Mansfield Unit 3, a pH system is planned, backed up by SO_2 feedback. Also, one system supplier uses a pH monitoring system as well as a supplemental signal based on boiler load.

Particulate Removal

The rigorous particulate emission regulations demand efficient and reliable removal devices. The trend is to utilize electrostatic precipitators (ESP) rather than wet scrubbers, although the latter approach offers the less expensive option of simultaneous removal of SO_2 and particulates. An availability exceeding 90% can probably be achieved without any excess capacity when using ESP. However, for low sulfur coals, the high ash resistivity may require hot ESP in which case fabric filters or wet scrubbers seem to be more attractive.

Wet particulate removal can be accomplished in a separate scrubber or in an absorber that also removes SO_2. In the latter case, the choices are limited since most absorbers are poor in particulate removal. Venturis are almost exclusively used as a separate scrubber for particulate removal. When a common slurry loop is used for both the scrubber and the absorber, particulate matter exists in the absorber. This can make it difficult to maintain the desired solids level, may increase mist eliminator plugging problems, and may increase wet-dry interface problems. It has been alleged that the particulates cause erosion in spray nozzles, venturi throats, areas of direct slurry impingement, and pumps. Although fly ash particles are harder than lime/limestone particles, they also can be much smoother and, thus, may be less erosive in some cases.

If the ESP is under-designed with respect to meeting the emission standards, the choice of an SO_2 absorber is limited. The types that have to be used, usually have a high potential for scaling and/or a high pressure drop. One possible exception is the Weir horizontal spray scrubber. However, available data and experience with this system are relatively limited. At Bruce Mansfield Unit 3, a Weir system is under construction. ESP designed for a removal efficiency of 95% will be used for primary particulate removal. A removal efficiency of greater than 99% is required to meet the emission regulations. It is claimed that the Weir scrubbers will remove 85% of the entering particulates,[13] so that the overall particulate removal efficiency will be 99.3%.

Mist Elimination

When the flue gas passes through the absorber units, small liquid droplets containing solids and dissolved species are entrained. It is desirable to remove this mist for several reasons:

- The droplets can deposit on downstream equipment and cause serious corrosion problems.
- If reheat is used, the operation of the reheater is adversely affected by the need to evaporate liquid droplets.
- If insufficient reheat is applied, rainout from the stack plume can occur.
- The mist contributes to the amount of particulate matter emitted.

The load on the mist eliminator depends on the type of absorber used and its effect on gas/liquid distribution. For instance a turbulent bed, with its high pressure drop and thus ability to distribute the gas and liquid, is better than grids. Although nozzles give a better distribution of slurry than an open pipe system, more liquid entrainment occurs when spray nozzles are used. A very important parameter is the gas velocity; in most cases a high velocity leads to a considerable amount of liquid entrainment. An exception may be the horizontal Weir scrubber. Once the liquid droplets have been entrained, they can only be removed by impaction or by a drastic change in the flow pattern. Thus, an increased spacing between the slurry distribution system and the mist eliminator does not significantly reduce the amount of entrainment.[14]

Various types of mist eliminators are available, almost all of which are based on the principle of inertial transport. One exception is the wet electrostatic precipitator. However, for lime/limestone scrubbing, the chevron type has become almost universal (Figure 5). The potential for plugging and scaling plays an essential role in this choice. The chevron mist eliminator seems to be the type that can combine low pressure drop and high collection efficiency with the lowest potential for plugging and scaling.

Figure 5. Horizontal chevron mist eliminator

One of the most extensive studies on the design of chevron mist eliminators has been conducted by TVA.[14] Also, design equations on pressure drop and efficiency have been developed by Calvert, *et al.*[15] However, much data are considered proprietary by the vendors. Most limestone systems are designed with a two-stage mist eliminator which allows more washing on the first stage because the second stage can remove the wash water mist. In the case of lime systems, about one-half use a single stage mist eliminator. The mist eliminator can also be designed with a method for bulk entrainment separation such as a perforated plate, a wash tray, a drastic change in flow direction, etc. Potential for scaling and high pressure drop are problems with the former two methods.

Although the chevron mist eliminator is in widespread use, operation is very troublesome, with scaling and plugging as the main problems. In fact, the mist eliminator is usually the device in the FGD system where scaling is first noted. Once scale has started to form it is very difficult to remove, especially when the main components are sulfate and sulfite. An uncontrolled growth can lead to shutdown of the whole FGD system due to the increased pressure drop. The severity of the problem depends on the excess capacity of the induced draft fans, the excess power consumption accepted, and the size of the plant. Therefore, scale formation may be tolerated for a period of 6 months in one case, while shut down after 1 week may occur in another case. The extent of the problem depends on the amount of liquid withdrawn from the absorber (higher blowdown allows washing the mist eliminator with more fresh water) and the amount of solids in the slurry, which can increase due to the presence of fly ash and thus cause more rapid plugging. Also, the material of construction is important. Solid plastic or stainless steel is preferable to thinly coated fiber-filled polymers because fibers exposed by erosion give sites for scale growth. However, stainless steel can be too heavy and too expensive, and some plastics cannot hold up against the stress caused by washing, the weight of deposits, and maintenance workers walking on them.

Spray washing, in combination with proper design, seems to be the only way to minimize scale formation in the mist eliminator. The present technology has developed as a result of trial and error and is still evolving. Continuous and/or intermittent washing can be used; the latter application provides a higher liquid flow rate which may remove hard scale, while the former is necessary to limit scale buildup. However, the effects are not fully understood. In some cases the total amount of washing liquid has been decreased by using brief intermittent high velocity washers, but this method is not universally accepted. Preferably, makeup water is used for washing if the water balance permits it. For instance, if thickener overflow water is used, the prevention of scale formation might not be successful at all. A collector tray allows the wash water to be handled separately from the scrubbing liquid at the expense of a higher pressure drop in the gas phase. If a two-stage mist eliminator is used, continuous underspray on the first stage and intermittent overspray or no wash on the second stage is common. The flow rate ranges from 30 gpm to as high as 2000 gpm for intermittent washing, while for continuous washing the range is 60 to 850 gpm. For each application, an upper limit exists due to the stress on the mist eliminators and the water balance.

Flue Gas Reheat

When flue gas is scrubbed it is cooled by evaporation of water to its adiabatic saturation temperature, typically about 125°F. In most cases it is considered to be of importance to reheat the gas, usually 20° to 60°F, in order to avoid the problems caused by the saturated gas and entrained mist. The moisture will otherwise condense on downstream surfaces, causing serious corrosion problems. Also, poor plume dispersion may cause high ground level concentrations of SO_2, and rainout from the stack may occur under certain weather conditions.

Different methods for flue gas reheat are listed in Table I, and an illustration of the most frequently used method, in-line reheat, is shown in Fig. 6. The major problem for this type of reheater is corrosion caused by chloride and sulfate. Neither carbon steel nor stainless steel have proved to be entirely satisfactory. The reason for this may, in many cases be attributed to inappropriate design of the reheat system. Plugging and deposition can also occur, but are more rare. Usually, proper use of soot blowers prevents this problem. Soot blowers may not remove hard scale, but frequent enough soot blowing may prevent hard scale deposition; generally soot blowing once every 4 hours with air or steam is enough.

Although there is a need for auxiliary fuel, or expensive alloys for in-line tubes, the cost of a reheater is not a major contributor to capital cost.

Fans and Ductwork

Dampers utilized for isolating sections of the duct system are of two types, namely louver and guillotine. Severe problems in operating dampers are experienced. Corrosion, erosion, fly ash buildup preventing opening and closing, and mechanical failures are some typical problems. However, the most serious deficiency is that all dampers leak and zero leakage can be achieved only by using double dampers with a higher pressure air barrier between them. However, even with this design, dampers can still leak in a dirty environment. Due to the leakage problem, it may be necessary to shut down the boiler to maintain the FGD system.[16] Louver dampers have a higher leakage rate than guillotine dampers, and therefore the latter offer an advantage with particulate-laden flue gas because of the more positive sealing action. On the other hand, guillotine dampers in the open position will leak to the atmosphere across the blade passage unless the blade is enclosed in a bonnet. Louver dampers are generally 10 to 15% less costly than guillotine dampers, but depending on service, louver dampers may not give the lowest cost installation.

The location and design of the fan is subject to differences of opinion. Some basic rules of thumb have however emerged. If wet particulate removal is used, the fan is preferably placed after the stack gas reheater in order to prevent condensation. Dry particulate removal gives the choice of placing the fan before or after the absorber, but in the former case the fan will require more horsepower because of the higher volume of flue gas. With a combination of wet/dry particulate removal, locating the fan before the scrubber is limited by the maximum particulate loading the fan can handle.

Wear by fly ash and deposition on the fan blades are the major operational problems with dry and wet fans, respectively. These problems can cause vibration and high torque leading to excessive noise and, in the worst case, rotor cracking. The scroll areas of wet fan housings have been protected with rubber linings but scale deposits can break off and cut the rubber. The trend is to use expensive materials of construction such as Inconel if a wet fan must be employed in the FGD system.[17]

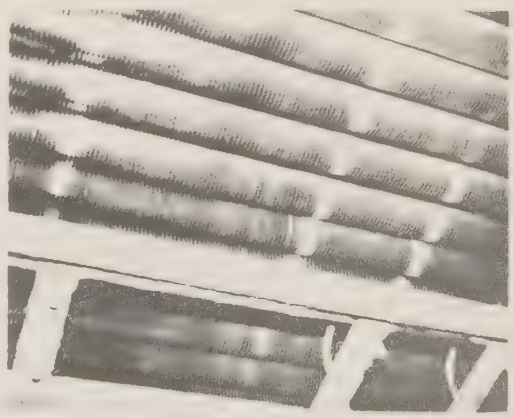

Figure 6. A finned tube in-line flue gas reheater

Sludge Disposal

A bleed stream from the reaction tank is sent to a thickener or directly to a pond. Thickener underflow, containing as much as 70% water, can be further dewatered if desirable; the

Table I. Classification of reheat methods.

In-line	Direct combustion	Indirect with hot air	Bypass	Exit gas recirculation	Waste heat recovery
Heating with steam or hot water in tubes	Firing of gas or low sulfur oil in the duct or an external chamber	Addition of ambient air, heat-exchanged with steam	Part of the flue gas is bypassed around the absorber	Part of the flue gas is heated and recirculated	Utilization of the heat in the flue gas before passing through the absorber

most common device for this is a vacuum filter but centrifuges are also used. A solids content as high as 90% can be obtained by filtering, but this value is highly dependent on the sulfate to sulfite ratio in the sludge. The amount of sludge depends on the stoichiometric ratio, which is usually higher for limestone than lime, the method of fly ash removal, and the degree of oxidation. The molar weight ratio of $CaSO_4 \cdot 2H_2O$ to $CaSO_3 \cdot \frac{1}{2}H_2O$ is 4 to 3, but on the other hand this is balanced by the fact that sulfate is easier to dewater than sulfite. Thus, the sludge consists of a mixture of sulfite and sulfate, and in some cases fly ash. The presence of fly ash in oxidized slurry appears to decrease the settling rate to 1.5 cm/min as compared to 2.4 cm/min with a very low fly ash content. If forced oxidation is applied in the absence of fly ash, for instance through air sparging in the reaction tank, a gypsum sludge can be obtained that may have a market value. In Japan, the gypsum market has become saturated[18] and in the U. S. only a very limited market, mainly for agricultural purposes, may exist. Consequently, most plants dispose of the sludge at a pond or use it for landfill. Both the disposal and transportation of the sludge, except slurry pipelines, require stabilization and/or an increase in the solids fraction. In order to be transported by truck or rail, the sludge must be stabilized because calcium sulfite is thixotropic and therefore can reliquefy under stress. For long hauling, conceivable options are addition of fly ash, forced oxidation, and addition of lime, or combinations of the methods mentioned. For stabilization of the sludge, additives can also be used to make the solids agglomerate and form a very hard and stable substance. The amount of fly ash that can be added depends on the sulfur and ash content in the coal and the degree of dewatering before disposal. If there is a surplus of fly ash, less dewatering can be used and more fly ash added. The bottom ash can also be used, and if all the ash is added the need for a separate ash disposal area is eliminated.

Table II. List of engineering properties that have to be considered for disposal of sludge.

1. Grain size
2. Moisture content
3. Angle of repose
4. Dry density
5. Angle of friction
6. Cohesion
7. Bearing capacity
8. Compressibility
9. Consolidation
10. Permeability

Sludge containing fly ash can be dewatered to a 50% solids content, but there probably is a need for additives if landfill is to be employed. There are many engineering properties of the sludge that have to be considered for the design of a landfill (see Table II). These depend on what the site will be used for, i.e., construction, recreation, pond. One of two possible design approaches must be adapted for landfills located over usable aquifers in the U. S.—either a natural liner of soil equivalent to at least 10 ft of clay, or a liner with a sump to collect leachate. The design depends on transport of salts to groundwater which, in turn, depends on permeability of indigenous soils. Figure 7 shows a lined clay pond supplied by sludge through a pipeline.

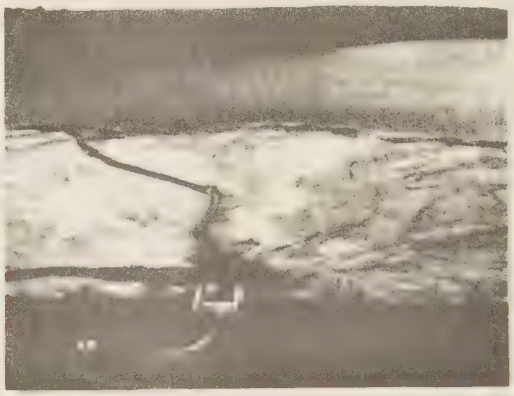

Figure 7. Clay-lined sludge pond.

One of the main problems in lime/limestone based FGD systems, closely related to sludge disposal, is the difficulty in closing the water loop. If the slurry is dewatered to a large extent, part of the overflow liquid must be blown down to prevent buildup of soluble species such as chlorides. Alternatively, if large amounts of water are used for pumping the slurry to a disposal pond, it may be necessary to dispose of part of the water to a natural water system when the pond level rises too high. In some areas, however, the air is so hot and dry that all of the water evaporates from the pond. Attempts have been made to return the liquid to the scrubber system, with considerable increase in scaling and shut down as a consequence.

Final Remarks

Although the number of lime/limestone FGD systems shows rapid growth, it may not be taken as an indication that the technology is commercially available. It seems to be possible to deduce from the experience of operating plants that safe and trouble-free equipment to be used for vital components system are not available. Nevertheless, great progress has been made, merely on an empirical basis, and hopefully this trend will accelerate.

References

Note: References 1 through 9 appeared in Part I. in *JAPCA* 30(6): 710 (1980).

10. S. Miller, private communication to H. S. Rosenberg, 1978.
11. H. N. Conkle, H. S. Rosenberg, and S. T. DiNovo, "Guidelines for the Design of Mist Eliminators for Lime/Limestone Wet Scrubbing Systems," EPRI FP-327, Palo Alto, CA, 1976.
12. D. T. Rabb, "Shawnee Operating Experience," paper presented at Industry Briefing Conference on Results of EPA Lime/Limestone Wet Scrubbing Test Programs, Raleigh, NC, Aug. 1978.

13. W. J. Raymond, A. G. Sliger, and J. J. O'Donnell, "Kellogg/Weir Scrubbing System for Bruce Mansfield Unit 3," paper presented at Fourth Annual International Conference on Coal Gasification, Liquefaction, and Conversion to Electricity, Pittsburgh, PA, Aug. 1977.
14. J. J. Schultz, T. M. Kelso, S. L. Glasgow, and R. M. Cole, "Performance of Entrainment Separators in Slurry Scrubbing Processes," Bulletin Y-93, National Fertilizer Development Center, Tennessee Valley Authority, Muscle Shoals, AL, June 1975.
15. S. Calvert, I. L. Jashnani, S. Yung, and S. Stalberg, "Entrainment Separators for Scrubbers—Initial Report," PB-241 189, National Technical Information Service, Springfield, VA, 1974.
16. R. W. McIlvaine, "Louver vs. guillotine dampers," *Wet Scrubber Newsletter* (30) 12 (1976).
17. A. V. Slack and J. D. Hatfield, "Removal of Sulfur Dioxide from Stack Gases by Scrubbing with Limestone Slurry: Operational Aspects of the Scaling Problem," paper presented at Second International Lime/Limestone Wet-Scrubbing Symposium, New Orleans, LA, Nov. 1971.
18. J. Ando, "SO_2 Abatement for Stationary Sources in Japan," EPA-600/7-78-210, National Technical Information Service, Springfield, VA, Nov. 1978.

Mr. Karlsson and Mr. Rosenberg are in the Chemical Process Development Section, Battelle Columbus Laboratories, 505 King Avenue, Columbus, OH 43201.

IX

Selective Catalytic Oxidation of NO to NO_2*

By Hans T. Karlsson and Harvey S. Rosenberg

Battelle Columbus Laboratories
Columbus, Ohio

Abstract – The objective of this program was to investigate the conversion of NO to the more readily absorbed NO_2 by means of selective catalytic gas-phase oxidation with the oxygen present in the flue gas.

A literature search and written request to catalyst manufacturers in the U.S. and Japan were used to identify candidate catalysts for the oxidation of NO. A total of 14 catalysts were tested in a fixed bed reactor using simulated flue gas of a composition that reflects the conditions when burning high sulfur coal. The catalysts were tested at a space velocity $\geq$ 1,500 hr^{-1} in the temperature range of 150 to 800 F.

Several catalysts exhibited optimum performance at 200 F. A total of 5 catalysts oxidized more than 50 percent NO at this temperature; Fe_2O_3/MnO/ZnO was the best one with 73 percent oxidation. However, when the catalysts were exposed to simulated flue gas in relatively long-term runs, deactivation was observed after about 14 hours. The causes for this deactivation have not been determined. Additional work is needed to solve the problem of deactivation as well as to find a more active catalyst.

---

* Final Report on "Development of a Flue Gas Treatment System for NO_x Removal at a Coal-Fired Power Plant" to Tennessee Valley Authority
January 23, 1981
Task 1.; pp. 4-38, and 68-70

TABLE OF CONTENTS

	Page
INTRODUCTION	1
BACKGROUND	2
OBJECTIVE AND SCOPE	5
CATALYSTS FOR OXIDATION OF NO	5
Literature Review for Identification of Catalysts	5
Selection of Catalysts for Experimental Program	11
Preparation of Catalysts	13
EXPERIMENTAL PROGRAM	14
Experimental Conditions	14
Description of Apparatus	15
Experimental Procedure	17
RESULTS	18
DISCUSSION	25
REFERENCES	27

INTRODUCTION

Nitric oxide (NO) and nitrogen dioxide (NO_2) are among the most active and undesirable pollutants in the atmosphere. The symbol NO_x is frequently used to collectively represent these two oxides of nitrogen. Six other nitrogen oxides are known to exist but they seldom occur in the atmosphere in measurable quantities and then only under special conditions. Not only are NO and NO_2 toxic in themselves, but also they are an important link in the chain of photochemical reactions leading to the formation of smog in the atmosphere.

The major component of worldwide atmospheric NO_x is biologically produced NO. Natural sources produce about 500×10^6 tons of NO per year while man-made sources emit 50×10^6 tons of NO_x per year. However, NO_x concentrations in urban areas are 10 to 100 times higher than those in non-urban areas, thus reflecting the importance of technological sources over natural sources.

Until recently, the NO_x emissions from stationary sources have not received as much attention as some other pollutants, namely, SO_2 and particulates. However, with progress being made in the areas of SO_2 and particulate control, the problems of NO_x control are becoming the focus of more intensive research and development. Although EPA officials currently believe that only three air quality regions -- Chicago, Denver, and Los Angeles -- definitely exceed the national ambient air quality standard for NO_2, the problem of NO_x emissions from stationary sources should not be overlooked. The need for NO_x control technologies from power generation systems has been emphasized by recently stated Federal research goals. It has been proposed that a suitable goal for coal-fired utility boilers is an NO_x emission standard of 100 ppm by 1985.

Generally speaking, two types of control technologies have been considered for NO_x -- combustion modification and stack gas treatment. However, if coal-fired utility boilers are required to achieve an emission level of 100 ppm of NO_x by 1985, stack gas treatment may be the only available technology to meet this standard in the required time frame.

Although the concentration of NO_x in flue gases is low (actual values range from 200 to 1500 ppm with an average value of 750 ppm), the volume of gas emitted by large installations is so great that significant amounts of NO_x are released into the atmosphere on an individual plant basis. The processing of large volumes of gas for NO_x emission control

presents formidable engineering problems in gas contacting, equipment size, pressure drop, and temperature control. Furthermore, other flue gas species such as H_2O, CO_2, SO_2 and O_2 can interfere with certain removal processes, especially for low concentrations of NO_x. The types of applicable processes include catalytic reduction, homogeneous reduction, catalytic decomposition, adsorption, absorption, etc. Absorption or wet scrubbing processes usually involve simultaneous removal of NO_x and SO_2 because when SO_2 is present in the gas, it is difficult to avoid SO_2 absorption. Furthermore, SO_2 absorbed from flue gas can assist in NO_x absorption. If nitrogenous by-products could be recovered for use as a fertilizer, the attractiveness of wet scrubbing processes would be further enhanced.

Most of the active process development work is taking place in Japan. The three leading stack gas treatment techniques for NO_x control are catalytic reduction with ammonia, non-catalytic reduction with ammonia, and direct scrubbing of NO with simultaneous absorption of SO_2. The wet processes are much less developed than the dry processes.

BACKGROUND

Wet methods for NO_x removal are limited by the relatively inert nature of NO. The NO_x in flue gas is approximately 90 percent NO. This difficulty can be overcome by oxidation of NO to the more reactive NO_2 in the gaseous phase using ozone or ClO_2 prior to absorption (oxidation absorption). Ozone is the best oxidizing agent but is very expensive. The cost of ClO_2 is 30 to 40 percent lower than that of ozone, but the use of ClO_2 introduces a considerable amount of chloride into the scrubbing liquor, thus causing waste disposal problems. Ozone and ClO_2 oxidize NO to NO_2 within a one-second residence time.

NO can be oxidized by the oxygen in flue gas, but with low NO concentrations the non-catalytic reaction is very slow and the rate decreases with increasing temperature. Figure 1 shows the percent conversion of NO to NO_2 as a function of residence time with temperature as a parameter, for flue gas containing 5 percent oxygen and 750 ppm NO. At 300 F, a residence time of about 150 minutes (space velocity of about 0.4 hr^{-1}) is required to convert 90 percent of the NO to NO_2.

Several oxidation absorption-reduction processes are under development in Japan for the simultaneous removal of NO_x and SO_2 from

stack gas. In this type of process, NO is first oxidized to the more reactive NO_2 which is then absorbed. Because of the nature of the process chemistry in the liquid phase, usually 4 to 5 moles of SO_2 are needed for each mole of NO_x for efficient removal of NO_x. Most of the absorbed NO_x is reduced to nitrogen or NH_3 by sulfite ions (absorbed SO_2) so that the formation of undesirable nitrites or nitrates is greatly reduced or eliminated. Any NH_3 produced must be either recovered for use or decomposed.

One of the simplest and potentially least expensive methods for converting NO to NO_2 is by catalytic oxidation using the oxygen present in the flue gas. It would be desirable to find a catalyst that:

- Oxidizes virtually all of the NO to NO_2 at a space velocity of 1,000 hr^{-1} or higher
- Shows optimum performance in the temperature range of 300 F down to 150 F
- Does not oxidize SO_2 to SO_3
- Does not become poisoned by sulfur compounds or other species present in the flue gas.

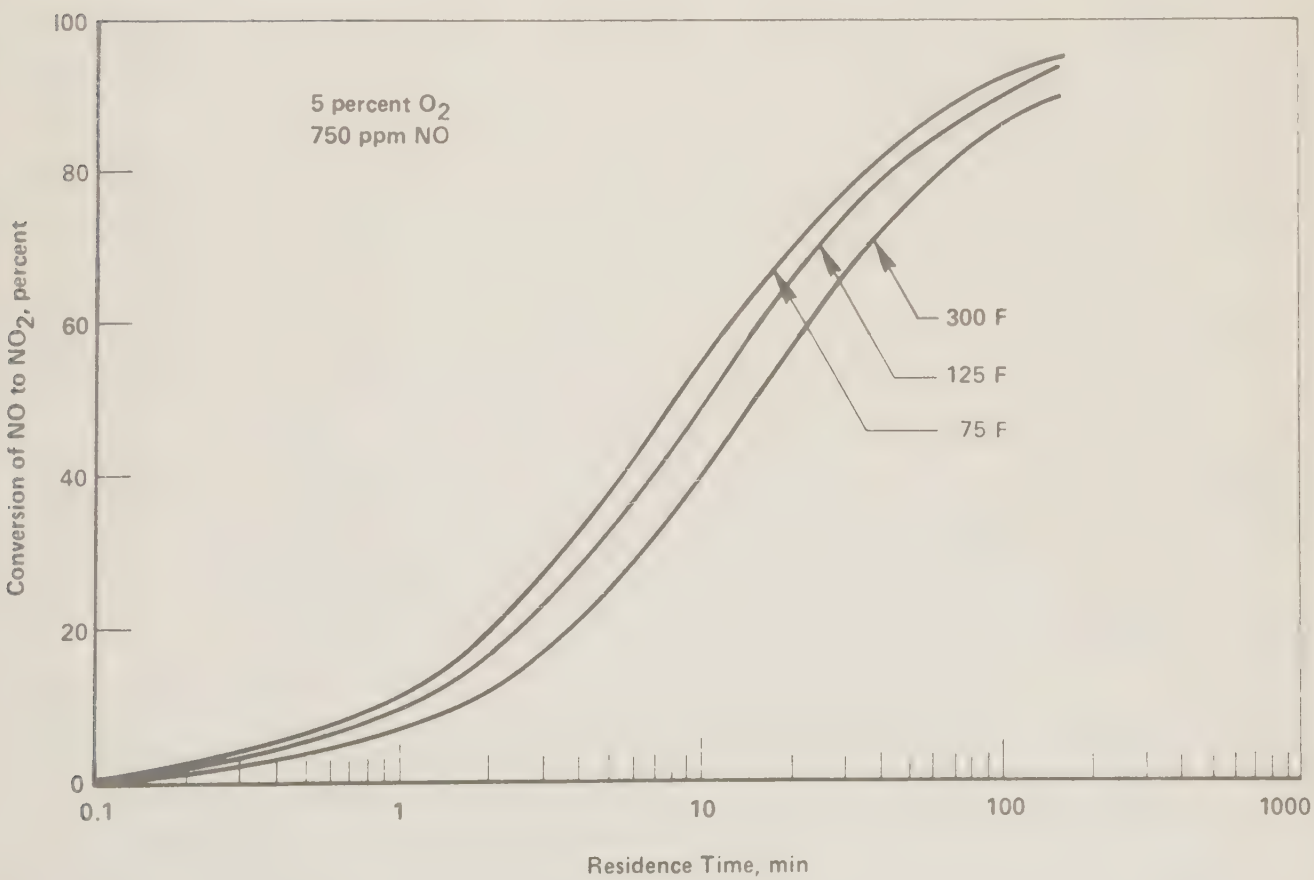

FIGURE 1. RESIDENCE TIMES FOR UNCATALYZED CONVERSION OF NO TO NO_2 IN FLUE GAS

Although the oxidation absorption-reduction processes under development are based on complete oxidation of NO to NO_2, it is still possible to remove NO_x along with SO_2 if some of the NO_x exists as NO. In this case, NO_x is absorbed in the form of N_2O_3 and N_2O_4, rather than N_2O_4 alone. For efficient removal, the molar ratio of NO_2 to NO must be at least one. However, equimolar absorption of NO and NO_2 may lead to the formation of undesirable nitrites and nitrates in the scrubbing liquor.

The size of a catalytic reactor is inversely proportional to the space velocity. Therefore, the lower limit of space velocity is determined by practical engineering considerations with regard to reactor size and pressure drop across the reactor. In processes employing selective catalytic reduction of NO_x with ammonia, the lowest space velocity used is about 1,000 hr^{-1} and this value can be considered as a guideline for engineering design.

Flue gas leaves the air preheater of a boiler at a temperature of about 300 F and usually enters an electrostatic precipitator for particulate removal. Therefore, if the catalytic reactor can be operated at 300 F or below, catalytic oxidation can be an add-on process and particulates should not affect the catalyst. If an operating temperature above 300 F is required, the air preheater would have to be divided into two units with the reactor inserted between the units. Also, the particulates would have to be removed ahead of the catalyst or the catalyst would have to tolerate the full particulate loading of the flue gas. An operating temperature below 300 F can be achieved by spray cooling the flue gas with water. At about 125 F, the flue gas becomes saturated with water (adiabatic saturation temperature) and cannot be cooled further by evaporation. Therefore, the catalytic reactor should be operated at a minimum temperature of 150 F to prevent condensation of water on the catalyst. After catalytic oxidation of NO to NO_2, the flue gas can be sent to a scrubber for simultaneous removal of NO_2 and SO_2. The scrubber will cool the flue gas to its adiabatic saturation temperature.

If SO_2 is oxidized to SO_3, condensation of sulfuric acid mist may occur in the catalytic reactor and in the ductwork downstream from the reactor, and may cause corrosion problems. Large amounts of SO_3 would also be expected to influence the wet scrubbing process with regard to process chemistry and sulfur removal efficiency. Absorption of SO_3 results in formation of sulfates rather than sulfites, and acid mist is very difficult to scrub from a gas stream.

OBJECTIVE AND SCOPE

The objective of this study was to experimentally investigate the conversion of NO to the more readily absorbed NO_2 by means of selective catalytic gas-phase oxidation with the oxygen present in flue gas. Gas mixtures in cylinders were used to simulate flue gas from a power plant burning high sulfur coal. Thus, a relatively high SO_2 concentration was established to make the concept suitable for wet scrubbing processes in which a high molar ratio of SO_2 to NO_x is needed for efficient removal of the latter. A total of about 85 experiments were performed with 14 catalysts on a uniform engineering basis by passing the simulated flue gas through a fixed bed reactor. The ranges of temperature and space velocity were chosen to reflect practical operating conditions.

CATALYSTS FOR OXIDATION OF NO

Literature Review for Identification of Catalysts

A comprehensive screening of pertinent literature was conducted in order to identify candidate catalysts and to obtain background information on the selective catalytic oxidation of NO to NO_2. Computerized searches of the five data files listed in Table 1 were conducted and a complete hand search of Chemical Abstracts was carried out. As a result of this effort, 180 references were obtained, out of which about 80 explicitly treat the subject of catalytic oxidation of NO. The number of references found in the different sources is summarized in Table 1.

The first documented study on catalytic gas phase oxidation of NO to NO_2 dates back to the early 1920's. At that time, McKee[1] obtained a patent for oxidation of NO by using silica gel as a catalyst. Since then, over 50 experimental investigations have been reported in the literature. Most of the studies are based on the behavior of a "clean" flue gas containing no SO_2.

The classification of catalysts investigated and the preparation of a review of published studies are difficult problems because catalysis is still an art rather than a well-defined science. The situation is exacerbated for the oxidation of NO because many publications are in Japanese.

TABLE 1. SUMMARY OF LITERATURE SEARCH

Source	Number of References			
	Printouts	Pertinent	Found in Hand Search	Net
Chemical Abstracts (1907-1979) (Hand Search)	--	166	--	166
Chemical Abstracts (1967-1979) (Computerized Search)	49	3	2	1
Air Pollution Technical Information Service (Computerized Search)	123	19	6	13
Pollution Abstracts (Computerized Search)	4	0	0	0
National Technical Information Service (Computerized Search)	6	0	0	0
Smithsonian Science Information Exchange (Computerized Search)	3	0	0	0
Total	--	--	--	180

The identified catalysts can be divided into three categories:

- Catalysts on a carrier
- Catalysts consisting of a mixture
- Catalysts consisting of a single compound.

Catalysts can also be classified on the basis of the active species or the method of preparation. The method of preparation is of utmost importance with regard to the properties of a catalyst. Common preparation methods for active species on a carrier include plasma spraying, precipitation of salts with subsequent calcining, and ion exchange. Catalysts consisting of a mixture are prepared by co-precipitation and extrusion of the solids, direct pelletizing, or from a paste or slurry with subsequent drying and crushing.

The first catalysts investigated consisted of single compounds such as activated carbon, silica gel, and different minerals. For instance, in 1922 Burdick[2] found that activated carbon and charcoal accelerate the oxidation rate as much as 500 fold. The activity was found to decrease in the presence of water vapor. Since then, several researchers have investigated the use of activated carbon as a catalyst for NO oxidation.[3-9]

The most comprehensive work on activated carbon has been conducted by Hougen and co-workers,[10-16] who determined the mechanism of the reaction, the rate equation, and the influence of water vapor and temperature. They also suggested a method to determine the optimum design of a catalytic reactor for NO oxidation. The reaction mechanism is of principal importance and can be represented by the following series:

$$2NO\ (g) \rightleftharpoons (NO)_2\ (g)$$

$$(NO)_2\ (g) \rightleftharpoons (NO)_2\ (ads)$$

$$(NO)_2\ (ads) + O_2\ (g) \rightleftharpoons 2NO_2\ (ads)$$

$$2NO_2\ (ads) \rightleftharpoons 2NO_2\ (g)$$

The overall rate was found to be controlled by the reaction between adsorbed $(NO)_2$ and oxygen in the gas phase to form adsorbed NO_2 (surface reaction). Water vapor was found to reduce the reaction by reversible adsorption on the active sites of the catalyst.

Szego[17] found that silica gel increased the oxidation rate by a factor of 20 at room temperature. Kurin, et al.[18] suggested a rate expression for the reaction. They also found water vapor to diminish the reaction rate.[19] Hougen and co-workers[10-16] also investigated silica gel, and found the reaction mechanism to be similar to the one for activated carbon. Several other researchers have studied the use of silica gel as a catalyst for the oxidation of NO.[20-27]

Although activated carbon exhibits a much greater activity than silica gel, the space velocity needed to oxidize NO to NO_2 with activated carbon is still too low. Using Burdick's[2] data for peach-kernal charcoal, the space velocity required to oxidize 50 percent of the NO to NO_2 in typical flue gas is about 450 hr^{-1}. According to the data of Rao and Hougen,[10] a space velocity of about 280 hr^{-1} is required to convert 90 percent of the NO to NO_2 at 350 F using activated carbon as a catalyst, with flue gas containing 5 percent oxygen and 750 ppm NO.

Research and development have gradually been focused on more complex catalysts involving metals in the form of elements, oxides, or exchanged (adsorbed on molecular sieves) ions. Over 20 different metals have been investigated in the form of mixtures or on a carrier. Since investigations are usually based on previous findings, the frequency of appearance of metals in the literature on catalytic oxidation of NO may reflect their desirable properties. Table 2 contains an estimate of the

TABLE 2. PREVIOUS INVESTIGATIONS OF VARIOUS METALS USED IN CATALYSTS FOR THE OXIDATION OF NO

Metal	Approximate Number of Investigations
Cr	15
Cu	15
Mn	15
Co	10
Fe	5
Ni	5
Pd	5
Pt	5
Ru	5
V	5

number of previous investigations with various metals. In addition, lead, magnesium, molybdenum, silver, and rhodium have been investigated once or twice. In general, previous investigators have selected metals that are known to have catalytic properties.

It is difficult to compare the various investigations because of the different conditions used in each case. However, a few individual studies have compared the activities of different catalysts.[28-30] Table 3 summarizes the findings of these studies which include mostly the same metallic elements, but on different carriers. The catalytic activity of the various metals is reversed when switching from an alumina to a zeolite carrier. Seiji[28] and Miyadera, et al.[29] also investigated noble metal catalysts, but these had much less activity than the oxides listed in Table 3.

Takayasu, et al.[31] performed test runs in a fixed bed reactor with Cr_2O_3 catalyst on eight different carriers. Table 4 summarizes the results which clearly show the Al_2O_3 carrier to be superior, especially when SO_2 and H_2O are present.

Takayasu, et al.[31] also studied the effect of the method of

TABLE 3. COMPARISON OF CATALYSTS FOR OXIDATION OF NO

Activity	Carrier	Temperature, F	Gas Composition	Reference
$CoO > MnO_2 > Fe_2O_3 > CuO$	Al_2O_3	480-700	500 ppm NO, 200 ppm SO_2, 4% O_2, balance H_2O and N_2	Seiji (28)
$MnO_2 = CoO > NiO > Cr_2O_3$	None	570-750	750 ppm NO, 4% O_2, balance N_2	Miyadera et al. (29)
$Cu = Cr^{3+} > Fe = Co^{2+} > Ni^{2+} = Mn^{2+}$	Zeolite	500-700	300 ppm NO, 6.4% O_2, balance N_2	Arai et al. (30)

catalyst preparation on the performance. Two samples of Cr_2O_3 catalyst on Al_2O_3 carrier were prepared, one by impregnation and the other by co-precipitation. Both samples were exposed to flue gas as specified in Table 4. The impregnated catalyst exhibited twice as much oxidation as the co-precipitated catalyst, both in the presence and absence of SO_2 and H_2O.

Most studies indicate that SO_2 and H_2O suppress the oxidation rate. However, Arai, et al.[30] found that the oxidation increased from 40 to 75 percent over a Cr^{3+}-zeolite catalyst when 8.3 percent by volume of H_2O was added to the flue gas. Takayasu, et al.[31,32] state that SO_2 and H_2O poisoning are reversible for Cr_2O_3 on Al_2O_3 and MnO_2 on Al_2O_3, respectively. The statements are based on the observations that the oxidation increased when SO_2 and/or H_2O were removed from the gas stream. The test runs were performed for a period of a few hours so that the findings may not be applicable to long term runs. Seiji[28] and Hattori, et al.[33] found the poisoning effect to be enhanced at low temperatures. A concentration of 500 ppm SO_2 is enough to cause a strong deactivation for metal oxides on Al_2O_3 according to Takayasu, et al.[31] and Hattori, et al.,[33] while Arai, et al.[30] observed strong deactivation at 200 ppm SO_2 for ion-exchanged zeolites. Findings by Takayasu, et al.[31] show the deactivation to be very low for a Cr_2O_3/Al_2O_3 catalyst at 300 ppm SO_2.

Hattori, et al.[33] investigated MnO_2 on SiO_2-Al_2O_3 and on

Al_2O_3, and found the former carrier to be superior with respect to SO_2 poisoning. This is in contradiction with the findings of Takayasu, et al.[31] for a Cr_2O_3 catalyst as reported in Table 4. Hattori, et al.[33] also found that SO_2 can be tolerated if V_2O_5, Sb_2O_3, or Bi_2O_3 is added to the catalyst. However, the investigation was limited to 500 ppm SO_2.

Takasu, et al.[34] found Sm_2O_3 to work as promotor when using NiO catalyst without a carrier. The optimum composition was determined to be 3.75 percent Sm_2O_3 and the activity increased 3.7 times due to increased surface area and monatomic oxygen chemisorption.

Two investigations showed that single metal oxides on Al_2O_3 work better than mixtures of oxides on Al_2O_3. Takayasu, et al.[31] observed no enhancing effect when some of a Cr_2O_3 catalyst was replaced by oxides

TABLE 4. EFFECT OF CARRIERS WITH Cr_2O_3 CATALYST ON NO OXIDATION[a][31]

Carrier	Percent Oxidation of NO	
	Clean Flue Gas[b]	SO_2/H_2O Present[c]
Al_2O_3	66	50
Bauxite	43	6
ZnO	19	6
SiO_2	9	11
SiO_2-Al_2O_3	22	6
MgO	14	6
SiC	19	8
Activated Carbon	2	-

(a) Space velocity is 24,000 hr^{-1} and temperature is 570 F.

(b) 500 ppm NO, 10% O_2, balance N_2.

(c) 500 ppm NO, 10% O_2, 500 ppm SO_2, 10% H_2O, balance N_2.

of cobalt, iron, copper, vanadium, or magnesium. In fact, the degree of oxidation decreased by about one-third. Seiji[28] studied some binary mixtures and found the activity to decrease in the following order: CuO/MnO_2 > CoO/CuO > CoO/MnO_2 > CoO/Fe_2O_3. The highest rate of conversion with the best mixture, CuO/MnO_2, was 80 percent, while with the best single oxide, CoO, it was 90 percent, with the temperature in the range of 480 to 660 F in both cases.

Selection of Catalysts for Experimental Program

Letters were sent to 23 catalyst companies in the U.S. and 19 in Japan to request catalyst samples to be tested for gas phase oxidation of NO to NO_2. One company in the U.S. (Climax Molybdenum) and one company in Japan (Tanaka Kikinyoku Kogyo) provided catalyst samples in response to this request. Table 5 summarizes the catalysts used in this study. The catalysts are divided into three groups. The first group was selected on the basis of the data in the literature and the samples were prepared at Battelle. The second group was also selected on the basis of the literature search, but the samples are commercially available. The third group consists of samples provided by manufacturers as a result of the request.

It was difficult to select the optimum set of catalysts on the basis of the information given in the literature. The ion-exchanged zeolite catalysts were selected because of findings by Arai, et al.,[30] who obtained a high degree of oxidation at a high space velocity. Catalysts Nos. 1 through 3 represent the catalysts which were reported to give the best performance. Catalyst No. 4 was selected because Kotera, et al.[35] removed more than 85 percent of the NO_x from real flue gas using this type of catalyst for oxidation of NO at a space velocity of 15,000 hr^{-1}, with subsequent scrubbing of the NO_x. Catalyst No. 5 was selected because Takeyama, et al.[36] were granted a patent which claims that the oxidation efficiency of a MnO_2/PbO catalyst is 90 percent at a space velocity of 7,500 hr^{-1}. Catalyst No. 6 was selected on the basis of the study by Hattori, et al.,[33] since they claimed that the poisoning effect of SO_2 can be tolerated in the presence of Sb_2O_3.

Catalyst Nos. 7, 8, and 9 are commercially available from The Harshaw Chemical Company and were selected for investigation because they have performed well in several studies as previously discussed.

Catalyst Nos. 10 through 13 were supplied by Climax Molybdenum Company, and Catalyst No. 14 by Tanaka Kikinyoku Kogyo in response to a specific request for catalysts to oxidize NO to NO_2.

TABLE 5. CATALYSTS SELECTED FOR INVESTIGATION

Catalyst Number	Active Species	Carrier	Size	Shape
		Prepared at Battelle		
1	Cr^{3+}	13X Zeolite	8-12 mesh	Spheres
2	Fe^{2+}	13X Zeolite	8-12 mesh	Spheres
3	Cu^{2+}	13X Zeolite	8-12 mesh	Spheres
4	$Fe_2O_3/MnO/ZnO$	None	3/16 in.	Pellets
5	MnO_2/PbO	None	< 1/4 in.	Irregular particle
6	$CuO/MnO_2/Sb_2O_3$	None	< 1/4 in.	Irregular particle
		Commercially Available		
7	Cr_2O_3	Al_2O_3	5/32 in.	Pellets
8	NiO	Al_2O_3	1/8 in.	Pellets
9	CoO	Al_2O_3	1/8 in.	Pellets
		Supplied by Manufacturers		
10	Fe_2O_3/MoO_3	Al_2O_3	1/8 in.	Granules
11	CuO/MoO_3	Al_2O_3	1/8 in.	Granules
12	Bi_2O_3/MoO_3	Al_2O_3	1/8 in.	Granules
13	V_2O_5/MoO_3	Al_2O_3	1/8 in.	Granules
14	Pt	Al_2O_3	< 1/4 in.	Spheres

Preparation of Catalysts

The zeolite-based catalysts were prepared with an 8 to 12 mesh 13X molecular sieve and chlorides of chromium, iron, and copper. The type of sieve used has the following molar formula:

$$Na_2O \cdot Al_2O_3 \cdot 2.8 \pm 0.2SiO_2 \cdot xH_2O.$$

The sieve was slowly added to distilled water while stirring in order to remove excess sodium by a thorough wash. Three solutions were prepared using chromium (III), iron (III), and copper (II) chloride. Each solution was divided into five portions and each portion contained the stoichiometric amount of positive ions required to replace all of the sodium ions in the sieve. One portion of a salt solution was added to molecular sieve and the slurry was stirred for 6 to 12 hours to achieve equilibrium. The sieve was then separated from the solution and washed with distilled water. The procedure was repeated with the remaining four portions of salt solution. The degree of ion exchange of a sieve increases as the ratio of sodium to metal ion in the solution decreases. Thus, a high total degree of exchange can be obtained by a step-wise procedure using fresh solution each time since sodium is removed in each step. The prepared catalysts were dried at 120 C for 48 hours.

An automatic tablet machine was used to prepare the $Fe_2O_3/MnO/ZnO$ catalyst. A mixture was made from powders of the three oxides in the proportion 52, 24, and 24 percent by weight, respectively. Starch was added to obtain 5 weight percent binder. The mixture was pressed to 3/16 in. diameter by 3/16 in. long pellets

The MnO_2/PbO catalyst was prepared by thoroughly mixing fine powders of MnO_2 and PbO. The mixture consisted of 95 percent by weight of the former and 5 percent by weight of the latter. Plaster of paris was suspended in water to be used as a binder. The suspension and powder were mixed and stirred for one hour. The mixture was dried overnight at 120 C to remove water. A solid mass of hard material containing 10 weight percent binder on a dry basis was obtained using this procedure. The solid mass was crushed to irregular particles with a size of less than 1/4 inch. The particles were calcined at 500 C for about 48 hours. The $CuO/MnO_2/Sb_2O_3$ catalyst was prepared using the same procedure, with 57, 38, and 5 weight percent CuO, MnO_2, and Sb_2O_3, respectively.

The four molybdenum-containing catalysts were prepared by Climax Molybdenum by impregnating 1/4 in. Al_2O_3 granules with metal salts. The granules were dried prior to calcination at 500 C.

EXPERIMENTAL PROGRAM

Experimental Conditions

Experiments were performed on a uniform engineering basis in a fixed bed reactor. Parameters such as space velocity, temperature, and gas composition were set to reflect the conditions at a coal-fired power plant. Table 6 summarizes the conditions under which the experiments were conducted.

Screening of the catalysts was started at a relatively low space velocity of 1,500 hr^{-1}. The space velocity is defined as the actual volumetric gas flow rate through the reactor divided by the bulk volume of catalyst charged in the reactor. The temperature range investigated was 150 to 800 F. However, it has previously been pointed out that at 300 F or b catalytic oxidation can be an add-on process. Also, the homogeneous decomposition of NO_2 to NO becomes important at high temperatures. Equilibrium data indicate that complete oxidation of NO cannot be obtained above 400 F. For instance, the equilibrium conversion for the homogeneous reaction is 92 percent at 500 F. However, higher temperatures may be of interest since recent data[30] indicate that it is possible to achieve higher than the

TABLE 6. EXPERIMENTAL CONDITIONS

Space Velocity: $\geq$ 1,500 hr^{-1}

Temperature: 150 to 800 F

Flue Gas Composition:

Component (volume basis)	Calculated from Cylinder Compositions and Experimental Conditions	Measured by Instrumental Analysis
NO_x (ppm)	720	620-670
NO_2/NO_x (mol/mol)	0.10	0.05-0.10
SO_2 (ppm)	2,600 - 2,800	2,400 - 2,800
H_2O (%)	7[a]	-
CO_2 (%)	11.2	-
O_2 (%)	5	4.9-5.1[b]
N_2 (%)	Balance	-

(a) 11% at 200 F; 13% at 150 F.

(b) Spot checks.

equilibrium conversion value in a catalytic reaction.

The composition of the simulated flue gas was chosen to reflect the conditions when burning high sulfur coal. This was done because wet scrubbing processes under development for simultaneous removal of SO_2 and NO_x require a molar ratio of SO_2 to NO_x of at least three. Water vapor contents of 11 and 13 volume percent were used for flue gas at 200 and 150 F, respectively, since the moisture content increases when the gas is cooled by evaporation of water. A heat balance for spray cooling flue gas at 300 F and 7 volume percent H_2O was used to calculate the appropriate moisture content at 200 and 150 F.

Description of Apparatus

The apparatus used in this study consisted of a flue gas manifold for mixing gases from cylinders to obtain a simulated flue gas, a vertical fixed bed reactor for catalytic conversion of NO to NO_2, an analysis system for measuring the concentrations of NO/NO_2, SO_2, SO_3, and O_2 in the simulated flue gas, and a multipoint digital temperature indicator for monitoring thermocouple readings at various locations. A schematic of the experimental set-up is shown in Figure 2.

The simulated flue gas was obtained from four gas cylinders with the following approximate composition on a volume basis:

Cylinder A - 20 percent O_2/balance N_2
Cylinder B - 2800 ppm NO/balance N_2
Cylinder C - 300 ppm NO_2/balance N_2
Cylinder D - 1.20 percent SO_2/48 percent CO_2/balance N_2.

Each cylinder was connected to a calibrated rotameter equipped with a pressure gauge and a flow controller to maintain a constant flow rate at varying downstream pressures. Each rotameter had two glass tubes and each tube had two floats of different materials so that the flow rate range per rotameter was from 20 to 6,900 cm^3/min

Teflon tubing was used for gas flow at ambient temperature and stainless steel tubing was used for elevated temperatures. The stainless steel tubing was wrapped with heating tapes and insulation to maintain and control the temperature of the simulated flue gas. The gas from Cylinder A flowed through a humidifier to provide water vapor. In most experiments,

the humidifier was maintained at 154 F so that the saturation level of the O_2/N_2 exit gas was 28 volume percent. The gases from all four cylinders were mixed together in equal proportions to provide simulated flue gas with the composition listed in Table 6.

The humidifier consisted of a 6-liter insulated stainless steel vessel wrapped with heating tape and equipped with a thermocouple. The temperature of the water in the humidifier was controlled at a desired level ($\pm$ 0.5F) by means of a proportional temperature controller. The gas was dispersed by a 1/2 in. stainless steel tube with a fine frit at the end. The humidifier was also equipped with a pressure gauge, an extra thermocouple connected to the digital indicator, and an external glass tube to measure the liquid level.

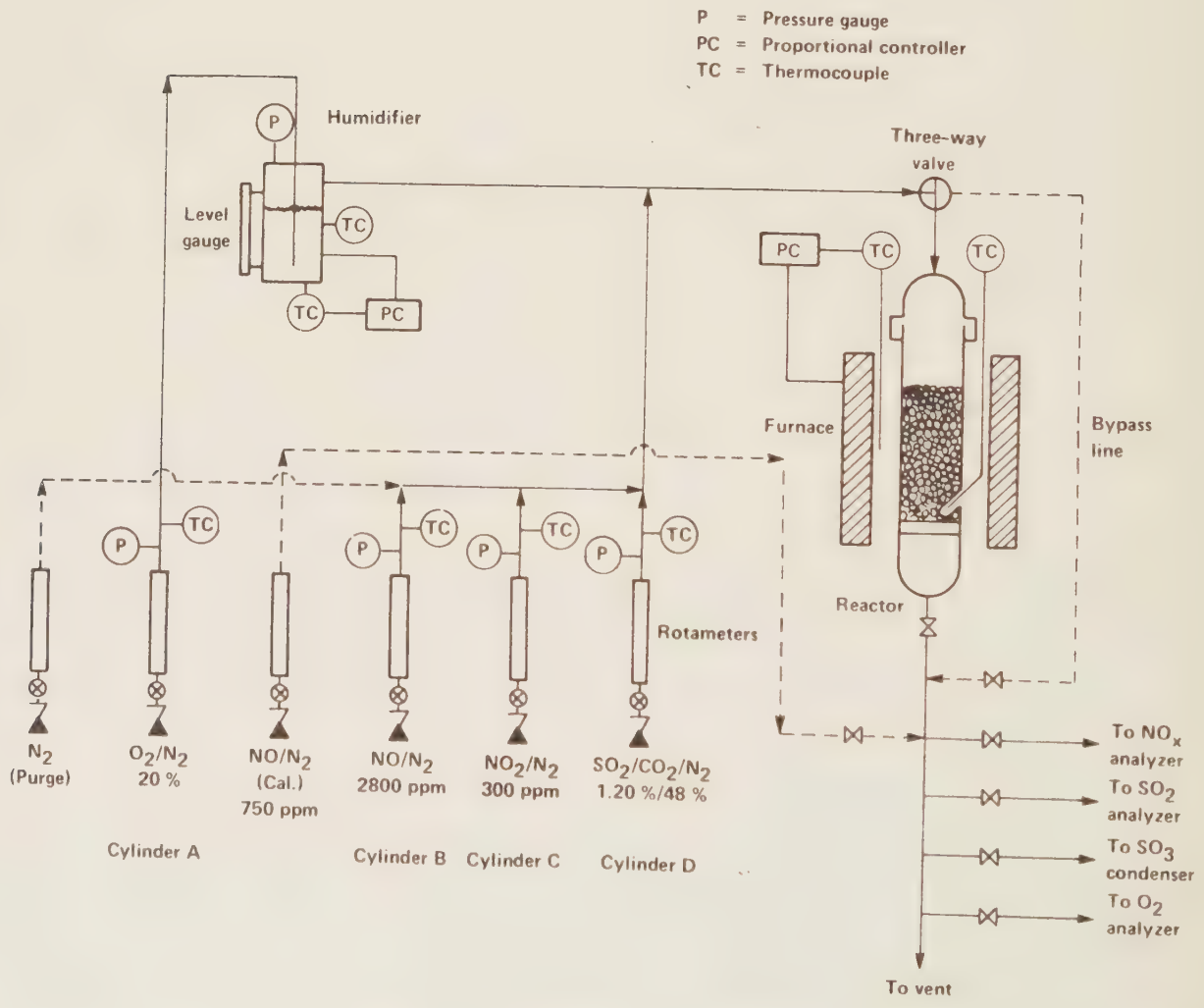

FIGURE 2. SCHEMATIC OF THE APPARATUS

The reactor consisted of a 25 in. long x 1 in. I.D. vertical quartz tube. The catalysts were supported on a coarse frit quartz disc and the simulated flue gas entered the reactor at the top. In most experiments, the catalyst bed had a depth of 10 in. Ball joints were used to connect the reactor inlet and outlet with the stainless steel tubing. A Solv-Seal joint was attached to the top of the reactor to allow the latter to be charged with catalyst. The reactor was surrounded by a tube furnace and the temperature was controlled by a proportional controller using a signal from a thermocouple attached to the reactor wall. There was an additional thermocouple located in a small well 1/4 in. above the quartz support disc and connected to the digital indicator.

Nitrogen was used to purge the system of any impurities, and another cylinder containing 750 ppm of NO in N_2 was used to calibrate the NO analyzer. A Thermo Electron Corporation (TECO) chemiluminescent instrument, Model 10A, was used to measure NO concentration. This instrument has a built-in thermal converter to decompose NO_2 to NO. The thermal converter can be used to measure NO_x (NO plus NO_2) or bypassed to measure NO only. For SO_2, an International Biophysics Corporation (IBC) Celeso instrument was used. This analyzer has a fuel cell detector which is specific for SO_2. A Beckman oxygen analyzer based on paramagnetism was used for spot checks of the oxygen concentration in the flue gas. The SO_2 and oxygen analyzers were preceded by U-tube cold traps immersed in ice water to remove moisture from the flue gas. A controlled condensation system based on the method of Goksoyr and Ross[37] was set up for detection of SO_3. This method consists of retaining the SO_3 by condensation as H_2SO_4 below the acid dew point but above the water vapor dew point. The H_2SO_4 is then determined by a simple acid-base titration.

Experimental Procedure

Blank runs were performed without catalyst in the reactor to determine if any oxidation occurred in the absence of catalyst. This step is important in order to establish that it is the catalysts that is responsible for the oxidation. The ratio of NO_2 to NO was found to be the same when flue gas in the temperature range of 150 to 800 F was passed through the empty reactor as when the gas was bypassed around the reactor.

The following procedure was used to perform a test run (experiment) with a catalyst sample. Simulated flue gas was passed through the

system while bypassing the reactor. The temperature of the humidifier was set to obtain the desired moisture content by assuming complete saturation of the gas leaving the humidifier. The temperature of the stainless steel tubing was set at about 30 F above the water dew point using the system of heating tapes and variacs. When the readings of NO_x and SO_2 concentrations in the flue gas attained constant levels as indicated by chart recorders, the flue gas was passed through the reactor by switching a three-way valve. The temperature of the catalyst bed was controlled at a desired value ($\pm$ 1 F) by using a proportional temperature controller. Steady state was considered to be achieved when the NO_x and SO_2 concentrations in the outlet gas from the reactor approached the inlet values within a deviation of 5 percent. The exposure time before steady state was reached varied from about one hour up to almost ten hours depending on temperature, type of catalyst, and space velocity. All analysis instruments were calibrated at least once a day.

RESULTS

An experimental matrix for the 14 catalysts tested at 8 temperatures is presented in Table 7. The number of experiments required for the complete matrix is 112 (14 x 8). However, each catalyst was not tested at every temperature so that the number of experiments performed from the matrix is 74. The catalysts are listed in Table 7 in the order that they were tested and qualitative results are presented on their oxidizing and reducing properties for NO_x; i.e., in most cases NO was oxidized to NO_2, but in some cases NO_2 was reduced to NO.

Quantitative data on the oxidation of NO to NO_2 at a space velocity of 1,500 hr^{-1} are presented in Table 8. Several catalysts exhibited optimum performance at a temperature of 200 F. Catalysts exhibiting greater than 50 percent oxidation of NO to NO_2 at this temperature in order of increasing performance are $V_2O_5/MoO-Al_2O_3$, $Bi_2O_3/MoO_3-Al_2O_3$, $Fe_2O_3/MoO_3-Al_2O_3$, $CoO-Al_2O_3$, $NiO-Al_2O_3$, and $Fe_2O_3/MnO/ZnO$. The latter catalyst, which was prepared at Battelle, exhibited 72.7 percent oxidation at 200 F. This catalyst and the $CoO-Al_2O_3$ catalyst were tested at a space velocity of 15,000 hr^{-1} to determine the optimum temperature. The results of these tests are summarized in Table 9. A high space velocity was used

TABLE 7. SUMMARY OF OXIDIZING/REDUCING PROPERTIES OF CATALYSTS[a]

Catalyst	Temperature, F							
	150	200	300	400	500	600	700	800
Cr_2O_3-Al_2O_3	?	+	+	-	?	?	?	?
Cr^{3+}-Zeolite	?	+	+	-	-	-	?	?
MnO_2/PbO	?	+	+	?	0	0	+	+
Pt-Al_2O_3	?	?	-	-	+	+	+	?
CuO/MnO_2/Sb_2O_3	?	0	+	+	+	+	?	?
CuO/MoO_3-Al_2O_3	?	?	-	-	0	+	+	+
V_2O_5/MoO_3-Al_2O_3	+	+	+	-	-	-0	?	?
Cu^{2+}-Zeolite	?	?	?	?	+	+	+	?
Fe^{2+}-Zeolite	?	0	0	0	0	?	?	?
Fe_2O_3/MoO_3-Al_2O_3	+	+	+	+	-	-	?	?
Bi_2O_3/MoO_3-Al_2O_3	+	+	+	+	?	?	?	?
NiO-Al_2O_3	+	+	+	+	?	?	?	?
CoO-Al_2O_3	+	+	+	-0	-	-	-	?
Fe_2O_3/MnO/ZnO	-	+	+	?	?	?	?	?

(a) + means NO → NO_2
- means NO_2 → NO
0 means no conversion
? means no data

because of the high degree of adsorption of NO_x exhibited by these catalysts. For example, at a space velocity of 1,500 hr^{-1} the CoO-Al_2O_3 catalyst was exposed to simulated flue gas at a temperature of 200 F for more than 7 hours before any NO_x was detected in the outlet gas from the reactor. The effect of space velocity on the oxidation of NO at a temperature of 200 F using CoO-Al_2O_3 or Fe_2O_3/MnO/ZnO catalyst is shown in Figure 3. The latter catalyst exhibited 50 percent or greater oxidation at space velocities below 3,500 hr^{-1}.

TABLE 8. PERCENT OXIDATION OF NO TO NO_2 AT A SPACE VELOCITY OF 1500 HR^{-1}[a]

Catalyst	150 F[b]	200 F[c]	300 F	400 F	500 F	600 F	700 F	800 F
Cr^{3+}-Zeolite	--	1.7	7.6	0	0	0	--	--
Fe^{2+}-Zeolite	--	0	0	0	0	--	--	--
Cu^{2+}-Zeolite	--	0	0	0	47.7	55.2	31.0	--
$Fe_2O_3/MnO/ZnO$	--	72.7[d]	--	--	--	--	--	--
MnO_2/PbO	--	18.2	11.7	0	0	0	4.8	11.2
$CuO/MnO_2/Sb_2O_3$	--	0	2.9	4.3	1.8	0.9	--	--
Cr_2O_3-Al_2O_3[e]	--	15.6	8.6[f]	0	--	--	--	--
NiO-Al_2O_3	57.6	63.5	47.2	10.6	0	--	--	--
CoO-Al_2O_3	--	53.9[d]	--	--	--	--	--	--
Fe_2O_3/MoO_3-Al_2O_3	6.6	53.4	37.0	1.0	0	0	--	--
CuO/MoO_3-Al_2O_3	--	--	0	0	0	7.1	13.9	7.9
Bi_2O_3/MoO_3-Al_2O_3	46.0	53.4	42.2	12.4	0	--	--	--
V_2O_5/MoO-Al_2O_3	35.3	53.0	34.1	0	0	0	--	--
Pt-Al_2O_3	--	0	0	0	12.0	43.6	18.7	--

(a) 12% CO_2; 7% H_2O; 5% O_2; 2400 to 2800 ppm SO_2; 620 to 670 ppm NO_x; balance N_2 (volume basis).

(b) 13% H_2O.

(c) 11% H_2O.

(d) Optimum temperature determined at a space velocity of 15,000 hr^{-1}.

(e) 500 ppm NO_x.

TABLE 9. PERCENT OXIDATION OF NO TO NO_2 AT A SPACE VELOCITY OF 15,000 HR^{-1}(a)

Catalyst	150 F(b)	200 F(c)	300 F	400 F	500 F	600 F	700 F
Fe_2O_3/MnO/ZnO	0	15.3	9.2	--	--	--	--
CoO-Al_2O_3	3.9	11.0	4.5	0	0	0	0

(a) 12% CO_2; 7% H_2O; 5% O_2; 2800 ppm SO_2; 630 to 650 ppm NO_x; balance N_2 (volume basis).

(b) 13% H_2O

(c) 11% H_2O

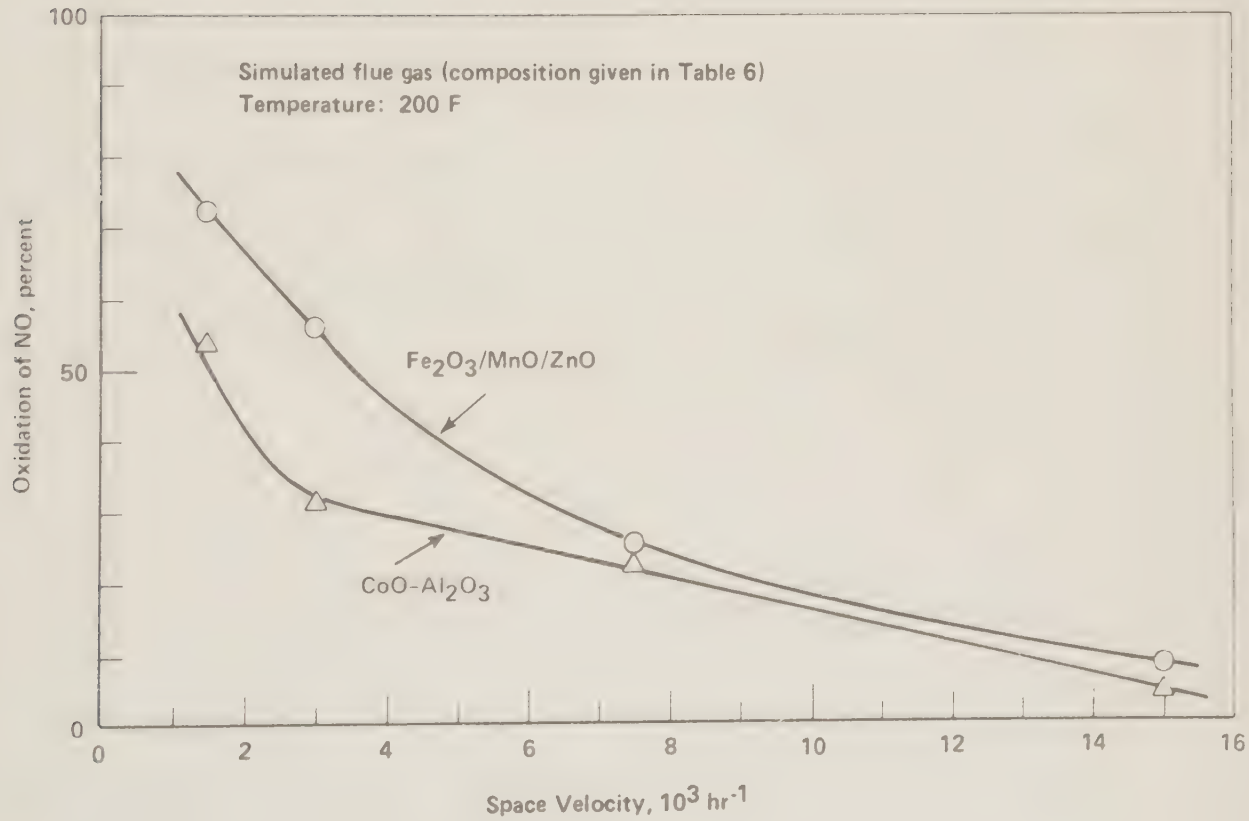

FIGURE 3. EFFECT OF SPACE VELOCITY ON THE CATALYTIC OXIDATION OF NO

The results summarized in Table 8 indicate that two of the catalyst exhibited optimum performance at a temperature of 600 F. The Cu^{2+}-zeolite catalyst and the Pt-Al_2O_3 catalyst exhibited 55.2 and 43.6 percent oxidation of NO, respectively, at this temperature. It appears that at temperatures of 600 F and above, SO_2 is catalytically oxidized to SO_3 because when the outlet gas was bubbled through water, a mist was formed which was probably due to the presence of H_2SO_4. Although the SO_3 in the outlet gas was not determined quantitatively, no SO_2 was detected in the outlet gas from the reactor when using the Pt-Al_2O_3 catalyst at 600 and 700 F. The effect of temperature on the oxidation of NO at a space velocity of 1,500 hr^{-1} with several catalysts is shown in Figure 4. These data illustrate that there usually is a region around the optimum temperature where the percent oxidation is relatively insensitive to changes in temperature.

The data presented in Table 8 for the Cr^{3+} ion-exchanged zeolite catalyst are somewhat in contradiction with the results reported by Arai, et al.[30] who obtained about 75 percent oxidation of NO at a temperature of 600 F and a space velocity of 20,000 hr^{-1} with this type of catalyst. However, there are some differences in experimental conditions between the two studies. In the work of Arai, et al.,[30] the SO_2 concentration was about 10 times lower and the NO_x concentration was about 5 times lower than in the present work. Also, the weight of catalyst used was about 50 times less than in the present study.

Three experiments were performed with the Cu^{2+}-zeolite catalyst using a gas stream with the following composition on a volume basis:

NO	640 ppm
O_2	5 percent
N_2	balance.

The results are listed in Table 10. These experiments were performed in order to determine the effect of deleting SO_2, CO_2, and H_2O from the gas stream used in the test runs, and to obtain data for comparison with data available from the literature. The equilibrium conversion for the homogeneous oxidation of NO is also given in Table 10 for comparison purposes. The equilibrium data indicate that complete oxidation of NO cannot be obtained above 400 F. However, it may be possible to achieve higher than the equilibrium conversion value in a catalytic reaction if the catalytic

TABLE 10. PERCENT OXIDATION OF NO TO NO_2 AT A SPACE VELOCITY OF 1500 HR^{-1}(a)

Catalyst	400 F	500 F	600 F
Cu^{2+}-Zeolite	60	76	70
Equilibrium conversion for homogeneous reaction	100	92	79

(a) 5% O_2; 630-640 ppm NO; balance N_2 (volume basis).

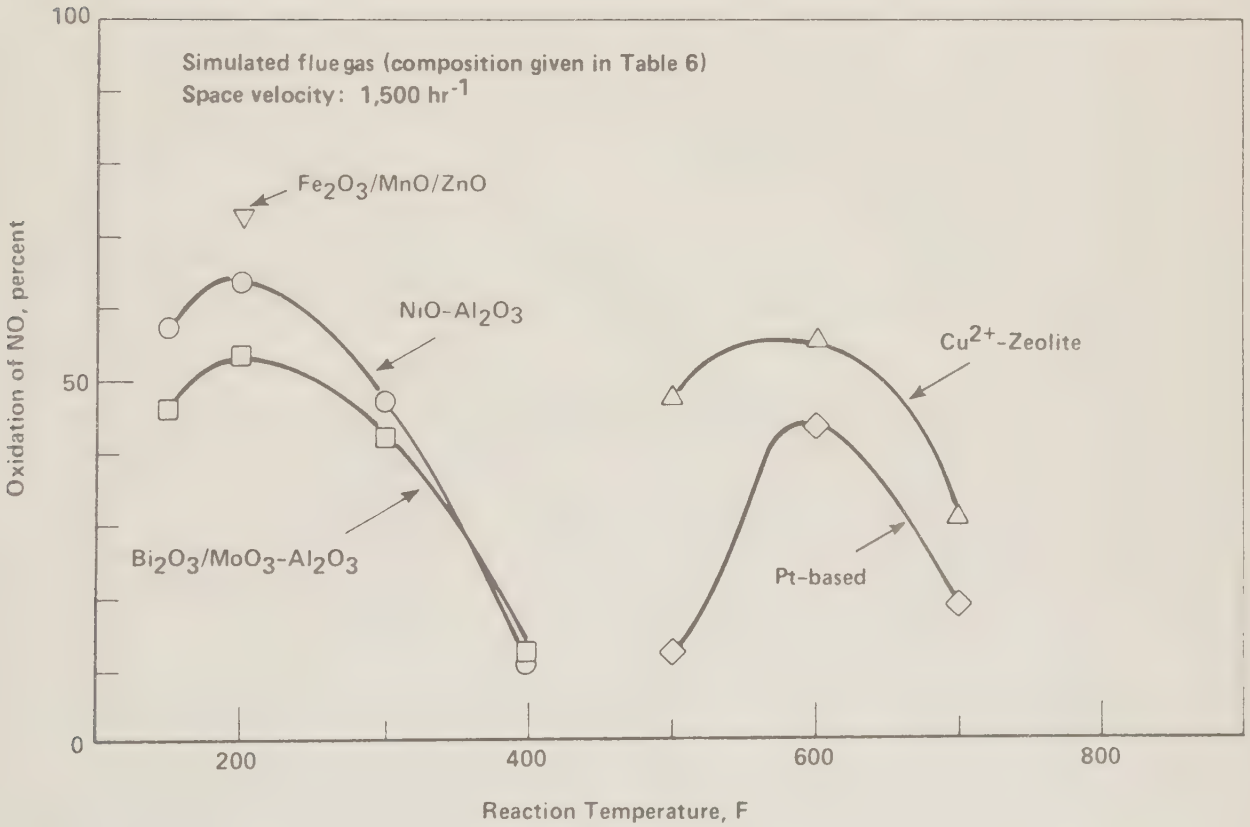

FIGURE 4. EFFECT OF REACTION TEMPERATURE ON THE CATALYTIC OXIDATION OF NO

reaction rate is much faster than the homogeneous reaction rate and if the last step in the catalytic reaction mechanism is irreversible.

A comparison of the data in Tables 8 and 10 for the Cu^{2+}-zeolite catalyst indicates that there is less oxidation of NO when SO_2, CO_2, and H_2O are present in the gas stream. The data obtained by Arai, et al.[30] agree with the data obtained from the present study for the Cu^{2+}-zeolite catalyst assuming that 60 percent of the available sites on the prepared zeolite are occupied by Cu^{2+}.

Four of the catalysts exhibiting high activity were selected for relatively long-term runs to study possible deactivation effects. These catalysts were $Fe_2O_3/MnO/ZnO$, $NiO-Al_2O_3$, $Bi_2O_3/MoO_3-Al_2O_3$, and Cu^{2+}-zeolite. The catalysts were exposed to simulated flue gas at a space velocity of 1,500 hr^{-1} for more than 20 hours; the temperature was 200 F for the first three catalysts and 550 F for the Cu^{2+}-zeolite. The first three catalysts exhibited a decreasing activity after 13 to 15 hours as shown in Figure 5, and the Cu^{2+}-zeolite was deactivated much faster. The causes for this deactivation have not been determined.

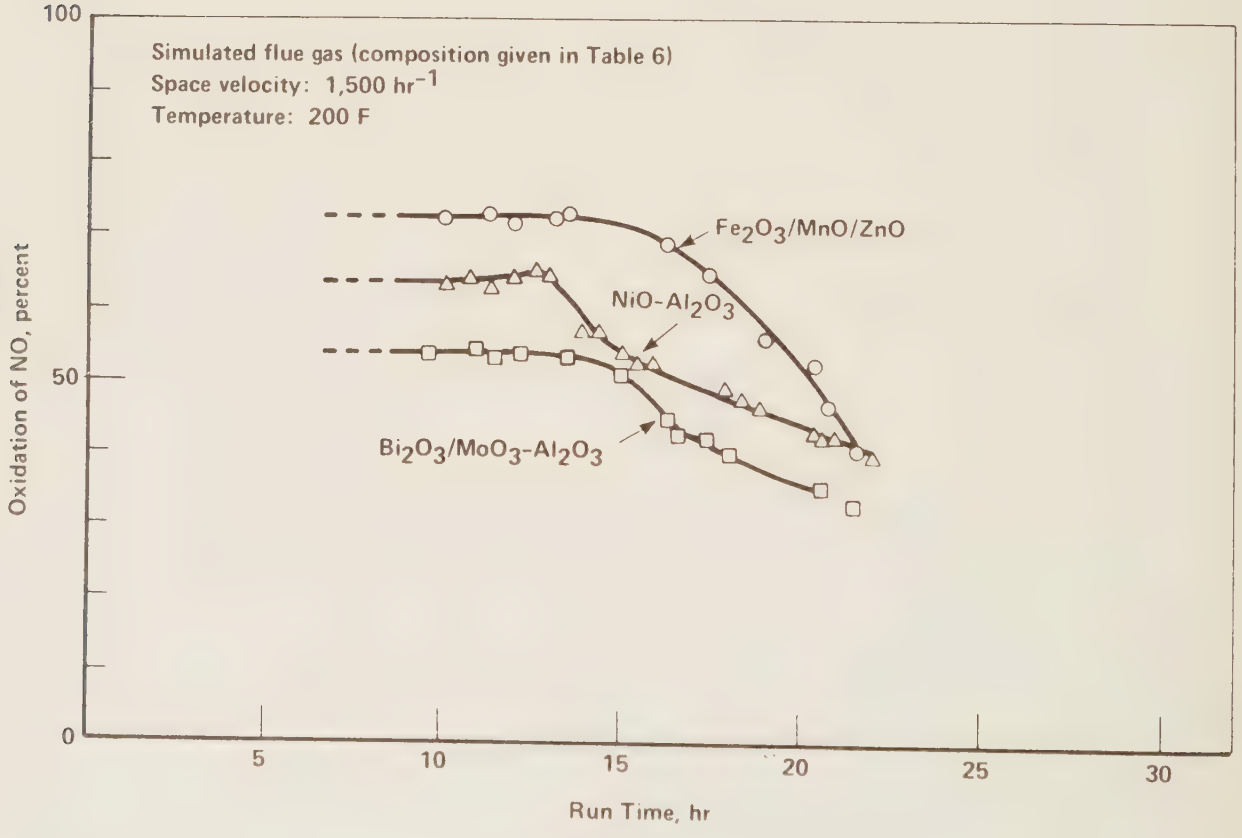

FIGURE 5. EFFECT OF RUN TIME ON THE CATALYTIC OXIDATION OF NO

DISCUSSION

The experimental results are very encouraging. A $Fe_2O_3/MnO/ZnO$ catalyst prepared at Battelle yielded over 70 percent oxidation of NO to NO_2 in simulated flue gas at a temperature of 200 F and a space velocity of 1,500 hr^{-1}. The optimum temperature for most of the catalysts tested appears to be around 200 F. This temperature is very suitable for an add-on process since particulates can be removed in a dry collection device ahead of the catalyst bed. The flue gas can then be spray cooled to 200 F with water. After catalytic oxidation of NO to NO_2, the flue gas can be sent to a limestone scrubber for removal of SO_2 and NO_2. The scrubber will cool the flue gas to its adiabatic saturation temperature of about 125 F.

It would be desirable to find a catalyst that yields more than 90 percent oxidation of NO at a space velocity greater than 1,500 hr^{-1}. The experimental results indicate that species such as SO_2 and H_2O, which are present in the flue gas, lower the oxidation level considerably. This effect has previously been reported in the literature and may be explained by adsorption of SO_2, H_2O, etc., on the catalyst surface so that there is a decrease in the number of available active sites.

The experimental results have revealed an additional problem with regard to catalytic oxidation of NO in flue gas. After about 14 hours of run time, the catalyst activity starts to decrease. No explanation has yet been found for this effect. Additional work is needed to solve the problem of catalyst deactivation as well as to find a more active catalyst.

The changes in catalyst properties when a catalyst is exposed to simulated flue gas should be investigated using methods such as BET surface area measurements and scanning electron microscopy. Long-term runs with catalyst candidates should be made without SO_2 and H_2O in the simulated flue gas to determine the effect of these components on catalyst activity. These runs should be repeated with each of the component, SO_2 and H_2O, present individually along with nitrogen, oxygen, CO_2 and NO_x.

Various experimental techniques should be utilized to identify the causes of catalyst deactivation. The following procedure is presented as an example:

(1) Select a promising catalyst candidate

(2) Add water to a sample of the catalyst

(3) Expose another sample of the same catalyst

to simulated flue gas and stop the test before breakthrough of NO_x; add water to the catalyst

(4) Repeat Step 3 with a fresh sample, but continue the run to steady state with respect to NO_x; add water to the catalyst

(5) Repeat Step 3 with a fresh sample, but continue to significant catalyst deactivation; add water to the catalyst

(6) Observe the color of the water extracts, measure pH, and analyze for nitrates, nitrites, sulfates, and sulfites.

The options for eliminating catalyst deactivation include selection of a catalyst that does not form nitrate and nitrite salts or sulfate and sulfite salts, modification of the catalyst carrier, modification of the catalyst preparation method, and modification of the catalyst operating conditions. The appropriate option(s) depends upon the causes of catalyst deactivation.

Although it may be difficult to find a catalyst that yields nearly complete oxidation of the NO at a space velocity of 1,500 hr^{-1} or greater, it should be possible to achieve 80 to 90 percent oxidation with a relatively modest effort. Several candidate catalysts should be prepared to achieve optimum performance based on the results of the investigation on causes of catalyst deactivation as well as the experimental results obtained previously. These catalysts should be subjected to a screening program similar to the one performed for the 14 catalysts that have already been tested.

REFERENCES

(1) McKee, R. H., "Gas Oxidation with Hydrated Silica Gel as a Catalyst", U. S. Patent 1,319,332 (September 20, 1921).

(2) Burdick, C. L., "Oxidation of Nitric Oxide and its Catalysts", J. Am. Chem. Soc., 44, 244-51 (1922).

(3) Boreskov, C. K., and Shogam, S. M., "Kinetics of the Oxidation of Nitrogen Oxide on Activated Charcoal", J. Phys. Chem. (U.S.S.R.), 8, 306-25 (1936).

(4) Kurin, N. P., and Novgorodova, E. M., "The Catalytic Oxidation of Nitrogen. III. Investigation of the Catalytic Activity of Activated Carbon", Izvest. Tomsk. Ind. Inst., 60 (3), 61-78 (1940).

(5) Varlamov, M. L., "Heterogeneous Oxidation of Nitric Oxide in the Mills-Packard Process of Sulfuric Acid Production", Nauch. Zapiski Odessk. Politekh. Inst., 20, 40-6 (1960).

(6) Tohata, H., Kato, S., and Arai, T., "Control Technique of Nitrogen Oxides", Taiki Osen Kenkyu (J. Japan. Soc. Air Pollution), 8, (3), 343 (1973).

(7) Eto, H., "NO_x Removal By Absorption", Nenryo Oyobi Nensho (Fuel and Combustion), 41 (6) 556-61 (1974).

(8) Takahata, K., Miki, H., Hashimoto, M. and Takabatake, M., "Oxidation of Nitrogen Monoxide in Waste Gas", Japanese Patent 75 41,798 (April 16, 1975).

(9) Urano, K., Tanikawa, N., Masuda, T., and Kobayashi, Y., "Studies on the Removal and Recovery of Waste Gas by Adsorption. II. Oxidation Adsorption of Nitrogen Monoxide on Activated Carbon", Nippon Kagaku Kaishi, (2) 303-9 (1978).

(10) Rao, M. N., and Hougen, O. A., "Catalytic Oxidation of Nitric Oxide on Activated Carbon", Chem. Eng. Progress Symposium Ser., 48 (4), 110-24 (1952).

(11) Kircher, O., and Hougen, O. A., "Effect of Water Vapor on the Catalytic Oxidation of Nitric Oxide", A.I.Ch.E. Journal, 3, 331-5 (1957).

(12) Chu, C., and Hougen, O. A., "Optimum Design of a Catalytic Nitric Oxide Reactor", Chem. Eng. Progr., 57, (6), 51-8 (1961).

(13) Chu, C., "Economic Design of a Nitric Oxide Reactor", Univ. Microfilms, Ann Arbor, Mich., L. C. Card No. Mic 61-2945 (1961).

(14) Hougen O. A., "Principles of Catalyzed Gaseous Reaction Rates and their Applications", Z. Elektrochem., 57, 479-96 (1953).

(15) Kircher, O., "Effect of Water Vapor on the Catalytic Oxidation of Nitric Oxide", Univ. Microfilms, Ann Arbor, Mich., Publ. No. 16181 (1956).

(16) Hougen, O. A., "Heterogeneous Catalysis and Reactor Design", Tidss. Kr. Kjemi, Bergvessen Met., 23, 6-14 (1963).

(17) Szego, L., "The Catalytic Oxidation of Nitrogen Oxide", Gazz. Chim. Ital., 60, 212-29 (1930).

(18) Kurin, N. P., and Blokh, I. O., "Catalytic Oxidation of Nitric Oxide. I.", J. Applied Chem. (U.S.S.R.), 11, 734-49 (1938).

(19) Kurin, N. P. and Blokh, I. O., Catalytic Oxidation of Nitric Oxide. II. Influence of Water Vapor on the Velocity of Oxidation in the Presence of Silica Gel, Chrome, Zinc, and Vanadium Catalyst", J. Applied Chem. (U.S.S.R.), 11, 750-3 (1938).

(20) Ozawa, M., "Method of Disposing Nitrogen Oxides in Flue Gas from Nitric Acid Treatment", Proc. Environmental Conservation Engineering Study Group (Japan), Semin. Meas., Attenuation, Removal Nitrogen Oxides Combust. Gas, Osaka, Japan (1973), pp. 165-79.

(21) Naruse, Y., Hata, T., and Kishidaka, H., "Catalytic Oxidation of NO and Adsorption Removal of NO_x", paper presented at the 34th Spring Term Annual Meeting of the Chemical Society of Japan, Tokyo (April, 1976)

(22) Jaffer, J. H., Jr., and Bliss, H., "Heat Transfer and Kinetics in a Catalyst Bed of Rectangular Cross Section: Air Oxidation of Nitric Oxide with Silica Gel", A.I.Ch.E. Joùrnal, 6, 510-16 (1960).

(23) Baker, R. W., Wong, H. N., and Hougen, O. A., "Catalytic Oxidation Of Nitric Oxide on Silica Gel", Chem. Eng. Progress Symposium Ser., 48, (4), 103-9 (1952).

(24) Roginskiĭ, S. Z., "Mechanism of Catalytic Oxidation by Molecular Oxygen at Low Temperatures", Acta Physicochim. (U.S.S.R.), 9, 475-500 (1938).

(25) Cambi, L., and Szego, L., "Adsorption of Nitrous Vapors by Means of Silica Gel", Giorn. Chim. Ind. Applicata, 9, 3-8 (1926).

(26) Bokhoven, C. and Zwietering, P., "The Catalytic Oxidation of Nitric Oxide", Chem. Weekblad (Meth.), 52, 83-7 (1956).

(27) Scholten, J. J. F., and Zwietering, P., "The Oxidation of Nitric Oxide over Silica. An Example of Physical Catalysis", Actes 2e Intern. Congr. Catalyse, Paris, 1960, 1, 389-403 (1961).

(28) Seiji, A., "Studies on Catalysts which Oxidize Nitric Oxide in Flue Gas", Kogai Hakua Shobo (Pollution Control), 10 (1), 32-42 (1975).

(29) Miyadera, T., et al., "Oxidation of NO by Metal Oxide Catalysts", Japan Chemical Society Preprint No. 2005 (1975).

(30) Arai, H., Tominaga, H., and Tsuchiya, J., "Oxidation of Nitrogen Monoxide over Transition-Metal Ion-Exchanged Zeolites", Proc. 6th Int. Congr. Catal., 1976, 2, 997-1006 (1977).

(31) Takayasu, M., Annen, Y., and Morita, Y., "Oxidation of Nitric Oxide on Chromia Catalysts", Waseda Daigaku Rikogaku Kenkyusho Hokoku (in English), 72, 17-21 (1976).

(32) Takayasu, M., Annen, Y., and Morita, Y., "Effects of Sulfur Dioxide and Water on Nitric Oxide Oxidation", Nenryo Kyokai-Shi, 54 (11), 930-5 (1975).

(33) Hattori, H., et al., "Studies on Oxidation Catalysts of Nitrogen (II) Oxide from Flue Gas", Kogai Hakua Shobo (Pollution Control), 12 (1), 62-74 (1977).

(34) Takasu, Y., Niwa, H., and Matsuda, Y., "Catalytic Properties of Oxygen Adsorbed on Nickel (II) Oxide-Samarium (III) Oxide Binary Oxides", J. Catal., 51 (2) 286-90 (1978).

(35) Kotera, T., Ozasa, M. and Takano, T., "Removal of Nitrogen Oxide from Waste Gas", Japanese Patent 76 44,558 (April 16, 1976).

(36) Takeyama, T., Masuda, K., and Takahashi, A., "Catalytic Oxidation of Nitrogen Monoxide", Japanese Patent 75 62,859 (May 29, 1975).

(37) Goksoyr, H., and Ross, K., "The Determination of Sulfur Trioxide in Flue Gases", J. Inst. Fuel, 35 (255), 177-79 (1962).